THE PAIRON PROBLEM IN HIGH TEMPERATURE SUPERCONDUCTIVITY

Ph. D. THESIS

by

SANJEEV KUMAR VERMA

DEPARTMENT OF PHYSICS
INDIAN INSTITUTE OF TECHNOLOGY ROORKEE
ROORKEE - 247 667 (INDIA)
MAY, 2019

THE PAIRON PROBLEM IN HIGH TEMPERATURE SUPERCONDUCTIVITY

A THESIS

Submitted in partial fulfilment of the requirements for the award of the degree

of

DOCTOR OF PHILOSOPHY

in

PHYSICS

by

SANJEEV KUMAR VERMA

DEPARTMENT OF PHYSICS
INDIAN INSTITUTE OF TECHNOLOGY ROORKEE
ROORKEE - 247 667 (INDIA)
MAY, 2019

INDIAN INSTITUTE OF TECHNOLOGY ROORKEE
ROORKEE

CANDIDATE'S DECLARATION

I hereby certify that the work which is being presented in the thesis entitled **"THE PAIRON PROBLEM IN HIGH TEMPERATURE SUPERCONDUCTIVITY"** in partial fulfilment of the requirements for the award of the Degree of Doctor of Philosophy and submitted in the Department of Physics of the Indian Institute of Technology Roorkee is an authentic record of my own work carried out during a period from January, 2014 to May, 2019 under the supervision of **Dr. B. D. Indu**, Professor, Department of Physics, Indian Institute of Technology Roorkee, Roorkee, INDIA.

The matter presented in this thesis has not been submitted by me for the award of any other degree of this or any other Institution.

(Sanjeev Kumar Verma)
Signature of Candidate

This is to certify that the above statement made by student is correct to the best of my knowledge.

(B. D. Indu)
Signature of Supervisor

The Ph.D. Viva-Voce Examination of **Mr. Sanjeev Kumar Verma**, Research Scholar, has been held on **September 24, 2019** at the Department of Physics, IIT Roorkee, Roorkee, INDIA.

Chair, SRC **Signature of External Examiner**

This is to certify that the student has made all the corrections in the thesis.

Signature of Supervisor **Head of the Department**

Dated: September 24, 2019

Abstract

The historic discovery of fascinating phenomenon of superconductivity by H. Kamerlingh Onnes promptly creates a striking impression among the Physics community. The two most important turning points of theoretical understanding of superconductivity are (i) phenomenological theory of superconductivity developed by Ginzburg and Landau known as Ginzburg-Landau (GL) theory and (ii) microscopic theory of superconductivity developed by J. Bardeen, L. N. Cooper, and J. R. Schrieffer known as BCS theory. Another breakthrough appears as a milestone when G. Bednorz and K. A. Müller discover the high-temperature superconductor (HTS) $La_{2-x}Sr_xCuO_4$ with transition temperature (T_c) up to 30 K. In the subsequent year the superconductor $YBa_2Cu_3O_{7-\delta}$ is discovered with critical temperature $T_c = 93$ K. Of many models proposed after the discovery of HTS, some of the worth mentioning are: RVB theory of HTS by P. W. Anderson and gauge theory of HTS for strongly correlated Fermi system by P. W. Anderson and G. Baskaran. It is identified that in cuprate HTS the charge carriers are holes and located in the same copper-oxide plane and it increases with the increasing number of copper-oxide layers. The role of the exchange of antiferromagnetic spin fluctuations in high-temperature superconductivity (HTSC) worked out by Moriya *et al.* and C. M. Varma.

The understanding of several unusual properties of HTS, namely; anisotropy of superconducting gap (SG), the high value of $2\Delta/k_BT_c$ (5 to 8), $d_{x^2-y^2}$ pairing symmetry, co-existence of superconducting and antiferromagnetic (AF) phases, etc. become

a challenge for theorists. None of these unusual properties could be explained by the BCS theory, and this enforced the researchers to think beyond the BCS model. To understand the mechanism of HTSC in cuprate superconductors Fujita *et al.* used the idea of attractive potential between two electrons from the BCS theory and showed the formation of d-wave Cooper-pair (pairon) in the copper-oxide plane. William *et al.* recently revealed that the holes in the cuprate superconductor get coupled to its local AF environment and creates the pairons. It is shown that pairon formation in cuprate superconductor is direction dependent due to anisotropic phonon exchange attraction which leads to anisotropic SG formation. Though the mechanism of HTSC is not fully understood, it appears that the understanding of pairons can provide some insight into the strange behaviour of HTS.

The electron-phonon interaction emerged as a key factor in the theoretical development of conventional superconductivity as well as HTSC. The effects of doping (impurity/defect)and that of anharmonicity, also has been noticed to be significant in the superconducting phenomenon. In the present work using a generalized (non-BCS) Hamiltonian, the contribution due to electrons, phonons, electron-phonon interactions, anharmonicity, and defects is taken care. The HTS has a very complex structure e.g., $La_{2-x}Sr_xCuO_4$ and $YBa_2Cu_3O_{7-\delta}$, which have layered structure with the different layer of copper-oxide planes that introduced a complex network interactions channels and are precisely taken care of by the modified form of Born-Mayer-Huggins potential (MBMHP). The Green's functions method based on many body quantum dynamics of electrons and phonons, has been adopted to investigate the properties of the SG.

Using the generalized EDOS of HTS followed by BCS formalism the two SG equations have been obtained which shows dependence on temperature, Fermi energy and renormalized electron, and phonon energies. The effect of AF spin fluctuations on the SG and pairing symmetry also seen. The expressions for pairing potential are

also obtained by utilizing the SG equations. Using Green's functions technique the renormalized electron-phonon dispersion is obtained from which the behaviour of SG, nodal and antinodal gap with doping are studied. The renormalized electron-phonon dispersion further used to analyze the anisotropy of the SG and pairing symmetry as well as a theory of renormalized phonon group velocity for HTS has been formulated using phonon Green's functions.

Publications

Articles in Journals

1. **S. K. Verma**, A. Kumari, A. Gupta, B. D. Indu, "The high-temperature superconductor gap equation", Phys. Scr., **94**, 035701 (2019). (doi: https://doi.org/10.1088/1402-4896/aafbc5)

2. **S. K. Verma**, A. Gupta, A. Kumari, B. D. Indu, "Superconducting gap anisotropy and d-wave pairing in $YBa_2Cu_3O_{7-\delta}$", Int. J. Mod. Phys. B **32**, 1850035 (2018). (doi: https://doi.org/10.1142/S0217979218500352)

3. **S. K. Verma**, A. Gupta, A. Kumari, B. D. Indu, "Pairing symmetry, nodal and antinodal superconducting gap in $La_{2-x}Sr_xCuO_4$: A doping scenario", J. Low Temp. Phys., **196**, 442-457, (2019). (doi: https://doi.org/10.1007/s10909-019-02199-2)

4. **S. K. Verma**, A. Gupta, A. Kumari, B. D. Indu, "Theory of Renormalized Phonon Group Velocity in High Temperature Superconductors", Mod. Phys. Lett. B, 1950337, (2019). (doi: https://doi.org/10.1142/S0217984919503378)

5. A. Gupta, **S. K. Verma**, A. Kumari, B. D. Indu, "Impurity induced renormalized phonon spectrum of cuprate superconductors", Int. J. Mod. Phys. B, **32**, 1850237, (2018). (doi: https://doi.org/10.1142/S0217979218502375)

6. A. Gupta, **S. K. Verma**, A. Kumari, B. D. Indu, "Analysis of electron and phonon heat capacities of $La_{2-x}Sr_xCuO_4$ cuprate superconductor", J. Phys. Chem. Solids, **134**, 83-88 (2019). (doi: https://doi.org/10.1016/j.jpcs.2019.05.037)

7. A. Gupta, A. Kumari, **S. K. Verma**, B. D. Indu, "The phonon and electron heat capacities of cuprate superconductors", Physica C, **551**, 55-65, (2018). (doi: https://doi.org/10.1016/j.physc.2018.05.010)

8. R. Chauhan, **S. K. Verma**, A. Gupta, A. Kumari, B. D. Indu, "A new approach to the potential energy of solid", Karbala International Journal of Modern Science, **5**, 97-104, (2019). (doi: https://doi.org/10.33640/2405-609X.1008)

9. A. Gupta, **S. K. Verma**, A. Kumari, B. D. Indu, "Generalized phonon density of states of $La_{2-x}Sr_xCuO_4$ cuprate superconductor", Int. J. Mod. Phys. B, (accepted).

10. R. Chauhan, **S. K. Verma**, A. Gupta, A. Kumari, B. D. Indu, "Pairon density of states of high-T_c cuprate superconductors", Physics C, (under review).

Proceedings/Conferences/Workshops

11. **S. K. Verma**, A. Kumari, A. Gupta, B. D. Indu, "Superconducting gap in cuprates high temperature superconductors", AIP Conf. Proc., **1953**, 120020, (2018). (doi: https://doi.org/10.1063/1.5033085)

12. **S. K. Verma**, A. Kumari, A. Gupta, B. D. Indu, "Anisotropy in superconducting gap in $YBa_2Cu_3O_{7-\delta}$ ", AIP Conf. Proc., **1942**, 130036, (2018). (doi: https://doi.org/10.1063/1.5029106)

13. A. Gupta, **S. K. Verma**, A. Kumari, B. D. Indu, "Effects of defect on phonon heat capacity in cuprate superconductors", AIP Conf. Proc., **1953**, 120014, (2018). (doi: https://doi.org/10.1063/1.5033079)

14. A. Gupta, A. Kumari, **S. K. Verma**, B. D. Indu, "Renormalized modes in cuprate superconductors", AIP Conf. Proc., **1942**, 130034, (2018). (doi: https://doi.org/10.1063/1.5029104)

15. A. Kumari, A. Gupta, **S. K. Verma**, B. D. Indu, "In-plane and cross-plane thermal conductivity in $La_{2-x}Sr_xCuO_4$", AIP Conf. Proc., **1953**, 120013, (2018). (doi: https://doi.org/10.1063/1.5033078)

16. A. Gupta, **S. K. Verma**, A. Kumari, B. D. Indu, "Study of electron density of states and electronic heat capacity of high temperature cuprate superconductor: $La_{2-x}Sr_xCuO_4$", JOSC Special Issue: Superstripes 2019, J. Supercond. Nov. Magn., (accepted).

17. **S. K. Verma**, A. Gupta, A. Kumari, B. D. Indu, "Angular superconducting gap in $YBa_2Cu_3O_{7-\delta}$", 12th International Conference on Materials and Mechanisms of Superconductivity and High Temperature Superconductors, Beijing, China, August 19-24, 2018.

18. **S. K. Verma**, A. Kumari, A. Gupta, B. D. Indu, "Anisotropy in superconducting gap in $YBa_2Cu_3O_{7-\delta}$", 62nd DAE Solid State Physics Symposium (DAE SSPS-2017), BARC – Mumbai, India, December 26-30, 2017.

19. **S. K. Verma**, A. Kumari, A. Gupta, B. D. Indu, "Superconducting gap in cuprates high temperature superconductors", 2nd International Conference on Condensed Matter & Applied Physics, Bikaner, India, November 24-25, 2017.

20. **S. K. Verma**, A. Gupta, A. Kumari, B. D. Indu, "Planer behaviour of renormalized and perturbed mode frequencies in cuprate superconductors $YBa_2Cu_3O_{7-\delta}$",

National Workshop on Recent Advances in Strong Correlated Electronic Materials-2017, Department of Physics, Indian Institute of Technology Roorkee, India, February 2-10, 2017.

21. A. Gupta, **S. K. Verma**, A. Kumari, B. D. Indu, "Effects of defect on phonon heat capacity in cuprate superconductors", 2nd International Conference on Condensed Matter & Applied Physics, Bikaner, India, November 24-25, 2017.

22. A. Kumari, A. Gupta, **S. K. Verma**, B. D. Indu, "In-plane and cross-plane thermal conductivity in $La_{2-x}Sr_xCuO_4$", 2nd International Conference on Condensed Matter & Applied Physics, Bikaner, India, November 24-25, 2017.

23. A. Gupta, A. Kumari, **S. K. Verma**, B. D. Indu, "Renormalized modes in cuprate superconductors", 62nd DAE Solid State Physics Symposium (DAE SSPS-2017), BARC – Mumbai, India, December 26-30, 2017.

24. INUP Familiarization Workshop on Nanofabrication Technologies, organized by INUP, IISC Bangalore, conducted at Indian Institute of Technology, Roorkee, India, April 27-28, 2017.

25. Radiation Effect in Semiconductor Device Physics, Modeling & Mitigation, organized by IEEE, conducted at Indian Institute of Technology, Roorkee, India, July 28, 2017.

26. Author Workshop on Book Publishing, organized by Mahatma Gandhi Central Library in association with Elsevier, Indian Institute of Technology Roorkee, Roorkee, India, September 26, 2016.

27. International conference on Science, Technology and Management, Delhi University, Delhi, India, September 27, 2015.

Acknowledgements

Firstly, I would genuinely like to express my deep and sincere gratitude to my Ph.D. supervisor Prof. B. D. Indu, Department of Physics, Indian Institute of Technology Roorkee for giving me a precious opportunity to work professionally with him. This scholarly work is only possible with his immense knowledge of the subject, creative thoughts, sharp and focused memory, intellectual guidance and continuous encouragement. I sincerely appreciate his humble nature, strictness for honesty and unique approach of handling students crucial situation that always gave me moral strength to continue my research work faithfully. His legitimate supervision generously helped me in all the time of fundamental research and academic writing of this doctoral thesis. I would like to express my sincere gratitude to my caretaker supervisor Prof. G. D. Varma for his moral and academic administrative support. After the retirement of my thesis supervisor, his sincere efforts for the smooth conduction of my Ph.D. viva on time is highly acknowledged.

My sincere thanks and heartfelt gratitude go to my supervisor family for providing the pleasant feeling of a family like precious environments.

I extend my sincere thanks to my SRC members: Prof. Tashi Nautiyal (Internal Expert), Prof. G. D. Varma (Chairman SRC, Former), Prof. K. L. Yadav (Chairman SRC, Present), Prof. D. Kaur (Chairman DRC) Department of Physics, Prof. R. C. Mittal (External Expert, Former) Department of Mathematics and Prof. Anil Kumar (External Expert, Present) Department of Chemistry who monitored my work thoroughly with valuable comments on several presentations of this work. I would like to express my sincere thanks to the official and technical staff of the Department of Physics.

I gratefully acknowledge my seniors Dr. Hempal Singh, Dr. Anu Singh and Dr. Rakhi Sharma for their moral support. I would like to express my special thanks to my lab-mates: Anushri Gupta, Anita Kumari, Radhika Chauhan and Ankita for valuable discussion of research work. My sincere thanks go to my friends: Dharmendra Singh Raghav, Divyanshu Dwivedi, Neeraj Singh, Pramod Kumar, Rakesh Kumar, Renu Bala, Rohit Kumar, Sandeep Sundriyal, Vikas Yadav, Vishnu Singh and Yogesh Kumar.

I gratefully acknowledge the Ministry of Human Resource Development (M.H.R.D.) Government of India, New Delhi, for providing financial assistance to complete this work. I would like to thanks the Students' Aid Committee (StAC) - Indian Institute of Technology Roorkee for providing further financial assistance in the extension period.

I gently take this unique opportunity to express the immense gratitude from my deep heart to my beloved parents for their unconditional lifelong support. From the 'Childhood' to become a 'Philosopher' is a very very precious moment and this long journey with countless obstacles was only possible with hearted love and dedicated support from my loving family.

Date: September 24, 2019 (Sanjeev Kumar Verma)

Dedicated to my parents
Sri. Raghuvansh Verma *and* ***Smt. Prabhawati Devi***

Contents

List of Figures

List of Tables

Abbreviations

AF:	**A**nti**f**erromagnetic
ARPES:	**A**ngle **R**esolved **P**hoto**e**mission **S**pectroscopy
BCS:	**B**ardeen-**C**ooper-**S**chrieffer
EDOS:	**E**lectron **D**ensity **o**f **S**tates
ERS:	**E**lectron **R**aman **S**pectroscopy
FS:	**F**ermi **S**urface
GL:	**G**inzburg-**L**andau
HTS:	**H**igh **T**emperature **S**uperconductors
HTSC:	**H**igh **T**emperature **S**uperconductivity
MBMHP:	**M**odified **B**orn-**M**ayer-**H**uggins **P**otential
QCP:	**Q**uantum **C**ritical **P**oint
RPGV:	**R**enormalized **P**honon **G**roup **V**elocity
RVB:	**R**esonating-**V**alence-**B**ond
SG:	**S**uperconducting **G**ap
STS:	**S**canning **T**unning **S**pectroscopy

Symbols

k_B:	Boltzmann Constant
$\hbar$:	Reduced Planck Constant
T_c:	Critical Temperature
$V_{ij}(r)$:	Modified Born-Mayer-Huggins Potential
H:	Hamiltonian
T:	Kinetic Energy
V:	Potential Energy
ε_F:	Fermi Energy
ω_D:	Debye Ffrequency
Δ:	Superconducting Gap
$D(\varepsilon)$:	Electron Density of States
x, δ:	Doping Concentration
v_g:	Phonon Group Velocity
$\tilde{v}_g$:	Renormalized Phonon Group Velocity
$a_k(a^*_{-k})$:	Phonon Annihilation (Creation) Operator
$A_k(B_k)$:	Phonon Field (Momentum) Operator
$b_{q\sigma}(b^*_{q\prime\sigma\prime})$:	Electron Annihilation (Creation) Operator
$G_{r,\underline{a},\underline{\underline{c}}}(t,t')$:	Retarded, Advanced, Causal Green's Functions
$G_m(\tau,\tau')$:	Matsubara Green's Functions
$\Gamma_k(\omega)(\Gamma_q(\omega))$:	Phonon (Electron) Frequency Line Widths
$\Delta_k(\omega)(\Delta_q(\omega))$:	Phonon (Electron) Frequency Line Shifts
$C(k_1,k_2)(D(k_1,k_2))$:	Mass (Force Constant) Change Parameter

Chapter 1

Introduction: Prospects and Retrospects

"The most beautiful thing we can experience is the mysterious. It is the source of all true art and science."

- - - Albert Einstein

1.1 The Discovery of Superconductivity

Before the discovery of superconductivity, people were attempting to study the temperature-dependent electrical conductivity of metals [1] and after three years of liquefaction of Helium (1908) [2] by H. Kamerlingh Onnes, he measures the electrical resistivity of Mercury (1911) at the extremely low temperature (~ 4.2 K) and surprisingly observed an unusual phenomenon - the ability to conduct electricity without any resistance [3] - known as superconductivity. In the beginning, the name "supraconduction" was given by Kamerlingh Onnes to this strange phenomenon which later on called as superconductivity [4] was reckoned as a landmark discovery in the history of low-temperature physics. In 1933, Meissner experimented with studying the behaviour of the superconductor in the magnetic field and found that

the magnetic field was expelled from the interior of superconductor when cooled below the critical temperature [5]. This experimental observation added a new feather to the phenomenon of superconductivity.

1.2 The Conventional Superconductivity

Even after the identification of a series of conventional superconductors [6], the theoretical understanding of superconductivity remained a puzzle for a long time and thus phenomenon of superconductivity appeared as a most mysterious and fascinating problem of the 20th century with several theoretical failures [7]. The discovery of Meissner effect projected the demarcation line between a perfect conductor and a superconductor with the inference that the superconductor behaves as a perfect conductor and as well as a perfect diamagnet which expels the magnetic field from inside of it [8]. The Gorter and Casimir's two fluid model [9] was an attempt to understand the phenomenon of superconductivity. The first and foremost phenomenological model of superconductivity based on two fluid model was presented by F. London and H. London [10] in 1935 which could explain the Meissner effect and introduced the concept of a parameter, known as London penetration depth, after which the magnetic field completely expelled by the superconductor. The conventional superconductor is categorized as type I and type II superconductor. The type I superconductor has only one critical magnetic field - the value of the magnetic field above which the superconductivity is destroyed. The type II superconductor has two critical magnetic fields and state of the superconductor between in these two fields known as vortex state (or Shubnikov phase). Such behaviour first experimentally discovered by Shubnikov *et al.* in 1937 [11]. To explain the Shubnikov phase, A. A. Abrikosov [12] used the Ginzburg-Landau theory [13] and proposed the concept of vortices. He showed that the Shubnikov phase is a state with vortices in a periodic fashion (triangular lattice). The idea of vertices accepted after the experimental confirmation by Hess *et al.* [14, 15]. In 1950, Fröhlich [16, 17] proposed a

theory of phonon mediated interaction in superconductivity. Since the vibrational frequency of lattice varies as $M^{1/2}$, this laid down the foundation of the isotopic effect in superconductivity. In the same year the isotopic effect was confirmed by Maxwell [18] and Reynolds *et al.* [19] and a relation between critical temperature T_c and isotopic mass M established as $T_c M^{1/2}$=constant. Among the several developed theoretical models there are two most important milestones in the field of conceptual understanding of superconductivity (i) phenomenological theory of superconductivity developed by Ginzburg and Landau known as Ginzburg-Landau theory (1950) [13] and (ii) microscopic theory of superconductivity developed by J. Bardeen, L. N. Cooper, and J. R. Schrieffer known as BCS theory (1957) [20].

Ginzburg and Landau (GL) Theory

Based on the Landau theory [21, 22] of second-order phase transition, Ginzburg and Landau (GL) proposed that the free energy of a superconductor near the superconducting transition can be expressed in terms of a complex order parameter. By minimizing the free energy, two equations pop-out which are known as GL equations and used to study the thermodynamic behaviour of superconductors [8]. The GL equations predict two characteristic lengths in a superconductor, namely; penetration depth (λ) which was initially introduced by the London brothers and coherence length (ξ). The ratio of these two parameters known as Ginzburg–Landau parameter $\kappa = \lambda/\xi$ and used to categorize the type of superconductors. For the limit, $0 < \kappa < 1/\sqrt{2}$ the superconductor falls under type I, and for $\kappa > 1/\sqrt{2}$ it falls under type II.

BCS (Bardeen–Cooper–Schrieffer) Theory

In 1957 J. Bardeen, L. N. Cooper, and J. R. Schrieffer formulated the first successful microscopic theory of superconductivity by introducing the concept of a phonon-mediated weak attractive electron-electron interaction that forms a bound pair of

electrons, known as Cooper pairs. [20]. The visualization of the Cooper pair formation involves electron-lattice-electron interaction. Surprisingly the electrons which obey the Fermi-Dirac statistics, after the formation of Cooper pairs behave like bosons. The BCS theory is based on the assumption that the phenomenon of superconductivity occurs when the attractive Cooper pair interaction dominates over the repulsive Coulombic force. Prior to the development BCS theory, L. N. Cooper earlier showed that due to the attractive interaction the electron-electron pair state can have energy less than that of the Fermi-energy of the material [23]. Though the first hint of the superconducting gap was observed by Corak *et al.* [24], but the BCS theory successfully explained the formation of the superconducting gap occurring due to electron-lattice-electron interaction [20].

There are several other important developments after the advent of BCS theory and much progress has been made in understanding the role of the electron-phonon interaction in the normal and superconducting state. Though the GL theory and BCS theory were developed separately but L. Gor'kov was able to derive GL theory from the BCS theory under some limits and related the Cooper pairs to the twice of the electronic charge which was appeared in the GL equations [25]. In 1958 P. W. Anderson used the random-phase approximation (RPA) in the theory of superconductivity and found that most of the elementary excitations in the superconducting state have the BCS type energy gap spectrum [26]. Further a new theoretical approach in superconductivity was carried out by N. N. Bogoliubov *et al.* [27, 28]. In 1958 Gor'kov [29] developed the Green's functions method which has been later applied to the superconductors by many authors [30–35]. Earlier, only weak electron-phonon coupling was considered, but Migdal [36] showed the possible strong electron-phonon interaction in normal metals. The concept of strong electron-phonon coupling extended to the superconducting state by Eliashberg [37] and Nambu [38] using Green's functions technique of Gor'kov [29]. In 1967 W. L. McMillian [39] applied the idea of strong-coupling theory to superconducting state and obtained the superconducting

transition temperature as a function of electron-phonon and electron-electron coupling constants which was further reanalyzed by Allen *et al.* [40]. Another significant development took place when B. D. Josephson [41] theoretically predicted an entirely new kind of behaviour of superconductor-the tunneling of current through an insulating barrier between two superconductors which later experimentally verified by P. W. Anderson and John Rowell [42], now known as the Josephson effect. Several new superconductors were discovered with increasing critical temperature such as Nb_3Sn (T_c=18 K) [43] in 1954, $Li_{1+x}Ti_{2-x}O_4$ (T_c=7 to 13 K) [44] in 1973, $BaPb_{1-x}Bi_xO_3$ (T_c=13 K) in 1975 [45], Nb_3Ge (T_c=23 K) [46] in 1978 and so on. Despite of much progress in the theory as well as in the experiments, many believed that the field was faded out until the high-temperature superconductor (HTS) is discovered [47].

1.3 The High-Temperature Superconductivity

Experimental Development

In 1986 G. Bednorz and K. A. Müller discovered a new class of superconductors heralding the possibility of high-temperature superconductivity (HTSC) in $La_{2-x}Sr_xCuO_4$(LaBaCuO) with transition temperature to 30 K [47]. The research in superconductivity opened new windows after this startling discovery and soon many HTS discovered. In the subsequent year the superconductivity in $YBa_2Cu_3O_{7-\delta}$ discovered with transition temperature 93 K [48], well above the boiling point of liquid nitrogen (77 K). This was a very significant development from the experimental point of view because it reduced the cost of the refrigeration system as well as it attracted the technological applications. Further the superconductivity discovered in BiSrCaCuO systems and it is found that the oxide $BiSrCaCu_2O_x$ has T_c about 105 K [49]. In the same group Bismuth can be replaced with Mercury and resulting compound $HgBa_2Ca_2Cu_3O_x$ has highest known T_c (∼135 K) [50] at normal pressure condition. The same compound $HgBa_2Ca_2Cu_3O_x$ exhibited superconductivity up to

150 K under high pressure (150 kbar) [51]. In all these HTS, CuO_2 being common component, therefore they are referred to as the cuprate HTS. In 2002 non-copper-oxide bulk superconductor MgB_2 was discovered by Akimitsu *et al.* with T_c=39 K [52]. In 2008, a new class of superconductor was discovered based on the iron compound by Hosono *et al.* [53] in $La[O_{1-x}F_x]FeAs$ with T_c=26 K. Further development took place in the field of iron-based superconductivity with increasing T_c up to 40 K [54–57]. The highest T_c in bulk iron-based superconductors reported is 55 K in $SmO_{1-x}F_xF_eAs$ [57].

Models of High-Temperature Superconductivity

Condensed matter theorists developed a rich heritage [58–66] to understand the mechanism of HTSC but the field is still lacking of mature understanding and thus the success is still awaited. Just after the discovery of superconductivity in $La_{2-x}Sr_xCuO_4$, in 1987 P. W. Anderson proposed resonating-valence-bond (RVB) theory [67] with the conclusion that the phenomenon of HTSC is predominantly electronic and magnetic. The idea of RVB further extended by P. W. Anderson *et al.* to study the phase transition phenomenon in La_2CuO_4 based compound [68]. Later P. W. Anderson and G. Baskaran developed the gauge theory of HTS for strongly correlated Fermi systems using RVB theory [69]. Emery [70] attempted to understand the mechanism of HTSC and identified that the charge carriers are holes and located in the same copper-oxide plane and it increases with increasing number of copper-oxide layers [71, 72]. An effective Hamiltonian was derived for high-T_c copper-oxide superconductor by Zhang *et al.* [73]. Varma *et al.* [74] worked out that the exchange of antiferromagnetic spin fluctuations mechanism is responsible for the HTSC in heavy fermion systems and the work of Moriya *et al.* [75–77] is worth mentioning in this regard. There are many properties of HTS found which are entirely different from the conventional superconductors and their explanation is still challenging problem. The experiments carried by D. A. Wollman *et al.* [78] using two superconducting-normal-superconducting (S-N-S) arrangements together,

reveals a new type of pairing symmetry in cuprate superconductors called $d_{x^2-y^2}$ wave pairing which was confirmed via flux quantization in a tri-crystal YBCO junction by Tsuei *et al.* [79]. It is now general agreement that a gap is formed in the close vicinity of Fermi level, but unlike the simple symmetric s-wave gap which is found in conventional superconductors, the gap is due to $d_{x^2-y^2}$ wave in HTS. The first $d_{x^2-y^2}$ wave pairing symmetry was theoretically predicted by D. J. Scalapino *et al.* [80] and later on by P. Monthoux *et al.* [81]. Masahiko *et al.* [82] investigated the mean-field theory of the Hubbard model and found the $d_{x^2-y^2}$ wave possibility in high T_c superconductors. Using the Heisenberg model G. Kotliar *et al.* [83] formulated an auxiliary-boson mean-field theory and observed the $d_{x^2-y^2}$ wave superconductivity and further investigation done by Zhang *et al.* [84] show the superconductivity with an order parameter which has $d_{x^2-y^2}$ wave symmetry. Structure of single vortex and vortex lattice in a superconductor with $d_{x^2-y^2}$ wave pairing symmetry has been analyzed by Ting *et al.* [85]. The superconducting properties of cuprates strongly depend on the doping level of impurity [86–98]. Overdoped cuprate behaves like conventional metal with Fermi surface, but underdoped cuprates act like superconductor and show disconnected Fermi arc [99]. The ratio of the superconducting gap (SG) to the critical temperature ($2\Delta/k_BT_c$) for conventional superconductor was found below 3.5 which is well taken care of by BCS theory, but in HTS this gap ratio was seen between 5 and 8 [100–102] and also showed a strong dependence on doping [93–98, 103]. The SG in HTS was found highly anisotropic [103–106] as well as the different magnitude of gap observed in nodal and antinodal direction [107]. Along with electron-phonon interaction [108–112], the anharmonicity also plays role in superconductivity [113–118]. In addition to SG, the HTS also exhibit pseudogap - an energy gap much larger than SG and persist above the T_c [119]. The experimental observations [120–122] on antiferromagnetic (AF) phase along with superconductivity was a surprising phenomenon since the magnetism tends to destroy the superconductivity as Abrikosov and Gor'kov showed that magnetic impurities disrupt superconductivity and suppress T_c. [123]. The co-existence of AF phase with superconductivity suggest that the pairing symmetry also influences by

AF spin fluctuations, though such scenario observed only at low temperature in a lightly doped superconductors, e.g., $La_{2-x}Sr_xCuO_4$ [120–122, 124].

Owing to BCS theory, the idea of the attractive potential between two electrons, Fujita *et al.* [125] further used it to the high-T_c cuprate and showed the formation of d-wave Cooper-pair (pairon) due to the longitudinal optical-phonon exchange in the copper-oxide plane. It is also demonstrated that the phonon mediated attraction and hence the pairon formation in cuprate superconductors is direction dependent leading to anisotropic SG formation [125]. Using GL theory Fujita and Godoy [126, 127] observed that below T_c the GL wave function yields the condensed pairon density and is proportional to the pairon energy gap. William *et al.* [128, 129] recently revealed that the holes in the cuprate superconductors coupled to its local AF environment and form the pairon. The understanding of pairon formation and its implication to HTSC is crucial and several efforts have been made in this regard [130–134]. The proposed mechanism of pairon formation in cuprates is shown in Fig. (1.1).

In transport problems of cuprate HTS, it is noted that the in-plane electronic transport is primarily affected by phonons [135] and lattice thermal conductivity depends on phonon velocity (sound velocity) along with various other parameters [136–142]. In 2008 Alexandrov [143] showed the role of anisotropic sound velocity in unconventional pairing in cuprate HTS. These results show that phonon is quite an essential component in the mechanism of HTSC and need further investigation in these complex structured HTS [86, 144, 145].

1.4 Motivation and State of the Art

In searching the fundamental principle behind the mysterious mechanism of HTSC extensive efforts has been made in the last 20 years yet an acceptable theory is still

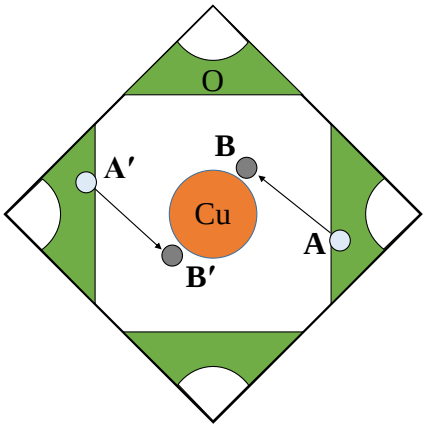

FIGURE 1.1: The two dimensional Fermi surface of a cuprate model has a small circle (electron) at the center and and four small pockets (holes) at the Brillouin corners. In the proposed mechanism of pairon formation, an exchange of a phonon can create the - pairon at $(\mathrm{B}, \mathrm{B}')$ and + pairon at $(\mathrm{A}, \mathrm{A}')$.

to come. The SG properties, e.g., its high value, anisotropy, and doping dependence remained a puzzle for a long time. The concrete role of the phonons in the superconducting mechanism of cuprate HTS is yet to be explored. Though there are theoretical achievements as specific scenario, but it's hard to find a well-developed model that successfully explains the strange behaviors with sound justification which motivate us to reinvestigate these problems in depth with a hope to add a further step to resolve the mystery of HTSC.

The HTS cuprates have a very complex structure (Figs. (1.2, 1.3)) that adds various difficulties for theoretical studies. In the present study two model cuprate HTS $YBa_2Cu_3O_{7-\delta}$ and $La_{2-x}Sr_xCuO_4$ have been taken for the study. Both the HTS have perovskite structure. In the crystal $YBa_2Cu_3O_{7-\delta}$ the oxidation states of Y, Ba, and O are +3, +2 and -2, respectively. The oxidation states of Cu are +3 and +2 due to different layers in the system, namely; CuO_2 and CuO. Similarly in superconductor $La_{2-x}Sr_xCuO_4$, the oxidation states of La (Sr), Cu and O are +3,

+2 and -2, respectively. The stability of a crystal depends on the equity of repulsive and attractive interaction. Among several interaction potentials, namely; Morse potential, Lennard-Jones potential, Buckingham potential, Born Mayer Potential, Born-Mayer-Huggins potential etc., the most appropriate potential for cuprates HTS appears to be Born-Mayer-Huggins potential ($V_{ij}(r) = a_{ij}e^{-b_{ij}r} + \frac{q_i q_j}{r}$) since it contains both, the long-range Coulombic interactions (repulsive for like changes, attractive for unlike charges) and short-range repulsive interactions, where i, j labels the ions of charges q_i and q_j separated by the distance $r_{ij} \equiv r$; a_{ij} and b_{ij} are the range and softening parameters, respectively. In the present work, the modified Born-Mayer-Huggins potential (MBMHP) has been used. The Green's functions method has been proven its importance in quantum field theory and widely used to explore the properties of HTS. The double-time temperature dependent Green's functions method has been taken as the state of the art - methodology. A generalized HTS (non-BCS) Hamiltonian used that take care contributions of electrons, phonons, electron-phonon interactions, anharmonicity, and defects. The electron Green's functions enable to obtain the electron density of states (EDOS) which further utilized to derive the SG equations following the BCS formalism. The phonon Green's functions permit to obtained the renormalized electron-phonon dispersion which is used to study the SG properties of $La_{2-x}Sr_xCuO_4$ and $YBa_2Cu_3O_{7-\delta}$. Further, the renormalized phonon dispersion enables to develop the theory of renormalized phonon group velocity for HTS.

1.5 Brief Outlay of All Chapters

This work reports the SG properties, pairing symmetry and theory of renormalized phonon group velocity for HTS whose organization consists of six chapters.

Chapter I contains a brief history of the origin of conventional and high temperature superconductivity. The systematic theoretical and experimental development

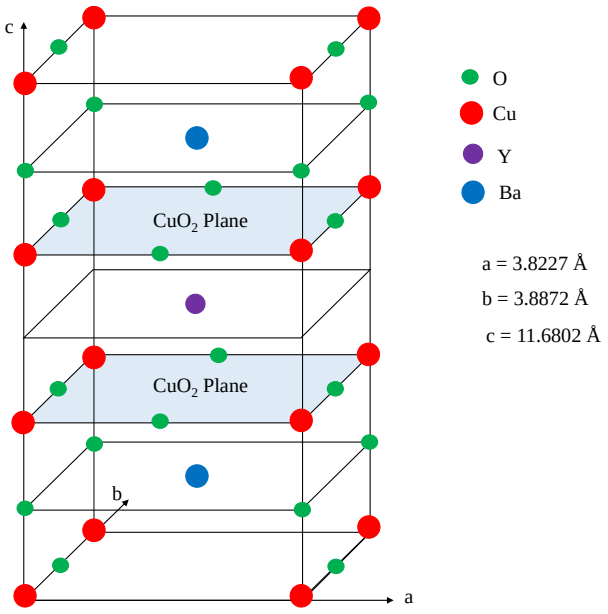

FIGURE 1.2: Crystal structure of $YBa_2Cu_3O_{7-\delta}$.

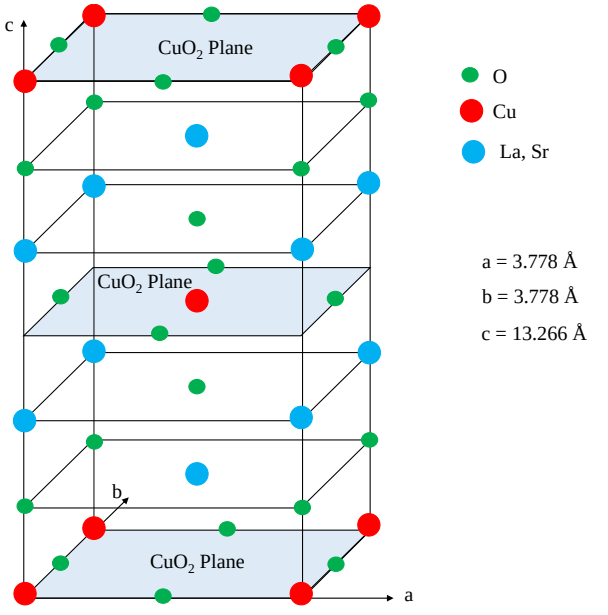

FIGURE 1.3: Crystal structure of $La_{2-x}Sr_xCuO_4$.

of conventional superconductors is presented with a concise discussion of GL and BCS theory along with other few models. A summary of HTSC given with various significant achievement in the experiment as well as in theory. In the end, a short note is provided about the motive of the present work and state of the art - "methodology".

Chapter II is devoted to discuss the methodology. The development of phonon and electron Green's functions is given with the help of quantum dynamical many-body problem. Further, the electron density of states is obtained using electron Green's functions in the Lehmann's representation and ended with the discussion and application of MBMHP.

Chapter III is devoted to study the SG properties. The SG equations are derived and successfully analyzed for representative HTS $YBa_2Cu_3O_{7-\delta}$. The effect of AF spin fluctuations on the SG worked out for $La_{2-x}Sr_xCuO_4$. The renormalized electron-phonon dispersion plot obtained for $La_{2-x}Sr_xCuO_4$ and $YBa_2Cu_3O_{7-\delta}$ which is further used to study the doping dependence of SG. The nodal and antinodal gap also studied for $La_{2-x}Sr_xCuO_4$ followed by the derivation of an expression of pairing potential and numerical analysis for $YBa_2Cu_3O_{7-\delta}$.

Chapter IV is dedicated to studying the anisotropy of SG and pairing symmetry. Using the renormalized electron-phonon dispersion plot anisotropy of SG and pairing symmetry is reported for $La_{2-x}Sr_xCuO_4$ and $YBa_2Cu_3O_{7-\delta}$. Effect of doping and AF spin fluctuations on pairing symmetry is also discussed.

Chapter V furnishes the development of renormalized phonon group velocity (RPGV) using the renormalized phonon dispersion. An expression of RPGV is derived and obtained result applied to $La_{2-x}Sr_xCuO_4$ system. The variation of RPGV with phonon frequency and doping is reported.

Chapter VI summaries all the results and conclusions obtained in this dissertation and at the end, a prototype of future work has been listed.

Chapter 2

Quantum Dynamics of Many-Particle System

"God used beautiful mathematics in creating the world."

- - - Paul Dirac

2.1 Introduction

The theoretical development of the condensed matter physics is devoted to establish the method to calculate the measurable physical quantities of an interacting system. The Green's functions [146] method has emerged as a powerful tool that deals with the problem of interacting particles. J. Schwinger [147, 148] developed an important concept of propagators or Greens's functions using quantum field theory which becomes very convenient to interpret the interaction problem of the particles with a quantized field, e.g., electron-phonon interaction or interaction problem of quantized fields, e.g., phonon-phonon interactions. In 1954 H. Lehmann used Green's functions to derive spectral representation that are useful in evaluating the energy spectrum of crystalline solids [149]. Matsubara defined Green's functions assuming time as complex quantity generally known as *'imaginary time Green's function'*. One of the most useful form of Green's functions was introduced by Bogolyubov and

Tyablikov in statistical physics in the form of double-time thermodynamic retarded and advanced Green's functions and found extremely useful in investigating quasi-particle spectra of the many-body system and superconductors [150–152]. Gorkov [29] introduced the pair correlation Green's functions in the context of Cooper pair formalism of superconductivity meanwhile, the same problem has been taken care by Eliashberg [37] via casual Green's functions and by Zubarev [153] vai retarded and advanced Green's functions. Using the Gorkov [29] pair correlation Green's functions, Nambu [38] has studied the strong electron-phonon coupling in the superconducting state. Freeman Dyson [154] introduced a very precise and accurate method to get the 'one-particle Green's functions' by summing up the Feynman diagrams following the perturbative approach. The Green's functions can also be defined as one-particle Green's functions, two-particle Green's functions or many-particle Green's functions and it describes the prorogation of the disturbance of a many-particle equilibrium system in which one, two or many particles are added or removed, respectively. Green's functions formalism is very important in the study of the many-body problem notably in the theoretical investigations in conventional and HTSC [152, 155–158] where the electron-phonon interaction plays an important role [108–112].

This chapter includes the development of electron and phonon Green's functions with the help of generalized (non-BCS) Hamiltonian followed by Dyson's equation. A short note is presented for the different type of Green's functions and a discussion of interacting potential is given in the end.

2.2 Double-Time Temperature Dependent Green's Functions

The external forces to an equilibrium system create a disturbance in the system, known as the 'response' and being examined by the response function, e.g., the

magnetic susceptibility and electrical conductivity is a response of applied magnetic and electric field, respectively. A smooth perturbation (applying a small external field an equilibrium system) corresponds to the linear response and well described by retarded Green's functions [159].

2.2.1 Retarded, Advanced, Causal and Matsubara Green's Functions

Green's functions are the thermodynamic expectation value of a product of operators evaluated at different times t and t' and depends only through the time difference $(t - t')$ [153, 157, 160]. Green's functions can be defined in the form of retarded $(G_r(t, t'))$, advanced $(G_a(t, t'))$, causal $(G_c(t, t'))$, and Matsubara $(G_m(\tau, \tau'), \tau = it)$ Green's functions as follows:

$$\begin{aligned}
G_r(t,t') &= -i\theta(t-t') < [A(t), B(t')]_\eta > \\
&= -i\theta(t-t')\{< A(t), B(t') - \eta < B(t'), A(t) >\} \qquad (2.1)\\
G_a(t,t') &= i\theta(t'-t) < [A(t), B(t')]_\eta > \\
&= -i\theta(t'-t)\{< A(t), B(t') - \eta < B(t'), A(t) >\} \qquad (2.2)\\
G_c(t,t') &= -i < TA(t), B(t') > \\
&= -i\theta(t-t') < A(t), B(t') > +i\eta\theta(t'-t) < B(t'), A(t) > \qquad (2.3)\\
G_m(\tau,\tau') &= - < TA(\tau), B(\tau') > \\
&= -\theta(\tau-\tau') < A(\tau), B(\tau') > +\eta\theta(\tau'-\tau) < B(\tau'), A(\tau) > \qquad (2.4)
\end{aligned}$$

where $\theta(t - t')$ is the Heaviside unit step function with the property

$$\theta(t-t') = \begin{cases} 1 & \text{for } t > t' \\ 0 & \text{for } t < t' \end{cases} \qquad (2.5)$$

and T is a time-ordering operator which arrange the operators in chronological order with the earliest time appearing on the right and latest on right, known as Wick's theorem and defined as:

$$TA(t)B(t') = \theta(t-t')A(t)B(t') + \eta\theta(t'-t)B(t')A(t) \tag{2.6}$$

where $\eta = \pm 1$, for Bosons the η take plus sign and for Fermions it takes the minus sign.

2.2.2 Time Correlation Functions and Spectral Representation

The average over the statistical ensemble of the product of the operators $A(t)$ and $B(t')$ in the Heisenberg representation known as the time correlation function and can be written as:

$$F_{AB}(t,t') =< A(t)B(t') >; \;\; F_{BA}(t,t') =< B(t')A(t) > \tag{2.7}$$

Which can be expressed in terms of spectral representation $J(\omega)$ as [31, 153, 161]:

$$F_{AB}(t-t') = \int_{-\infty}^{\infty} e^{\beta\hbar\omega} J(\omega) e^{-i\omega(t-t')} d\omega \tag{2.8}$$

$$F_{BA}(t-t') = \int_{-\infty}^{\infty} e^{-i\omega(t-t')} J(\omega) d\omega \tag{2.9}$$

and is related to the one-particle Green's functions by the relation [32].

$$J(\omega) = \lim_{\epsilon \to 0} \frac{-2}{[exp(\beta\hbar\omega) - 1]} Im\ G[\omega + i\epsilon] \tag{2.10}$$

2.3 The Hamiltonian

The Hamiltonian (H) of a system is written as a sum of kinetic energy (T) and total potential energy (V) [32, 162–167]: $H = T + V$ where

$$T = \frac{1}{2}M\sum_{ll'}\sum_{i}(\dot{u}_{x_i}^{ll'})^2 \tag{2.11}$$

$$V = \sum_{ll'}\sum_{x_1,x_2}\left(\frac{1}{2!}\right)\phi^{(2)}_{x_1,x_2}(ll')u^{ll'}_{x_1}u^{ll'}_{x_2} + \sum_{ll'}\sum_{x_1,x_2,x_3}\left(\frac{1}{3!}\right)\phi^{(3)}_{x_1,x_2,x_3}(ll')u^{ll'}_{x_1}u^{ll'}_{x_2}u^{ll'}_{x_3} + \sum_{ll'}\sum_{x_1,x_2,x_3,x_4}\left(\frac{1}{4!}\right)\phi^{(4)}_{x_1,x_2,x_3,x_4}(ll')u^{ll'}_{x_1}u^{ll'}_{x_2}u^{ll'}_{x_3}u^{ll'}_{x_4} + \cdots \tag{2.12}$$

where

$$\phi^{(n)}_{x_1,x_2,\cdots x_n}(ll') = \left.\frac{\partial V^{(n)}}{\partial x_1\partial x_2\cdots\partial x_n}\right|_{r=r_0} \tag{2.13}$$

are the atomic force constant of various order n. In writing the total potential energy, the potential energy term (V_0) corresponding to the equilibrium configuration is left out and consequently the first order atomic force constant ($\phi^{(1)}_{x_1}(ll') = \frac{\partial V}{\partial x_1}$) at equilibrium condition ($r = r_0$) must vanish i.e., $\phi^{(1)}_{x_1}(ll') = 0$. In the above equations, $u^{ll'}_{x_i} = u^{l}_{x_i} - u^{l'}_{x_i}$, $u^{l}_{x_i}$ is the atomic displacement of the x^{th} coordinate of the atom at i^{th} site from the equilibrium position can be expressed in terms of phonon creation (a^*_{kj}) and annihilation (a_{kj}) operators as:

$$u^{l}_{x_i} = \left(\frac{\hbar}{2MN}\right)^{1/2}\sum_{kj}\frac{e_x(k_j)}{(\omega_{k_j})^{1/2}}(a_{kj} + a^*_{-kj})e^{2\pi ik.R_i} \tag{2.14}$$

where M is the atomic mass, N is the total number of the atoms in the crystal, $e_x(k_j)$ is the x^{th} component of the eigenvector of dynamical matrix of the lattice with j^{th} branch index of the frequency spectrum, ω_{k_j} is the normal mode frequency with wave vector k and polarization index j.

An exact eigenstate of the crystal Hamiltonian can be established from the harmonic (quadratic) approximation in Eq. (2.12) which capably describes the infinitely long-lasting, non-interacting normal modes of vibration. Although the harmonic approximation successfully explains the dispersion relations, frequency spectra, some thermal and elastic properties with some drawbacks of fitting parameters, but unfortunately many physical properties of the crystals, for example, the thermal expansion, thermal conductivity, temperature dependence of infrared absorption and Raman scattering, etc. could not be explained and this enforces the inclusion of the higher order namely; cubic, quartic, etc. terms to investigate these features of a crystals.

In a real situation, it is hard to find a system with perfection. The presence of impurities like isotopic point impurities, vacancies, faults, dislocations, etc. changes the structure of the lattice and consequently the associated dynamical properties and energy scenario of the crystal changed [168, 169]. In the context of quantum mechanics, the Hamiltonian is written in the form of field operator. The model generalized Hamiltonian (H) which have contribution due to electrons (H_e), phonons (H_p), electron-phonon interactions (H_{ep}), anharmonicities (H_A) and defects (H_D) can be conveniently expressed as:

$$H = H_e + H_p + H_{ep} + H_A + H_D \tag{2.15}$$

where

$$H_e = \sum_q \hbar(\omega_{q\uparrow} b^*_{q\uparrow} b_{q\uparrow} + \omega_{q\downarrow} b^*_{q\downarrow} b_{q\downarrow} + \omega_{-q\uparrow} b^*_{-q\uparrow} b_{-q\uparrow} + \omega_{-q\downarrow} b^*_{-q\downarrow} b_{-q\downarrow}) \quad (2.16a)$$

$$H_p = \sum_k \frac{\hbar\omega_k}{4}(A^*_k A_k + B^*_k B_k) \quad (2.16b)$$

$$H_{ep} = \sum_{qk}(g_k b^*_{Q\uparrow} b_{q\uparrow} + g^*_k b^*_{q\uparrow} b_{Q\uparrow} + g_k b^*_{Q\downarrow} b_{q\downarrow} + g^*_k b^*_{q\downarrow} b_{Q\downarrow}) B_k \quad (2.16c)$$

$$H_A = \sum_{s\geq 3} \sum_{k_1 \cdots k_s} \hbar V_s(k_1, k_2 \cdots k_s) A_{k_1} A_{k_2} \cdots A_{k_s} \quad (2.16d)$$

$$H_D = \sum_{k_1,k_2} \hbar[-C(k_1,k_2) B_{k_1} B_{k_2} + D(k_1,k_2) A_{k_1} A_{k_2}] \quad (2.16e)$$

The anharmonicity impacts the electron-phonon interactions [115] and the well-known fact that doping has a decisive role in HTSC, the corresponding Hamiltonian H_A and H_D have been scrutinized, respectively. The notation $A_k = a_k + a^*_{-k}$ represents the phonon field operator and $B_k = a_k - a^*_{-k} = -B^*_{-k}$ represents phonon momentum operator with phonon annihilation (a_k) and creation (a^*_{-k}) operators where $\mathbf{k}$ is phonon wave vector. The operator A_k and B_k satisfy the commutation relations as $[B_k, A_{k'}] = 2\delta_{k-k'}$ and $[A_k, A_{k'}] = [B_k, B_{k'}] = 0$. Also, $b_k(b^*_{-k}) \equiv [b_{q\sigma}(t)(b^*_{q'\sigma'})(t')]$ are electron annihilation (creation) operators with wave vector $\mathbf{q}$, $\mathbf{Q} = \mathbf{k} + \mathbf{q}$ for electrons with spin $\sigma(\uparrow\downarrow)$. The coefficients $V_s(k_1, k_2 \cdots k_s)$ are the Fourier transform of s^{th} order force constants. For the brevity, the index kj is denoted by k, where j is the the polarization branch of phonon wave vector k. The other terms in Eq. (2.16) are given as:

$$V_3(k_1,k_2,k_3) = \frac{1}{3!}\left(\frac{\hbar}{8N}\right)^{1/2} \frac{\Delta(k_1,k_2,k_3)\phi_3(k_1,k_2,k_3)}{(\omega_{k_1}\omega_{k_2}\omega_{k_3})^{1/2}} \quad (2.17)$$

$$\phi_3(k_1,k_2,k_3) = \frac{1}{M^{3/2}} {\sum_{l,l'}}' \sum_{x_1,x_2,x_3} \phi^{(3)}_{x_1,x_2,x_3}(l,l') e(k_1) e(k_2) e(k_3) \times \mathrm{e}^{2\pi \mathrm{i}(k_1,k_2,k_3)\cdot r_0(l,l')}$$

and

$$V_4(k_1,k_2,k_3,k_4) = \frac{1}{4!}\left(\frac{\hbar}{4N}\right)\frac{\Delta(k_1,k_2,k_3,k_4)\phi_4(k_1,k_2,k_3,k_4)}{(\omega_{k_1}\omega_{k_2}\omega_{k_3}\omega_{k_4})^{1/2}} \tag{2.18}$$

$$\phi_4(k_1,k_2,k_3,k_4) = \frac{1}{M^2}\sum_{l,l'}{}' \sum_{x_1,x_2,x_3,x_4} \phi^{(4)}_{x_1,x_2,x_3,x_4}(l,l')e(k_1)e(k_2)e(k_3)e(k_4) \times \mathrm{e}^{2\pi \mathrm{i}(k_1,k_2,k_3,k_4)\cdot r_0(l,l')}$$

where,

$$\Delta k = \begin{cases} 1 & \text{if } k = 0 \text{ or a reciprocal lattice vector,} \\ 0 & \text{otherwise.} \end{cases} \tag{2.19}$$

In the above equations, $\phi^{(s)}_{x_1,x_2,\ldots x_s}(l,l')$ are the expansion coefficients [170, 171] and the prime over summation show the exclusion of the terms with $l = l'$ from the expressions. The parameters $C(k_1,k_2)$ and $D(k_1,k_2)$ are mass change parameter and force constant change parameter, respectively and given as:

$$C(k_1,k_2) = \left(\frac{M_0}{4N\mu}\right)(\omega_{k_1}\omega_{k_2})^{1/2}[e(k_1).e(k_2)]\left[\sum_{l}^{N} c e^{\mathrm{i}(k_1+k_2).R_l} - \sum_{\mathrm{i}}^{n} e^{\mathrm{i}(k_1+k_2).R_{\mathrm{i}}}\right] \tag{2.20}$$

$$D(k_1,k_2) = (4N)^{-1}(\omega_{k_1}\omega_{k_2})^{-1/2}\sum_{l,l'}\left(\frac{\phi_{l,l'}}{M_0}\right)[e(k_1).e(k_2)]e^{\mathrm{i}(k_1\cdot R_l + k_2\cdot R'_l)} \tag{2.21}$$

where $\mu = MM'/(M'-M)$ and $c = n/N$. Here $M_0^{-1}(= c/M' + (1-c)/M)$ is the effective atomic mass, the change in the harmonic force constant due to defect is given by $\phi_{l,l'}$, ω_k is the angular frequency of the normal mode of the wave vector k, $e(k)$ is the polarization vector and equilibrium position of the l^{th} atom in the crystal is given by R_l. In the model study, crystal consisting of N atom hypothesized such that impurities of equal mass M' are randomly scattered at n lattice sites and rest sites $(N-n)$ are occupied by atoms of mass M. Since it is well known that physical

properties change dramatically on impurity concentration (doping) therefore n taken as variable to regulate the doping.

2.4 Phonon Green's Functions

To achieve the phonon energy spectrum, consider the double-time temperature dependent retarded one phonon Green's functions [153]

$$\begin{aligned} G_{k,k'}(t-t') &= \ll A_k(t); A^*_{k'}(t') \gg \\ &= -\mathrm{i}\theta(t-t')\langle [A_k(t), A^*_{k'}(t')] \end{aligned} \tag{2.22}$$

Using the quantum dynamical equation of motion approach $i\hbar\frac{dA_k(t)}{dt} = [A_k(t), H]$ via Hamiltonian (2.15) one can obtain:

$$i\hbar\frac{\partial G_{k,k'}(t-t')}{\partial t} = \hbar\delta(t-t')\langle [A_k(t), A^*_{k'}(t')]\rangle - i\theta(t-t')\langle [i\hbar\frac{\partial A_k(t)}{\partial t}, A^*_{k'}(t')]\rangle \tag{2.23}$$

Taking differentiation of Eq. (2.23) with respect to t once again and following the Fourier transformation one can have

$$(\omega^2 - \omega_k^2)G_{k,k'}(\omega) = \frac{\omega_k}{\pi}\left(\eta_{k,k'} + \ll F_k(t); A^*_{k'}(t') \gg\right) \tag{2.24}$$

where

$$\eta_{k,k'} = \delta_{k,k'} + 4\omega_k^{-1}\sum_{k_1} C(k_1, -k)\delta_{k_1,k'} \tag{2.25}$$

A hierarchy of higher order Green's functions appears in the second term of Eq. (2.24). To simplify it further we write the equation of motion with respect to t' for the Green's functions $\ll F_k(t); A^*_{k'}(t') \gg$ and using the resulting expression in Eq. (2.24) the equation of motion for $G_{k,k'}$ can be worked out in terms of Dyson's

equation as:

$$G_{k,k'}(\omega) = G^0_k(\omega)\delta_{k,k'} + G^0_k(\omega)\tilde{P}(k,k',\omega)G^0_{k'}(\omega) \quad (2.26)$$

$$= G^0_k(\omega)\delta_{k,k'} + G^0_k(\omega)\pi(k,k',\omega)G_{k'}(\omega) \quad (2.27)$$

Here $G^0_k(\omega) = \omega_k/\pi(\omega^2 - \omega_k^2)$, $\pi(k,k',\omega)$ and $\tilde{P}(k,k',\omega)$ are the unperturbed Green's functions, self-energy function and response function, respectively and are associated as:

$$\pi(k,k',\omega) = \frac{\tilde{P}(k,k',\omega)}{[1 + G^0_k(\omega)\tilde{P}(k,k',\omega)]} \quad (2.28)$$

We can expend the denominator of Eq. (2.28) in the form of power series if frequency is far from zeroes. In the first order approximation $\pi(k,k',\omega) \cong \tilde{P}(k,k',\omega)$ as this term gives the maximum contribution and the contribution from the rest term is negligibly small. This leads to the new form of the Green's functions as [170, 172]

$$G_{k,k'}(\omega) = \frac{\omega_k \eta_{k,k'}}{\pi[\omega^2 - \tilde{\omega}_k^2 - 2\omega_k \tilde{P}(k,k',\omega)]} \quad (2.29)$$

In order to carefully investigate the response function

$$\tilde{P}(k,k',\omega) = \frac{1}{2\pi} \ll F_k(t); F^*_{k'}(t') \gg_\omega \quad (2.30)$$

we write

$$F_k(t) = F^{(1)}_k(t) + F^{(2)}_k(t) + F^{(3)}_k(t) + F^{(4)}_k(t) + F^{(5)}_k(t) \quad (2.31)$$

where

$$F_k^{(1)}(t) = 4\pi\Bigg[\sum_{k_1} D(k_1,-k) + \sum_{k_1} C(k_1,-k) + 4\omega_k^{-1}\sum_{k_1} C(k_1,-k) \times D(k_1,-k_1)\Bigg]A_{k_1} \tag{2.32}$$

$$F_k^{(2)}(t) = 6\pi\Bigg[\sum_{k_1,k_2} V_3(k_1,k_2,-k) + 4\omega_k^{-1}\sum_{k_1} C(k_1,-k) \times \sum_{k_1,k_2} V_3(k_1,k_2,-k_1)\Bigg]A_{k_1}A_{k_2} \tag{2.33}$$

$$F_k^{(3)}(t) = 8\pi\Bigg[\sum_{k_1,k_2,k_3} V_4(k_1,k_2,k_3,-k) + 4\omega_k^{-1}\sum_{k_1} C(k_1,-k) \times \sum_{k_1,k_2,k_3} V_4(k_1,k_2,k_3,-k_1)\Bigg]A_{k_1}A_{k_2}A_{k_3} \tag{2.34}$$

$$\begin{aligned} F_k^{(4)}(t) = -2\pi\omega_k^{-1}\sum_q \Big[& g_k(3\omega_{q\uparrow} + \omega^c_{q\uparrow} + 3\omega_{Q\uparrow} + \omega^c_{Q\uparrow})b^*_{Q\uparrow}b_{q\uparrow} \\ & + g_k^*(3\omega_{Q\uparrow} + \omega^c_{Q\uparrow} + 3\omega_{q\uparrow} + \omega^c_{q\uparrow})b^*_{q\uparrow}b_{Q\uparrow} \\ & + g_k(3\omega_{q\downarrow} + \omega^c_{q\downarrow} + 3\omega_{Q\downarrow} + \omega^c_{Q\downarrow})b^*_{Q\downarrow}b_{q\downarrow} \\ & + g_k^*(4\omega_{q\downarrow} + \omega^c_{q\downarrow} + 2\omega_{Q\downarrow} + \omega^c_{Q\downarrow})b^*_{q\downarrow}b_{Q\downarrow}\Big] \end{aligned} \tag{2.35}$$

$$\begin{aligned} F_k^{(5)}(t) = -2\pi\omega_k^{-1}B_k\sum_{k,q}\Big[& 4|g_k|^2(b^*_{Q\uparrow}b_{Q\uparrow} + b^*_{q\uparrow}b_{q\uparrow} + b^*_{Q\downarrow}b_{Q\downarrow} + b^*_{q\downarrow}b_{q\downarrow}) \\ & + |g_k|^2(2b^*_{Q\uparrow}b_{q\uparrow}\delta_{q\uparrow,Q\downarrow} + 2b^*_{Q\downarrow}b_{q\uparrow}\delta_{Q\uparrow,q\downarrow} + 2b^*_{Q\uparrow}b_{Q\downarrow}\delta_{q\uparrow,q\downarrow} \\ & + 2b^*_{q\downarrow}b_{q\uparrow}\delta_{Q\uparrow,Q\downarrow} + 2b^*_{q\uparrow}b_{q\downarrow}\delta_{Q\uparrow,Q\downarrow} + 2b^*_{Q\downarrow}b_{Q\uparrow}\delta_{q\uparrow,q\downarrow} \\ & + 2b^*_{q\uparrow}b_{Q\downarrow}\delta_{Q\uparrow,q\downarrow} + 2b^*_{q\downarrow}b_{Q\uparrow}\delta_{q\uparrow,Q\downarrow})\Big] \end{aligned} \tag{2.36}$$

and

$$F^*_{k'}(t') = F^{*(1)}_{k'}(t') + F^{*(2)}_{k'}(t') + F^{*(3)}_{k'}(t') + F^{*(4)}_{k'}(t') + F^{*(5)}_{k'}(t') \tag{2.37}$$

with

$$F^{*(1)}_{k'}(t') = 4\pi\Bigg[\sum_{k'_1} D(k'_1,-k') + \sum_{k'_1} C(k'_1,-k') + 4\omega_k^{-1}\sum_{k'_1} C(k'_1,-k') \times D(k'_1,-k'_1)\Bigg]A_{k'_1} \tag{2.38}$$

$$F^{*(2)}_{k'}(t') = 6\pi\Bigg[\sum_{k'_1,k'_2} V_3(k'_1,k'_2,-k') + 4\omega_{k'}^{-1}\sum_{k'_1} C(k'_1,-k') \times \sum_{k'_1,k'_2} V_3(k'_1,k'_2,-k'_1)\Bigg]A_{k'_1}A_{k'_2} \tag{2.39}$$

$$F^{*(3)}_{k'}(t') = 8\pi\Bigg[\sum_{k'_1,k'_2,k'_3} V_4(k'_1,k'_2,k'_3,-k') + 4\omega_{k'}^{-1}\sum_{k'_1} C(k'_1,-k') \times \sum_{k'_1,k'_2,k'_3} V_4(k'_1,k'_2,k'_3,-k'_1)\Bigg]A_{k'_1}A_{k'_2}A_{k'_3} \tag{2.40}$$

$$\begin{aligned} F^{*(4)}_{k'}(t') = -2\pi\omega_{k'}^{-1}\sum_{q'}\Big[& g_{k'}(3\omega_{q'\uparrow}+\omega^c_{q'\uparrow}+3\omega_{Q'\uparrow}+\omega^c_{Q'\uparrow})b^*_{Q'\uparrow}b_{q'\uparrow} \\ & + g^*_{k'}(3\omega_{Q'\uparrow}+\omega^c_{Q'\uparrow}+3\omega_{q'\uparrow}+\omega^c_{q'\uparrow})b^*_{q'\uparrow}b_{Q'\uparrow} \\ & + g_{k'}(3\omega_{q'\downarrow}+\omega^c_{q'\downarrow}+3\omega_{Q'\downarrow}+\omega^c_{Q'\downarrow})b^*_{Q'\downarrow}b_{q'\downarrow} \\ & + g^*_{k'}(4\omega_{q'\downarrow}+\omega^c_{q'\downarrow}+2\omega_{Q'\downarrow}+\omega^c_{Q'\downarrow})b^*_{q'\downarrow}b_{Q'\downarrow}\Big] \end{aligned} \tag{2.41}$$

$$\begin{aligned} F^{*(5)}_{k'}(t') = -2\pi\omega_{k'}^{-1}B_{k'}\sum_{k',q'}\Big[& 4|g_{k'}|^2(b^*_{Q'\uparrow}b_{Q'\uparrow}+b^*_{q'\uparrow}b_{q'\uparrow}+b^*_{Q'\downarrow}b_{Q'\downarrow}+b^*_{q'\downarrow}b_{q'\downarrow}) \\ & + |g_{k'}|^2(2b^*_{Q'\uparrow}b_{q'\uparrow}\delta_{q'\uparrow,Q'\downarrow}+2b^*_{Q'\downarrow}b_{q'\uparrow}\delta_{Q'\uparrow,q'\downarrow}+2b^*_{Q'\uparrow}b_{Q'\downarrow}\delta_{q'\uparrow,q'\downarrow} \\ & + 2b^*_{q'\downarrow}b_{q'\uparrow}\delta_{Q'\uparrow,Q'\downarrow}+2b^*_{q'\uparrow}b_{q'\downarrow}\delta_{Q'\uparrow,Q'\downarrow}+2b^*_{Q'\downarrow}b_{Q'\uparrow}\delta_{q'\uparrow,q'\downarrow} \\ & + 2b^*_{q'\uparrow}b_{Q'\downarrow}\delta_{Q'\uparrow,q'\downarrow}+2b^*_{q'\downarrow}b_{Q'\uparrow}\delta_{q'\uparrow,Q'\downarrow})\Big] \end{aligned} \tag{2.42}$$

While calculating the response function ($\tilde{P}(k,k',\omega)$), a total 268 Green's functions are encountered. The higher order Green's functions are decoupled using proper decoupling scheme [32, 153].

$$\ll abcd \gg = < ab > \ll cd \gg + < ac > \ll bd \gg + < ad > \ll ab \gg \tag{2.43}$$

Here a, b, c, d represent the operators B_k or A_k. Only 39 Green's functions are left after the simplification and rest give either a very small contribution or vanish. Using a renormalized phonon and electron Hamiltonian the remaining Green's functions are calculated:

$$H^e_{Ren} = \sum_q \hbar(\tilde{\omega}_{q\uparrow} b^*_{q\uparrow} b_{q\uparrow} + \tilde{\omega}_{q\downarrow} b^*_{q\downarrow} b_{q\downarrow} + \tilde{\omega}_{-q\uparrow} b^*_{-q\uparrow} b_{-q\uparrow} + \tilde{\omega}_{-q\downarrow} b^*_{-q\downarrow} b_{-q\downarrow}) \quad (2.44)$$

$$H^p_{Ren} = \frac{\hbar}{4} \sum_k [\frac{\tilde{\omega}^2_k}{\omega_k} A^*_k A_k + \omega_k B^*_k B_k] \quad (2.45)$$

The excitation spectrum, i.e., a response function ($P(k, k', \omega)$) can be written in a universally accepted form as

$$\tilde{P}(k, k', \omega + i\varepsilon) = \lim_{\varepsilon \to 0^+} \Delta_k(\omega) - i\Gamma_k(\omega) \quad (2.46)$$

where $\Gamma_k(\omega)$ is the imaginary part of $\tilde{P}(k, k', \omega + i\varepsilon)$ known as phonon frequency linewidth at the half maximum of the phonon frequency peak and $\Delta_k(\omega)$ is the real part known as the shift in the phonon frequency line of the perturbed mode. After relevant algebraic simplifications, the Green's functions takes the form as:

$$G_{k,k'}(\omega + i\epsilon) = \frac{\omega_k \eta_{k,k'}}{\pi(\omega^2 - \bar{\omega}^2_{kq} + 2i\omega_k \Gamma_{kq}(\omega))} \quad (2.47)$$

The perturbed mode frequency ($\bar{\omega}_{kq}$) and renormalized frequency ($\tilde{\omega}_{kq}$) are accomplished in the following form:

$$\bar{\omega}^2_{kq} = \tilde{\omega}^2_{kq} + 2\omega_k \Delta_k(\omega); \qquad \tilde{\omega}^2_{kq} = \tilde{\omega}^2_k + \tilde{\omega}^2_q \quad (2.48)$$

$$\tilde{\omega}^2_k = \omega^2_k - \omega_k[\omega^D_k + \omega^A_k + \omega^{AD}_k]; \qquad \tilde{\omega}^2_q = \omega_k \omega_{ep} \quad (2.49)$$

$$\begin{aligned}\omega_{ep} =& -8\omega_k^{-1}|g_k|^2N + 32\omega_k^{-2}\sum_q |g_k|^2[(2\omega_{qQ}^c + 6\omega_q^c)n_c(Q) + (2\omega_{qQ}^c + 3\omega_q^c)n_c(q) \\ &+ 3\omega_{Q\uparrow}N(Q\uparrow) + 3\omega_{Q\downarrow}N(Q\downarrow) + 3\omega_{Q\uparrow}N(q\uparrow) + (4\omega_{q\downarrow} + 2\omega_{Q\downarrow})N(q\downarrow)]\end{aligned} \tag{2.50}$$

$$\begin{aligned}\omega_k^D =& 8D(k_1,-k) + 8C(k_1,-k) + 32\omega_k^{-1}C(k_1,-k)D(k_1,-k_1) \\ &+ 32\omega_k^{-1}\sum_{k_1} C(k_1,-k_1)D(k_1,-k) + 32\omega_k^{-1}\sum_{k_1} C(k_1,-k_1)C(k_1,-k) \\ &+ 128\omega_k^{-2}\sum_{k_1} C(k_1,-k_1)C(k_1,-k)D(k_1,-k_1)\end{aligned} \tag{2.51}$$

$$\omega_k^A = 48\sum_{k_1,k_2} V_4(k_1,k_2,k_1,-k)n_{k_1} \tag{2.52}$$

$$\begin{aligned}\omega_k^{AD} =& 192\omega_k^{-1}\sum_{k_1,k_2} C(k_1,-k_1)V_4(k_1,k_2,k_1,-k_1)n_{k_1} \\ &+ 64\omega_k^{-1}\sum_{k_1,k_2} C(k_1,-k_1)V_4(k_1,k_2,k_1,-k_1) \\ &+ 256\omega_k^2\sum_{k_1,k_2} C(k_1,-k_1)C(k_1,-k)V_4(k_1,k_2,-k_1,-k_1)\end{aligned} \tag{2.53}$$

The some of the symbols appearing in above expressions may be expressed as follows:

$$N = N(Q_\uparrow)+N(q\uparrow)+N(Q\downarrow)+N(q\downarrow); \quad \omega_{qQ}^c = \omega_q^c+\omega_Q^c; \quad n_{k_1} = \frac{\omega_{k_1}}{\tilde{\omega}_{k_1}}\coth(\beta\hbar\omega_{k_1}/2) \tag{2.54}$$

Where $N(\gamma\sigma)$ represent Fermi functions and $n_c(\gamma)$ Bose functions with $\gamma = (q, Q)$; $\sigma = (\uparrow,\downarrow)$, ω_q^c and ω_Q^c are the pairon frequencies before and after scattering with phonons respectively.

2.4.1 Phonon Frequency (Energy) Line Widths

The phonon line width $\Gamma_k(\omega)$ can be obtained in the following form:

$$\Gamma_k(\omega) = \Gamma_k^D(\omega) + \Gamma_k^A(\omega) + \Gamma_k^{AD}(\omega) + \Gamma_k^{ep}(\omega) \tag{2.55}$$

where

$$\Gamma_k^D(\omega) = \sum_{k_1} \pi\epsilon(\omega) R^D(k,k_1)\omega_{k_1}\delta(\omega^2-\tilde{\omega}_{k_1}^2) + 8\pi\omega_k^{-1} N R^{Dep}(k,k_1)\Big[\delta(\omega-\tilde{\omega}_{k_1}) + \delta(\omega+\tilde{\omega}_{k_1})\Big] \tag{2.56}$$

$$\Gamma_k^A(\omega) = \Gamma_k^{3A}(\omega) + \Gamma_k^{4A}(\omega) \tag{2.57}$$

$$\Gamma_k^{3A}(\omega) = 18\pi\epsilon(\omega)\sum_{k_1,k_2}|V_3(k_1,k_2,-k)|^2\eta_1\Big[S_{+\alpha}\omega_{+\alpha}\delta(\omega^2-\tilde{\omega}_{+\alpha}^2) + S_{-\alpha}\omega_{-\alpha}\delta(\omega^2-\tilde{\omega}_{-\alpha}^2)\Big] \tag{2.58}$$

$$\Gamma_k^{4A}(\omega) = 48\pi\epsilon(\omega)\sum_{k_1,k_2,k_3}|V_4(k_1,k_2,k_3,-k)|^2\eta_2\Big[S_{+\beta}\omega_{+\beta}\delta(\omega^2-\tilde{\omega}_{+\beta}^2) + 3S_{-\beta}\omega_{-\beta}\delta(\omega^2-\tilde{\omega}_{-\beta}^2)\Big] \tag{2.59}$$

$$\Gamma_k^{AD}(\omega) = \Gamma_k^{3D}(\omega) + \Gamma_k^{4D}(\omega) \tag{2.60}$$

$$\Gamma_k^{3D}(\omega) = 144\pi\epsilon(\omega)\sum_{k_1,k_2}|V_3(k_1,k_2,-k)|^2 R^c(k,k_1)\omega_k^{-1}\eta_1\Big[S_{+\alpha}\omega_{+\alpha} \times \delta(\omega^2-\tilde{\omega}_{+\alpha}^2) + S_{-\alpha}\omega_{-\alpha}\delta(\omega^2-\tilde{\omega}_{-\alpha}^2)\Big] \tag{2.61}$$

$$\begin{aligned}\Gamma_k^{4D}(\omega) &= \pi\epsilon(\omega)\sum_{k_1,k_2,k_3}|V_4(k_1,k_2,k_3,-k)|\Big[\tilde{R}(k,k_1)n_{k_2}\frac{\omega_{k_1}\omega_{k_2}}{\tilde{\omega}_{k_2}}\delta(\omega^2-\tilde{\omega}_{k_1}^2)\\ &+\tilde{R}^*(k,k_1)n_{k_1}\frac{\omega_{k_1}\omega_{k_3}}{\tilde{\omega}_{k_1}}\delta(\omega^2-\tilde{\omega}_{k_3}^2)\Big]\\ &+384\pi\epsilon(\omega)\sum_{k_1,k_2,k_3}|V_4(k_1,k_2,k_3,-k)|^2\\ &\times R^c(k,k_1)\omega^{-1}\eta_2\Big[S_{+\beta}\omega_{+\beta}\delta(\omega^2-\tilde{\omega}_{+\beta}^2)+S_{-\beta}\omega_{-\beta}\delta(\omega^2-\tilde{\omega}_{-\beta}^2)\Big] \quad (2.62)\end{aligned}$$

$$\begin{aligned}\Gamma_k^{ep}(\omega) &= \pi\omega_k^{-2}|g_k|^2\sum_q\Big[\bar{N}_{qQ\uparrow}(3\omega_{qQ\uparrow}+\omega_{qQ}^c)\omega_{1q\uparrow}^c\delta(\omega-4\tilde{\omega}_{qQ\uparrow})+\bar{N}_{qQ\uparrow}\\ &\times(3\omega_{qQ\uparrow}+\omega_{qQ}^c)\omega_{2Q\uparrow}^c\delta(\omega-3\tilde{\omega}_{qQ\uparrow}-\tilde{\omega}_{qQ}^c)+3\bar{N}_{qQ\downarrow}(3\omega_{qQ\downarrow}+\omega_{qQ}^c)\\ &\times\omega_{3q\downarrow}^c\delta(\omega-3\tilde{\omega}_{qQ\downarrow}-\tilde{\omega}_{qQ}^c)+\bar{N}_{qQ\downarrow}(4\omega_{q\downarrow}+2\omega_{Q\downarrow}+\omega_{qQ}^c)\omega_{4Q\downarrow}^c\\ &\times\delta(\omega-3\tilde{\omega}_{qQ\downarrow}-\tilde{\omega}_{qQ}^c)\Big]+128\pi\sum_{k,q}\omega_k^{-2}|g_k|^4\Big[\tilde{n}_kN(Q_\uparrow)\delta(\omega-7\tilde{\omega}_{Q\uparrow}-\tilde{\omega}_Q^c)\\ &+\tilde{n}_kN(q_\uparrow)\delta(\omega-7\tilde{\omega}_{q\uparrow}-\tilde{\omega}_q^c)+\tilde{n}_kN(Q_\downarrow)\delta(\omega-6\tilde{\omega}_{Q\downarrow}-2\tilde{\omega}_Q^c)\\ &+\tilde{n}_kN(q_\downarrow)\delta(\omega-6\tilde{\omega}_{Q\downarrow}-2\tilde{\omega}_q^c)-2\omega_k^{-1}\tilde{\omega}_k^2\hat{N}^2\epsilon(\omega)\delta(\omega^2-\tilde{\omega}_k^2)\Big] \quad (2.63)\end{aligned}$$

In the above equations the various symbols are identify as:

$$R^{Dep}(k,k_1) = |g_k|^2[D(k_1,-k)+C(k_1,-k)(1+4\omega_k^{-1}D(k_1,-k_1))] \quad (2.64)$$

$$\begin{aligned} R^{D}(k,k_1) &= |D(k_1,-k)|^2+8|C(k_1,-k)|^2[1+16\omega_k^{-2}|D(k_1,-k_1)|^2 \\ &\quad +8\omega_k^{-1}D(k_1,-k_1)]+16C(k_1,k)[D(k_1,-k) \\ &\quad +4\omega_k^{-1}|D(k_1,-k)|^2] \end{aligned} \quad (2.65)$$

$$\begin{aligned} \tilde{R}^{*}(k,k_1) &= 16D(k_1,k)+16C(k_1,k)[1+8\omega_k^{-1}D(k_1,-k_1)] \\ &\quad +16\omega_k^{-1}|C(k_1,-k)|^2[1+4\omega_k^{-1}D(k_1,-k_1)] \end{aligned} \quad (2.66)$$

$$\begin{aligned} \tilde{R}(k,k_1) &= 16D(k_1,-k)+16C(k_1,-k)[1+8\omega_k^{-1}D(k_1,-k_1)] \\ &\quad +16\omega_k^{-1}|C(k_1,-k)|^2[1+4\omega_k^{-1}D(k_1,-k_1)] \end{aligned} \quad (2.67)$$

$$R^{c}(k,k_1) = C(k_1,k)+2\omega_k^{-1}|C(k_1,-k)|^2 \quad (2.68)$$

$$S_{\pm\alpha} = n_{k_2}\pm n_{k_1} \quad (2.69)$$

$$S_{\pm\beta} = 1\pm n_{k_1}n_{k_2}\pm n_{k_2}n_{k_3}\pm n_{k_3}n_{k_1} \quad (2.70)$$

$$\omega_{\pm\alpha} = \tilde{\omega}_{k_1}\pm\tilde{\omega}_{k_2};\quad \omega_{\pm\beta}=\tilde{\omega}_{k_1}\pm\tilde{\omega}_{k_2}\pm\tilde{\omega}_{k_3} \quad (2.71)$$

$$\eta_{i-1} = \frac{\omega_{k_1}\omega_{k_2}\ldots\omega_{k_i}}{\tilde{\omega}_{k_1}\tilde{\omega}_{k_2}\ldots\tilde{\omega}_{k_i}};\quad \tilde{n}_{k_i}=\frac{\tilde{\omega}_{k_i}}{\omega_{k_i}}\coth\frac{\beta\hbar\tilde{\omega}_{k_i}}{2} \quad (2.72)$$

$$n_{k_i} = \coth(\beta\hbar\omega_{k_i}/2)\ i=1,2,\cdots,n \quad (2.73)$$

$$\omega_{qQ\binom{\uparrow}{\downarrow}} = \omega_{q\binom{\uparrow}{\downarrow}}+\omega_{Q\binom{\uparrow}{\downarrow}};\quad \tilde{\omega}_{qQ\binom{\uparrow}{\downarrow}}=\tilde{\omega}_{q\binom{\uparrow}{\downarrow}}+\tilde{\omega}_{Q\binom{\uparrow}{\downarrow}};\quad \omega^c_{qQ}=\omega^c_q+\omega^c_Q \quad (2.74)$$

$$N = N(Q_\uparrow)+N(q_\uparrow)+N(Q_\downarrow)+N(q_\downarrow) \quad (2.75)$$

$$\hat{N}^2 = N^2(Q_\uparrow)+N^2(q_\uparrow)+N^2(Q_\downarrow)+N^2(q_\downarrow) \quad (2.76)$$

$$\bar{N}_{qQ\binom{\uparrow}{\downarrow}} = N_{q\binom{\uparrow}{\downarrow}}+N_{Q\binom{\uparrow}{\downarrow}} \quad (2.77)$$

$$\omega^c_{\binom{1q\uparrow}{2Q\uparrow}} = 13\omega_{\binom{q\uparrow}{Q\uparrow}}+11\omega_{\binom{Q\uparrow}{q\uparrow}}+4\omega^c_{qQ} \quad (2.78)$$

$$\omega^c_{\binom{3q\downarrow}{4Q\downarrow}} = 7\omega_{\binom{q\downarrow}{Q\downarrow}}+5\omega_{\binom{Q\downarrow}{q\downarrow}}+4\omega^c_{qQ} \quad (2.79)$$

2.4.2 Phonon Frequency (Energy) Line Shifts

The Phonon spectrum frequency shift is given as:

$$\Delta_k(\omega) = \Delta_k^D(\omega) + \Delta_k^A(\omega) + \Delta_k^{AD}(\omega) + \Delta_k^{ep}(\omega) \tag{2.80}$$

$$\begin{aligned}
\Delta_k^D(\omega) &= \sum_{k_1} \frac{R^D(k,k_1)\omega_{k_1}}{(\omega^2 - \tilde{\omega}_{k_1}^2)} + 16\omega_k^{-1} N \left(\frac{1}{(\omega - \tilde{\omega}_{k_1})} - \frac{\tilde{\omega}_{k_1}}{(\omega^2 - \tilde{\omega}_{k_1}^2)} \right) \\
&\quad \times R^{Dep}(k,k_1) && (2.81) \\
\Delta_k^A(\omega) &= \Delta_k^{3A}(\omega) + \Delta_k^{4A}(\omega) && (2.82) \\
\Delta_k^{3A}(\omega) &= 18 \sum_{k_1,k_2} |V_3(k_1,k_2,-k)|^2 \eta_1 \left(\frac{S_{+\alpha}\omega_{+\alpha}}{(\omega^2 - \tilde{\omega}_{+\alpha}^2)} + \frac{S_{-\alpha}\omega_{-\alpha}}{(\omega^2 - \tilde{\omega}_{-\alpha}^2)} \right) && (2.83) \\
\Delta_k^{4A}(\omega) &= 48 \sum_{k_1,k_2,k_3} |V_4(k_1,k_2,k_3,-k)|^2 \eta_2 \left(\frac{S_{+\beta}\omega_{+\beta}}{(\omega^2 - \tilde{\omega}_{+\beta}^2)} + \frac{3S_{-\beta}\omega_{-\beta}}{(\omega^2 - \tilde{\omega}_{-\beta}^2)} \right) && (2.84) \\
\Delta_k^{AD}(\omega) &= \Delta_k^{3D}(\omega) + \Delta_k^{4D}(\omega) && (2.85) \\
\Delta_k^{3D}(\omega) &= 144 \sum_{k_1,k_2} |V_3(k_1,k_2,-k)|^2 \omega_k^{-1} \eta_1 \left(\frac{S_{+\alpha}\omega_{+\alpha}}{(\omega^2 - \omega_{+\alpha}^2)} + \frac{S_{-\alpha}\omega_{-\alpha}}{(\omega^2 - \omega_{-\alpha}^2)} \right) \\
&\quad \times R^c(k,k_1) && (2.86)
\end{aligned}$$

$$\begin{aligned}
\Delta_k^{4D}(\omega) &= \sum_{k_1,k_2,k_3} |V_4(k_1,k_2,k_3,k)| \left(\frac{\tilde{R}(k,k_1) n_{k_2} \omega_{k_1} \omega_{k_2}}{\tilde{\omega}_{k_2}(\omega^2 - \tilde{\omega}_{k_1}^2)} + \frac{\tilde{R}^*(k,k_1) n_{k_1} \omega_{k_1} \omega_{k_3}}{\tilde{\omega}_{k_1}(\omega^2 - \tilde{\omega}_{k_3}^2)} \right) \\
&\quad + 384 \sum_{k_1,k_2,k_3} |V_4(k_1,k_2,k_3,-k)|^2 R^c(k,k_1) \frac{\eta_2}{\omega_k} \left(\frac{S_{+\beta}\omega_{+\beta}}{(\omega^2 - \tilde{\omega}_{+\beta}^2)} \right. \\
&\quad \left. + \frac{3S_{-\beta}\omega_{-\beta}}{(\omega^2 - \tilde{\omega}_{-\beta}^2)} \right) && (2.87)
\end{aligned}$$

$$\begin{aligned}\Delta_k^{ep}(\omega) &= \omega_k^{-2}|g_k|^2\sum_q\Bigg[\bar{N}_{qQ\uparrow}(3\omega_{qQ\uparrow}+\omega_{qQ}^c)\Bigg(\frac{\omega_{1q\uparrow}^c}{(\omega-4\tilde{\omega}_{qQ\uparrow})}+\frac{\omega_{2Q\uparrow}^c}{(\omega-3\tilde{\omega}_{qQ\uparrow}-\tilde{\omega}_{qQ}^c)}\Bigg)\\ &+\bar{N}_{qQ\downarrow}\Bigg(\frac{3(3\omega_{qQ\downarrow}+\omega_{qQ}^c)\omega_{3q\downarrow}^c}{(\omega-3\tilde{\omega}_{qQ\downarrow}-\tilde{\omega}_{qQ}^c)}+\frac{(4\omega_{q\downarrow}+2\omega_{Q\downarrow}+\omega_{qQ}^c)\omega_{4Q\downarrow}^c}{(\omega-3\tilde{\omega}_{qQ\downarrow}-\tilde{\omega}_{qQ}^c)}\Bigg)\Bigg]\\ &+128\sum_{k,q}\omega_k^{-2}|g_k|^4\Bigg[\frac{\tilde{n}_kN(Q_\uparrow)}{(\omega-7\tilde{\omega}_{Q\uparrow}-\tilde{\omega}_Q^c)}+\frac{\tilde{n}_kN(q_\uparrow)}{(\omega-7\tilde{\omega}_{q\uparrow}-\tilde{\omega}_q^c)}\\ &+\frac{\tilde{n}_kN(Q_\downarrow)}{(\omega-6\tilde{\omega}_{Q\downarrow}-2\tilde{\omega}_Q^c)}+\frac{\tilde{n}_kN(q_\downarrow)}{(\omega-6\tilde{\omega}_{Q\downarrow}-2\tilde{\omega}_q^c)}-\frac{2\tilde{\omega}_k^2\hat{N}^2}{\omega_k(\omega^2-\tilde{\omega}_k^2)}\Bigg]\end{aligned}\tag{2.88}$$

2.5 Electron Green's Functions

The double-time thermodynamic electron Green's functions can be written as [153]:

$$\begin{aligned}G_{q,q'}(t-t') &= \ll b_{q\sigma}^*(t);b_{q'\sigma'}(t')\gg\\ &= -\mathrm{i}\theta(t-t')\langle[b_{q\sigma}^*(t),b_{q'\sigma'}(t')]\rangle\end{aligned}\tag{2.89}$$

Using quantum dynamical equation of motion to the Eq. (2.89) via Hamiltonian (2.15) one can obtain

$$i\hbar\frac{\partial G_{q,q'}(t-t')}{\partial t}=\hbar\delta(t-t')\langle[b_{q\sigma}^*(t),b_{q'\sigma'}(t')]\rangle-i\theta(t-t')\langle[[b_{q\sigma}^*(t),H],b_{q'\sigma'}(t')]\rangle\tag{2.90}$$

Differentiating Eq. (2.90) with respect to t and following the fourier transformation we get

$$G_{q,q'}(\omega)=G_{q,q'}^0(\omega)\{\delta_{qq'}\delta_{\sigma\sigma'}+[\omega+(3\omega_q+\omega_q^c)]^{-1}\ll F_q^*(t);b_{q'\sigma'}(t')\gg\}\tag{2.91}$$

$G_{q,q'}^0(\omega)$ is the unperturbed Green's functions which can be written as

$$G_{q,q'}^0(\omega)=\frac{1}{2\pi[\omega-(3\omega_q+\omega_q^c)]}\tag{2.92}$$

and

$$\begin{aligned} F_q^*(t) &= 4\pi \sum_k (g_k + g_k^*) \Big[\{(3\omega_{q\sigma} + \omega_q^c) + (3\omega_{Q\sigma} + \omega_q^c)\} b_{Q\sigma}^* B_k + 2 \sum_k g_k b_{Q\sigma}^* B_k B_k \\ &+2 \sum_{k,q} g_k^* b_{q\sigma}^* B_k B_k + \omega_k b_{Q\sigma}^* A_k + 6 \sum_{k_1,k_2} V_3(k_1, k_2, -k) b_{Q\sigma}^* A_{k_1} A_{k_2} \\ &+ 8 \sum_{k_1,k_2,k_3} V_4(k_1, k_2, k_3, -k) b_{Q\sigma}^* A_{k_1} A_{k_2} A_{k_3} + \sum_{k_1} D(k_1, -k) b_{Q\sigma}^* A_k \Big] \end{aligned} \tag{2.93}$$

To avoid the tedious expressions of higher order Green's functions $\ll F_q^*(t); b_{q'\sigma'}(t') \gg$ the Dyson's equation approach used to get

$$\begin{aligned} G_{q,q'}(\omega) &= G_q^0(\omega)\delta_{qq'}\delta_{\sigma\sigma'} + G_q^0(\omega)\tilde{P}(q, q', \omega)G_{q'}^0(\omega) && (2.94) \\ &= G_q^0(\omega)\delta_{qq'}\delta_{\sigma\sigma'} + G_q^0(\omega)\pi(q, q', \omega)G_{q'}(\omega) && (2.95) \end{aligned}$$

which lead to the following form of configuration

$$G_{q,q'}(\omega) = \frac{(3\omega_q + \omega_q^c)\delta_{qq'}\delta_{\sigma\sigma'}}{2\pi[\omega^2 - \tilde{\omega}_q^2 + (3\omega_q + \omega_q^c)\tilde{P}(q, q', \omega)]} \tag{2.96}$$

Here ω_q and ω_q^c are the electron and pairon frequencies. The response function $(\tilde{P}(q, q', \omega))$ for electron can be written as

$$\begin{aligned} \tilde{P}(q, q', \omega + i\epsilon) &= \frac{1}{2\pi(3\omega_q + \omega_q^c)^2} \ll F_{q,\sigma}^*(t); F_{q',\sigma'}(t) \gg && (2.97) \\ &= \lim_{\epsilon \to 0^+} \Delta_q(\omega) - i\Gamma_q(\omega) \end{aligned}$$

The final form of the electron Green's functions can be obtained as

$$G_{q,q'}(\omega) = \frac{(3\omega_q + \omega_q^c)\delta_{qq'}\delta_{\sigma\sigma'}}{2\pi[\omega^2 - \bar{\omega}_q^2 + i(3\omega_q + \omega_q^c)\Gamma_q(\omega))]} \tag{2.98}$$

with electron perturbed mode ($\bar{\omega}_q$) and renormalized electron mode ($\tilde{\omega}_q$) frequencies are given by

$$\bar{\omega}_q^2 = \tilde{\omega}_q^2 + (3\omega_q + \omega_q^c)\Delta_q(\omega) \tag{2.99}$$

$$\begin{aligned}\tilde{\omega}_q^2 &= (3\omega_q + \omega_q^c)^2 - \sum_k 16|g_k|^2\tilde{n}_{k_1} - \sum_{k,k_1} 24|g_k|V_3(k_1,k_1,-k)n_{k_1} \\ &\quad - \sum_k 16|g_k|^2[2(3\omega_q + \omega_q^c)\tilde{n}_{k_1} + 2\omega_k\tilde{n}_{k_1} + \sum_{k_1} 48V_4(k_1,k_1,k,-k) \\ &\quad \times n_{k_1}\tilde{n}_{k_1} + 8D(k,-k)\tilde{n}_{k_1}](3\omega_q + \omega_q^c)^{-1}\end{aligned} \tag{2.100}$$

2.5.1 Electron Frequency (Energy) Line Widths

The electron frequency line width can be achieved in the form

$$\Gamma_q(\omega) = \Gamma_q^D(\omega) + \Gamma_q^A(\omega) + \Gamma_q^{ep}(\omega) \tag{2.101}$$

where

$$\begin{aligned}\Gamma_q^D(\omega) &= 512\sum_{k,k_1}\pi|g_k|^2|D(k_1,k)|^2\Big[\epsilon(\omega)\omega_{k_1}N(\omega_{kc})\delta(\omega^2-\tilde{\omega}_{k_1}^2) \\ &\quad + n_{k_1}\delta(\omega-(3\tilde{\omega}_q+\tilde{\omega}_q^c))\Big](3\omega_q+\omega_q^c)^{-2}\end{aligned} \tag{2.102}$$

$$\Gamma_q^A(\omega) = \Gamma_q^{3A}(\omega) + \Gamma_q^{4A}(\omega) \tag{2.103}$$

$$\begin{aligned}\Gamma_q^{3A}(\omega) &= 1152\sum_{k,k_1,k_2}\pi|g_k|^2|V_3(k_1,k_2,k)|^2\Big[\epsilon(\omega)\eta_1 N(\omega_{kc}) \\ &\quad \times (S_{+\alpha}\tilde{\omega}_{+\alpha}\delta(\omega^2-\tilde{\omega}_{+\alpha}^2) + S_{-\alpha}\tilde{\omega}_{-\alpha}\delta(\omega^2-\tilde{\omega}_{-\alpha}^2)) \\ &\quad + n_{k_1}n_{k_2}\delta(\omega-(3\tilde{\omega}_q+\tilde{\omega}_q^c))\Big](3\omega_q+\omega_q^c)^{-2}\end{aligned} \tag{2.104}$$

$$\Gamma_q^{4A}(\omega) = 6144 \sum_{k,k_1,k_2,k_3} \pi |g_k|^2 |V_4(k_1,k_2,k_3,k)|^2 \Big[\epsilon(\omega)\eta_2 N(\omega_{kc}) + (S_{+\beta}\tilde{\omega}_{+\beta}\delta(\omega^2-\tilde{\omega}_{+\beta}^2) + 3S_{-\beta}\tilde{\omega}_{-\beta}\delta(\omega^2-\tilde{\omega}_{-\beta}^2)) + 3n_{k_1}n_{k_2}n_{k_3}\delta(\omega-(3\tilde{\omega}_q+\tilde{\omega}_q^c))\Big](3\omega_q+\omega_q^c)^{-2} \quad (2.105)$$

$$\Gamma_k^{ep}(\omega) = 16\sum_k \pi |g_k|^2 \Big[\epsilon(\omega)(\frac{-8\tilde{\omega}_k^2}{\omega_k} + \frac{2\omega_k^3}{(3\omega_q+\omega_q^c)^2})N(\omega_{kc})\delta(\omega^2-\tilde{\omega}_k^2) + (\frac{\omega_k^2 n_k}{(3\omega_q+\omega_q^c)^2} + \frac{4\omega_k\tilde{n}_k}{(3\omega_q+\omega_q^c)} + \tilde{n}_k)\delta(\omega-(3\tilde{\omega}_q+\tilde{\omega}_q^c))\Big] \quad (2.106)$$

2.5.2 Electron Frequency (Energy) Line Shifts

The electron line shift for impurity induced anharmonic crystal can be expressed as

$$\Delta_q(\omega) = \Delta_q^D(\omega) + \Delta_q^A(\omega) + \Delta_q^{ep}(\omega) \quad (2.107)$$

where

$$\Delta_q^D(\omega) = 512\sum_{k,k_1} |g_k|^2 |D(k_1,k)|^2 \Big[\frac{\omega_{k_1}N(\omega_{kc})}{(\omega^2-\tilde{\omega}_{k_1}^2)} + \frac{n_{k_1}}{(\omega-(3\tilde{\omega}_q+\tilde{\omega}_q^c))}\Big] \times (3\omega_q+\omega_q^c)^{-2} \quad (2.108)$$

$$\Delta_q^A(\omega) = \Delta_q^{3A}(\omega) + \Delta_q^{4A}(\omega) \quad (2.109)$$

$$\Delta_q^{3A}(\omega) = 1152\sum_{k,k_1,k_2} |g_k|^2 |V_3(k_1,k_2,k)|^2 \Big[\eta_1 N(\omega_{kc})(\frac{S_{+\alpha}\tilde{\omega}_{+\alpha}}{(\omega^2-\tilde{\omega}_{+\alpha}^2)} + \frac{S_{-\alpha}\tilde{\omega}_{-\alpha}}{(\omega^2-\tilde{\omega}_{-\alpha}^2)}) + \frac{n_{k_1}n_{k_2}}{(\omega-(3\tilde{\omega}_q+\tilde{\omega}_q^c))}\Big](3\omega_q+\omega_q^c)^{-2} \quad (2.110)$$

$$\Delta_q^{4A}(\omega) = 6144\sum_{k,k_1,k_2,k_3} |g_k|^2 |V_4(k_1,k_2,k_3,k)|^2 \Big[\eta_2 N(\omega_{kc})(\frac{S_{+\beta}\tilde{\omega}_{+\beta}}{(\omega^2-\tilde{\omega}_{+\beta}^2)} + \frac{3S_{-\beta}\tilde{\omega}_{-\beta}}{(\omega^2-\tilde{\omega}_{-\beta}^2)}) + \frac{3n_{k_1}n_{k_2}n_{k_3}}{(\omega-(3\tilde{\omega}_q+\tilde{\omega}_q^c))}\Big](3\omega_q+\omega_q^c)^{-2} \quad (2.111)$$

$$\Delta_k^{ep}(\omega) = 16\sum_k |g_k|^2 \Big[(\frac{-8\tilde{\omega}_k^2}{\omega_k} + \frac{2\omega_k^3}{(3\omega_q+\omega_q^c)^2})\frac{N(\omega_{kc})}{(\omega^2-\tilde{\omega}_k^2)} + (\frac{\omega_k^2 n_k}{(3\omega_q+\omega_q^c)^2} + \frac{4\omega_k\tilde{n}_k}{(3\omega_q+\omega_q^c)} + \tilde{n}_k)(\omega-(3\tilde{\omega}_q+\tilde{\omega}_q^c))^{-1}\Big] \quad (2.112)$$

2.5.3 Electron Density of States

Using the Lehmann's representation [149] the electron density of states (EDOS) $N_{el}(\omega)$ can be expressed as:

$$N_{el}(\omega) = -\sum_{q} Im\ G_{q,q'}(\omega) \tag{2.113}$$

The imaginary part of $G_{q,q'}(\omega)$ is given by

$$G_{q,q'}(\omega) = -\frac{(3\omega_q + \omega_q^c)^2 \delta_{qq'}\delta_{\sigma\sigma'}\Gamma_q(\omega)}{2\pi[(\omega^2 - \bar{\omega}_q^2)^2 + (3\omega_q + \omega_q^c)^2\Gamma_q^2(\omega)]} \tag{2.114}$$

Using the imaginary part of electron Green's functions from Eq. (2.114) to Eq. (2.113) gives

$$N_{el}(\omega) = \sum_{q} \frac{(3\omega_q + \omega_q^c)^2 \delta_{qq'}\delta_{\sigma\sigma'}\Gamma_q(\omega)}{2\pi[(\omega^2 - \bar{\omega}_q^2)^2 + (3\omega_q + \omega_q^c)^2\Gamma_q^2(\omega)]} \tag{2.115}$$

For smaller values of $\Gamma_q(\omega)$ the Breit-Wigner approximation [32] can be used to get simplified form of EDOS as:

$$N_{el}(\omega) \quad = \quad \sum_{q} \frac{(3\omega_q + \omega_q^c)^2 \Gamma_q^i(\omega)}{[2\pi(\omega^2 - \bar{\omega}_q^2)^2]}; \quad i = D, 3A, 4A, ep \tag{2.116}$$

The EDOS used to calculate the superconducting gap (SG) equation in chapter (3) following the fact that the electron-phonon has an inevitable role in the phenomenon of superconductivity. Therefore considering only electron-phonon interaction, i.e., taking only $\Gamma_q^{ep}(\omega)$ the simplified EDOS ($D(\omega)$) can be written as:

$$D(\omega) = \sum_{q} \frac{\omega_{qc}^2 \Gamma_q^{ep}(\omega)}{[2\pi(\omega^2 - \bar{\omega}_q^2)^2]} \tag{2.117}$$

where $\omega_{qc} = 3\omega_q + \omega_q^c$.

2.6 Interaction Potential

The model cuprate HTS $YBa_2Cu_3O_{7-\delta}$ and $La_{2-x}Sr_xCuO_4$ have been taken for the study. Both the HTS have perovskite structure. The superconductor, $YBa_2Cu_3O_{7-\delta}$ consist different layer of CuO, CuO_2, and BaO. Considering Y at the center of the unit cell of $YBa_2Cu_3O_{7-\delta}$ there emerges a network of Y-Cu, Y-Ba, and Y-O. Similarly, in $La_{2-x}Sr_xCuO_4$, having different layers of LaO and CuO_2 with Cu at the center of the unit cell, there are a complex interactions network of Cu-O, Cu-La, and Cu-Sr. A precise potential function is essential to understand the behaviour of complex structured HTS. This problem is carefully addressed by choosing the most suited form of modified Born-Mayer-Huggins potential (MBMHP) [173]:

$$V_{ij}(r) = a_{ij}e^{-b_{ij}r} + \frac{q_i q_j}{r} \tag{2.118}$$

where i, j labels the ions of charges q_i and q_j separated by the distance $r_{ij} \equiv r$; a_{ij} and b_{ij} are the range and softening parameters, respectively. The MBMHP have been plotted in Fig. (2.1) for $La_{2-x}Sr_xCuO_4$ and $YBa_2Cu_3O_{7-\delta}$ to check the stability of crystal. The MBMHP has been used to calculate the harmonic and anharmonic interacting force constant for $YBa_2Cu_3O_{7-\delta}$ and $La_{2-x}Sr_xCuO_4$ which is further utilized in the calculation of renormalized electron-phonon dispersion relation via dynamical matrix.

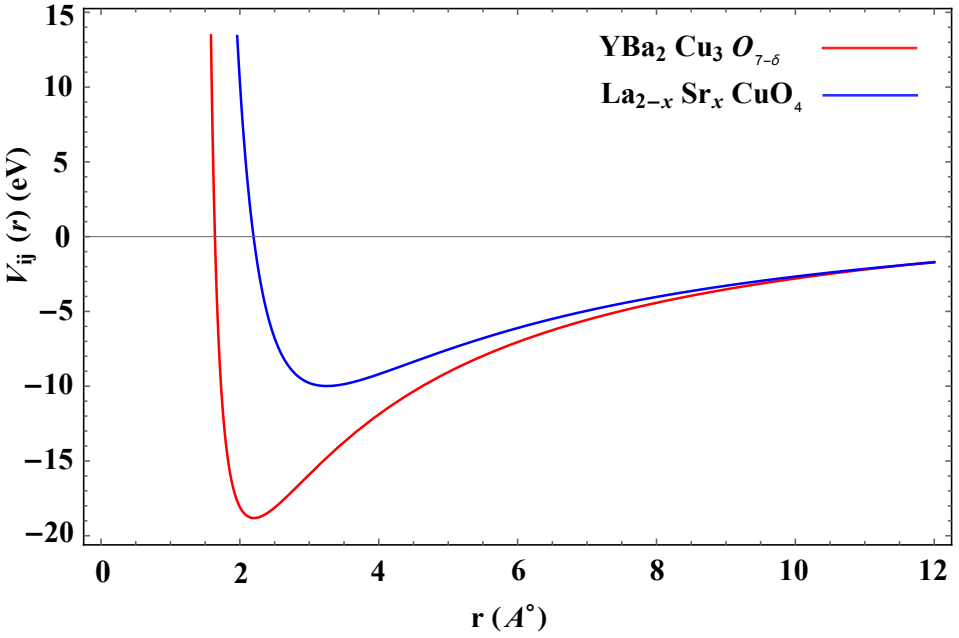

FIGURE 2.1: Potential plots for $La_{2-x}Sr_xCuO_4$(blue) and $YBa_2Cu_3O_{7-\delta}$ (red).

Chapter 3

The Superconducting Gap

"We have no right to assume that any physical laws exist, or if they have existed up until now, that they will continue to exist in a similar manner in the future."

- - - Max Planck

Work presented in this chapter is partially published as follows:

1. Superconducting gap anisotropy and d-wave pairing in $YBa_2Cu_3O_{7-\delta}$.
   S. K. Verma, A. Gupta, A. Kumari, B. D. Indu.
   Int. J. Mod. Phys. B, **32**, 1850035 (2018).
   DOI: https://doi.org/10.1142/S0217979218500352.

2. The high-temperature superconductor gap equation.
   S. K. Verma, A. Kumari, A. Gupta, B. D. Indu.
   Phys. Scr., **94**, 035701 (2019).
   DOI: https://doi.org/10.1088/1402-4896/aafbc5.

3. Pairing symmetry, nodal and antinodal superconducting gap in $La_{2-x}Sr_xCuO_4$: A doping scenario.
   S. K. Verma, A. Gupta, A. Kumari, B. D. Indu.
   J. Low Temp. Phys., **196**, 442-457, (2019).
   DOI: https://doi.org/10.1007/s10909-019-02199-2.

4. Superconducting gap in cuprates high temperature superconductors.
   S. K. Verma, A. Kumari, A. Gupta, B. D. Indu.
   AIP Conf. Proc., **1953**, 120020, (2018).
   DOI: https://doi.org/10.1063/1.5033085.

5. Anisotropy in superconducting gap in $YBa_2Cu_3O_{7-\delta}$.
   S. K. Verma, A. Kumari, A. Gupta, B. D. Indu.
   AIP Conf. Proc., **1942**, 130036, (2018).
   DOI: https://doi.org/10.1063/1.5029106.

3.1 Introduction

Superconducting gap (SG) - the energy difference between the ground state and lowest quasiparticle excitation of superconductor, is an inherent and temperature dependent property of superconductor which appears below critical temperature (T_c) of superconductor [174]. Historically, the first experimental evidence of SG observed by Corak *et al.* [24] while measuring the temperature dependent specific heat below T_c and by the Biondi *et al.* [175] as first spectroscopic measurement but there was no theoretical justification of these results. The SG successfully explained by the first microscopic theory of superconductivity known as the Bardeen-Cooper-Schrieffer (BCS) theory [20], which emerges due to the formation of Cooper pairs via phonon-mediated electron-electron interaction in the close vicinity of the Fermi surface [119, 176–178] as the superconductor cooled down below T_c. The temperature dependence of SG in aluminum was measured which followed exactly the predicted results of BCS theory [179]. The BCS theory predicted the reduced SG limit, R ($\equiv 2\Delta/k_BT_c$) $\simeq 3.5$, which is a fairly good justification for the conventional superconductors. After the discovery of HTS, various experimental techniques, namely, angle-resolved photoemission spectroscopy (ARPES), Andreev reflection, scanning tunneling spectroscopy (STS), etc. have been used to measure the SG in HTS and the increased reduced gap ratio emerged in the range $R = 5 - 8$ [47, 100–102]. The

large reduced gap ratio observed in HTS which is beyond the BCS predictions and opened new challenges for researchers to understand the pairing mechanism in new perspective. Along with the larger value of SG, the other surprising property of SG found in HTS was its doping dependence [93, 94] and highly anisotropic nature [103–106]. Many authors attempted to justify the anomaly of SG with various methodologies [37, 180–188]. These anomalies could not be explained by BCS theory and this was sufficient to motivate to consider the reformulation of the problem. In this chapter the problem of anomaly in the SG has been dealt via two different approaches namely; (i) the derivation of SG equation with new approach and (ii) use of renormalized electron-phonon dispersion.

In the first approach, the expression of SG derived following the BCS formalism but using generalized electron density of states (EDOS) which was considered as a constant quantity in the BCS theory as oversimplification. Since the EDOS plays a crucial role in the investigation of physical properties of superconductors, therefore it should be treated very carefully as EDOS depends on various quantities such as electron-phonon interaction, doping, anharmonicity, and temperature [189–191]. Therefore, treating the generalized EDOS offers the possibility to explore a detailed study of the pairing mechanism. The fact that the electron distribution functions change drastically below T_c as the phenomenon of pair formation occurs that prompts the new type of distribution functions; namely, the pairon distribution functions [192], which should be taken care of in the SG formulation. In the present formulation, such a diverse situation has been undertaken via generalized EDOS [189] which provides a tool to get significant information about the SG. The simultaneous presence of antiferromagnetic (AF) and superconducting phases being a mysterious phenomenon has also currently become an interesting topic of debate. The coexistence of AF and superconductivity is observed against the generalized behaviour of superconductors, since it is thought that the AF phase and superconducting phase can't coexist; for, the magnetism has the tendency to destroy the superconductivity. The experimental observations [120–122] of the AF phase along

with superconductivity certainly trigger to study this strange behaviour. Although the effect of AF spin fluctuations is either absent or minimal in some cuprate superconductor, e.g., $YBa_2Cu_3O_{7-\delta}$ [193], the pairing mechanism also influenced by antiferromagnetic spin fluctuations in some cuprate superconductors at low temperatures and low doping concentration, e.g., $La_{2-x}Sr_xCuO_4$ [120–122, 194, 195]. Without going into the details of the analysis of spin-Green's functions, the model of SG formulation further extended with the consideration of AF spin fluctuations and some effect has been encountered on SG of $La_{2-x}Sr_xCuO_4$ [196].

The second approach corresponds to the evaluation of SG in momentum space using the renormalized electron-phonon dispersion because the electron-phonon interactions play a deterministic role in the phenomenon of HTSC [115, 134, 192, 197–200] and in doping dependent SG [93–98, 103]. The renormalized electron-phonon dispersion used to calculate the SG. The renormalized electron-phonon dispersion opens the window to study the anisotropic nature of SG and pairing symmetry.

3.2 The High-Temperature Superconducting Gap Equation

3.2.1 Formulation of the Problem

The Interaction Energy

Since the reduced gap limit for the HTS is found to $R \simeq 5-8$ [100, 101, 103], inferring that the BCS gap equation become less significant where as the EDOS have a sophisticated form, depending on temperature [189–191] and doping concentration [201–203]. The marginal Fermi liquid theory of Varma *et al.* [204] considers two different cases of electron density of states in which for one case it is taken as a function of temperature at low electron frequency, and is constant otherwise. EDOS

[189] being a very sensitive quantity and depend on temperature along with other parameters namely; renormalized electron and phonon energies, etc. Consequently, a much generalized EDOS has become inevitable to incorporate these effects. Therefore the development of the SG equation for the HTS using a simple Copper pair formalism [205] needs to be investigated more attentively with

$$V^{-1} = \int_{2\varepsilon_F}^{2(\varepsilon_F+\hbar\omega_D)} (\varepsilon - 2\varepsilon_F + 2\Delta)^{-1} D(\varepsilon) d\varepsilon \tag{3.1}$$

where V, ε_F, ω_D and Δ stand for the effective (positive) averaged attractive potential, Fermi energy, Debye frequency and binding energy of pair (SG) [206], respectively. However, V has been oversimplified in the BCS problem, but here the appearance of EDOS $\rightarrow D(\varepsilon)$ leaves ample scope to deal with the problem to extract much of the additional physics.

The Electron Density of States

Using electron Green's functions ($G_{q,q'}(\varepsilon)$)

$$G_{q,q'}(\varepsilon) = \{2\pi[\varepsilon^2 - \bar{\varepsilon}_q^2 + i\varepsilon_{qc}\Gamma_q(\varepsilon)]\}^{-1} \varepsilon_{qc}\delta_{qq'}\delta_{\sigma\sigma'} \tag{3.2}$$

and following the Lehmann representation the intact form of the EDOS has been obtained [189] as:

$$N_{el}(\varepsilon) = \sum_q \frac{\Gamma_q(\varepsilon)\varepsilon_{qc}^2\delta_{q,q'}\delta_{\sigma,\sigma'}}{2\pi[(\varepsilon^2 - \bar{\varepsilon}_q^2)^2 + \varepsilon_{qc}^2\Gamma_q^2(\varepsilon)]} \tag{3.3}$$

Here $\Gamma_q(\varepsilon)$ $(= \Gamma_q^D(\varepsilon) + \Gamma_q^A(\varepsilon) + \Gamma_q^{ep}(\varepsilon))$ is total line width where $\Gamma_q^D(\varepsilon)$, $\Gamma_q^A(\varepsilon)$ and $\Gamma_q^{ep}(\varepsilon)$ stand for defects, anharmonicites and electron-phonon line width, respectively. It is an established fact that the electron-phonon interaction has an inevitable role

in the phenomenon of superconductivity. In order to make the theory simpler, the main contribution of $\Gamma_q^{ep}(\varepsilon)$ has been taken up in the EDOS [189], namely:

$$D(\varepsilon) = \sum_q \frac{\varepsilon_{qc}^2 \Gamma_q^{ep}(\varepsilon)}{2\pi(\varepsilon^2 - \bar{\varepsilon}_q^2)^2} \tag{3.4}$$

with

$$\Gamma_q^{ep}(\varepsilon) = 16\pi \sum_k |g_k|^2 \left[\xi(\varepsilon) \left(\frac{-8\tilde{\varepsilon}_k^2}{\varepsilon_k} + \frac{2\varepsilon_k^3}{\varepsilon_{qc}^2} \right) N(\varepsilon_{kc}) \delta(\varepsilon^2 - \tilde{\varepsilon}_k^2) + \left(\frac{\varepsilon_k^2 n_k}{\varepsilon_{qc}^2} + \frac{4\varepsilon \tilde{n}_k}{\varepsilon_{qc}} + \tilde{n}_k \right) \delta(\varepsilon - \tilde{\varepsilon}_{qc}) \right] \tag{3.5}$$

where

$$N(\varepsilon_{kc}) = \frac{1}{2} \left[(e^{3\beta\varepsilon_F} + 1)^{-1} + (e^{\beta\varepsilon_{qc}} - 1)^{-1} \right]; n_k = \coth\left(\frac{1}{2}\beta\varepsilon_k\right); \tilde{n}_k = \frac{\tilde{\varepsilon}_k}{\varepsilon_k} \coth\left(\frac{1}{2}\beta\varepsilon_k\right) \tag{3.6}$$

In the above equations the numerous symbols are described at the appropriate place.

3.2.2 The Superconducting Gap Equation

The use of Eq. (3.4) in gap Eq. (3.1) followed by some algebraic simplification one obtains

$$\frac{\alpha(\tilde{\varepsilon}_k, \bar{\varepsilon}_q)}{(\tilde{\varepsilon}_k - 2\varepsilon_F + 2\Delta)} + \frac{\gamma(\tilde{\varepsilon}_{qc}, \bar{\varepsilon}_q)}{(\tilde{\varepsilon}_{qc} - 2\varepsilon_F + 2\Delta)} + V^{-1} = 0 \tag{3.7}$$

where

$$\alpha(\tilde{\varepsilon}_k, \bar{\varepsilon}_q) = \frac{\tilde{\varepsilon}_{qc}^2 |g_k|^2 (2\varepsilon_k^4 - 8\tilde{\varepsilon}_k^2 \varepsilon_{qc}^2) N(\varepsilon_{kc})}{4\pi\varepsilon_k \tilde{\varepsilon}_k (\tilde{\varepsilon}_k^2 - \bar{\varepsilon}_q^2)^2} \tag{3.8}$$

and

$$\gamma(\tilde{\varepsilon}_{qc}, \bar{\varepsilon}_q) = \frac{\tilde{\varepsilon}_{qc}^2 |g_k|^2 (\varepsilon_k^2 n_k + 4\varepsilon_k \varepsilon_{qc} \tilde{n}_k + \varepsilon_{qc}^2 \tilde{n}_k)}{4\pi(\tilde{\varepsilon}_{qc}^2 - \bar{\varepsilon}_q^2)^2} \tag{3.9}$$

Further simplification of Eq. (3.7) yields the two expressions for SG as:

$$\Delta_{\frac{1}{2}}(T) = \frac{1}{4}\{(4\varepsilon_F - \tilde{\varepsilon}_k - \tilde{\varepsilon}_{qc}) - V[\alpha(\tilde{\varepsilon}_k, \bar{\varepsilon}_q) + \gamma(\tilde{\varepsilon}_{qc}, \bar{\varepsilon}_q)] \pm f)\} \tag{3.10}$$

where subscript '1' and '2' stand for '+' and '-' sign, respectively with

$$f = [\{V[\alpha(\tilde{\varepsilon}_k, \bar{\varepsilon}_q) + \gamma(\tilde{\varepsilon}_{qc}, \bar{\varepsilon}_q)] - (\tilde{\varepsilon}_k - \tilde{\varepsilon}_{qc})\}^2 + 4\alpha(\tilde{\varepsilon}_k, \bar{\varepsilon}_q)V(\tilde{\varepsilon}_k - \tilde{\varepsilon}_{qc})]^{\frac{1}{2}} \tag{3.11}$$

which can be rearranged as

$$f = V[\alpha(\tilde{\varepsilon}_k, \bar{\varepsilon}_q) + \gamma(\tilde{\varepsilon}_{qc}, \bar{\varepsilon}_q)] - (\tilde{\varepsilon}_k - \tilde{\varepsilon}_{qc}) + 2\varepsilon_1 \tag{3.12}$$

where

$$\varepsilon_1 = \frac{\alpha(\tilde{\varepsilon}_k, \bar{\varepsilon}_q)V(\tilde{\varepsilon}_k - \tilde{\varepsilon}_{qc})}{V[\alpha(\tilde{\varepsilon}_k, \bar{\varepsilon}_q) + \gamma(\tilde{\varepsilon}_{qc}, \bar{\varepsilon}_q)] - (\tilde{\varepsilon}_k - \tilde{\varepsilon}_{qc})} \tag{3.13}$$

Using Eq. (3.12), the SG equations (Eq. (3.10)), $\Delta_1(T)$ and $\Delta_2(T)$ can be written, respectively as:

$$\Delta_1(T) = \varepsilon_F - \frac{1}{2}[\tilde{\varepsilon}_k - \varepsilon_1] \tag{3.14}$$

$$\Delta_2(T) = \varepsilon_F - \frac{1}{2}\{\tilde{\varepsilon}_{qc} + V[\alpha(\tilde{\varepsilon}_k, \bar{\varepsilon}_q) + \gamma(\tilde{\varepsilon}_{qc}, \bar{\varepsilon}_q)] + \varepsilon_1\} \tag{3.15}$$

3.2.3 Analysis of Superconducting Gap Equations

Present formulation describes the two possible gap equations (Eq. (3.14) and (3.15)) with complex dependence on various terms, namely; Fermi energy and dimensionless temperature dependent quantities $\alpha(\tilde{\varepsilon}_k, \bar{\varepsilon}_q)$ and $\gamma(\tilde{\varepsilon}_{qc}, \bar{\varepsilon}_q)$. $\alpha(\tilde{\varepsilon}_k, \bar{\varepsilon}_q)$ and $\gamma(\tilde{\varepsilon}_{qc}, \bar{\varepsilon}_q)$ both incorporate the effects of anharmonicities and defects in terms of renormalized phonon and electron energies, and subsequently, the obtained SG equations evidently portray that in gap formation (and hence pair formation) the anharmonicity and defect play a decisive role. These effects of anharmonicity on electron-phonon coupling leading to gap formation have also been discussed by Amy *et al.* [115]. However, the conventional and HTS usually exhibit a single-gap structure, but there is evidence that many superconductors depict two or multiple gap structure [207–210]. The two gap phenomenon has been theoretically studied by the two-band model based on work of Suhl *et al.* [211] using σ and π band structures.

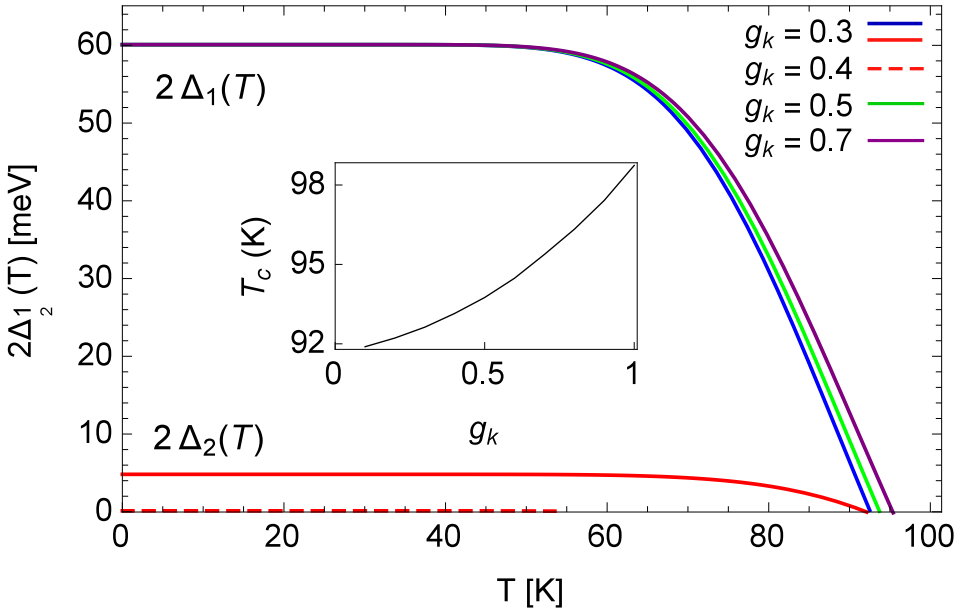

FIGURE 3.1: Variation of computed SG $2\Delta_1(T)$ and $2\Delta_2(T)$ with temperature for $YBa_2Cu_3O_{7-\delta}$. Both the SG approach towards the same $T_c = 93.8K$ at $g_k = 0.3$. Inset exhibits the variation of T_c with g_k.

In order to numerically analyze the new results and to evaluate the temperature dependence of the SG for $YBa_2Cu_3O_{7-\delta}$ the following physical constant [173, 189, 192, 212] have been used:

$\varepsilon_k = 8.7490 \times 10^{-14}$ erg, $\tilde{\varepsilon}_k = 1.0321 \times 10^{-14}$ erg, $\varepsilon_q^c = 2.9278 \times 10^{-14}$ erg, $\bar{\varepsilon}_q = 2.3702 \times 10^{-14}$ erg, $\varepsilon_F = 6.5690 \times 10^{-14}$ erg and using (Born-Mayer-Huggins potential) $V_{BMH} = 1.0410 \times 10^{-12}$ erg.

The temperature variant plots for gaps $\Delta_1(T)$ and $\Delta_2(T)$ for $g_k = 0.3$, 0.4, 0.5 and 0.7 are shown in Fig. (3.1) for $YBa_2Cu_3O_{7-\delta}$. The temperature variation of the SG calculated by Monthoux *et al.* [81, 213] and Pao *et al.* [214] show the saturation of the SG in the low-temperature region. The present result also shows the saturation of the SG in the low-temperature region in agreement with the previous work [81, 213]. For different coupling constants $g_k = 0.3$, 0.5 and 0.7; zeros of $\Delta_1(T)$ reveal $T_c = 93.8K$, $94K$ and $95.4K$, respectively. The reduced gap ratio obtained as $(2\Delta_1(0)/k_BT_c)_{g_k=0.3,\,0.5,\,0.7} = 7.5$, 7.4, 7.2 appear within the limit, i.e., $5-8$ of HTS

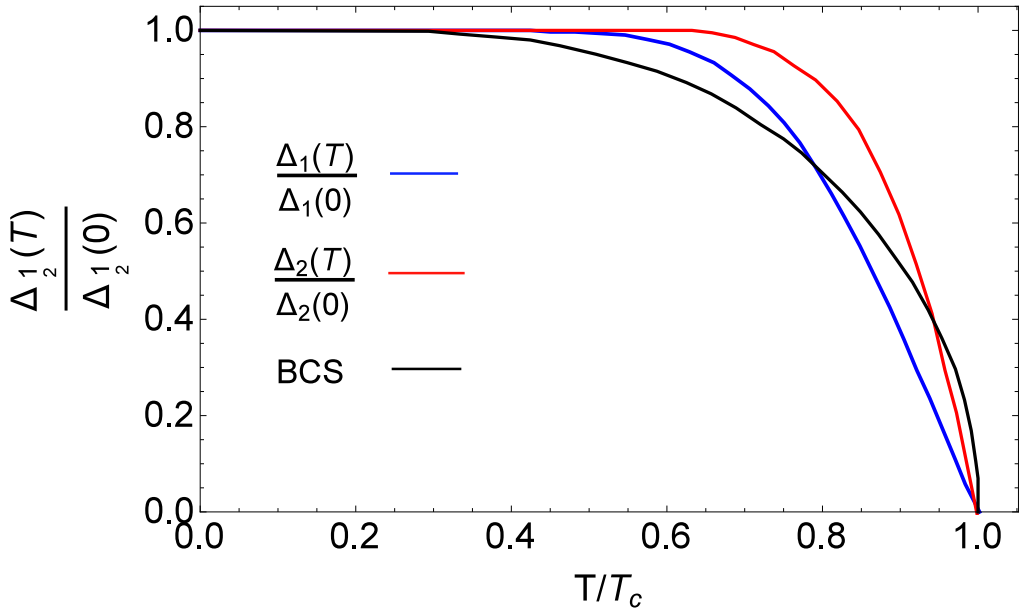

FIGURE 3.2: At $g_k = 0.3$, normalized SG plot $\Delta_1(T)/\Delta_1(0)$ and $\Delta_2(T)/\Delta_2(0)$ along with the normalized BCS gap curve. Both SGs are in agreement with the BCS gap curve in the low-temperature regime.

[100, 101, 103]. The inset of Fig. (3.1) show the variation of T_c with g_k obtained from zeros of $\Delta_1(T)$ for different electron-phonon coupling constant g_k, which indicates slight non-linearity with rising T_c, which is consistent with the work of Monthoux *et al.* [213]. The experiments [215] reveal that with the change in doping profile from underdoped to overdoped there appears an increase in T_c of HTS. Therefore, it can be inferred that with increasing doping (within superconducting limits) the electron-phonon coupling constant increases [216] leading to a higher critical temperature, indicating that the mechanisms of HTSC are highly influenced by the strength of the electron-phonon interactions. For $g_k = 0.3$, the gap equation $\Delta_2(T)$ computes a small reduced gap ratio $2\Delta_2(0)/k_B T_c = 0.6$ for $YBa_2Cu_3O_{7-\delta}$. Such a low value of reduced gap ratio could not be observed experimentally, manifesting that $YBa_2Cu_3O_{7-\delta}$ is the strongly correlated system. For $g_k = 0.4$ and above, $\Delta_2(T)$ tends to disappear (red dashed line of Fig. (3.1)) or becomes physically insignificant negative. However, Souma *et al.* [209] remarked that with reference to multi-gap superconductor such as MgB_2, the electrons in the σ bands are strongly coupled

with phonons responsible for the large gap, while in π band small gap appears due to weak electron-phonon coupling. The small gap for weak electron-phonon coupling ($g_k \ll 1$) provides the possible background for the formation of a smaller SG in two-gap superconductor. Hence, the present theory can be utilized to explain the two-gap superconductivity via variable strength of electron-phonon coupling. Both SG equations $\Delta_1(T)$ and $\Delta_2(T)$ are normalized at $g_k = 0.3$ to their maximum gap values $\Delta_1(0)$ and $\Delta_2(0)$, respectively; where $\Delta(0)$ represents the gap at $T = 0K$ and is plotted in Fig. (3.2) along with BCS results. The temperature dependence of the computed SG obeys the BCS gap curve in the low-temperature region and deviates near T_c.

However, both the temperature-dependent SG equations give different values of SG, but both approach the same T_c, for $g_k = 0.3$ as observed for $YBa_2Cu_3O_{7-\delta}$ in Fig. (3.1) and predicts $T_c \simeq 93.8K$, slightly above the experimental gap value of $YBa_2Cu_3O_{7-\delta}$ ($T_c \simeq 92K$). It is well established that gap and pair formation depend on temperature and start showing their presence below T_c and increased as $T \to 0$. The present work achieved similar temperature dependence (Fig. (3.1)) via various occupancies. The dependence of the SG equations $\Delta_1(T)$ and $\Delta_2(T)$ on Fermi energy also supports the fact that the SG and pair formation takes place in the vicinity of the Fermi level [20]. In support of the work of Amy *et al.* [115], present investigations establish that the anharmonic effects through renormalized electron and phonon frequencies do significantly contribute to the SG and pair formation [192, 217]. As the BCS gap equation is relevant to the isotropic gap superconductor (or conventional superconductor) having s-wave pairing, the computed gap show deviation from BCS gap curve and reduced gap ratio (for $YBa_2Cu_3O_{7-\delta}$, $2\Delta_1(0)/k_BT_c \simeq 7.2 - 7.5$) is found to be larger than the BCS gap limit ($2\Delta/k_BT_c \simeq 3.5$). The symmetry of the SG is attributed to renormalized energy (frequency). In chapter (4), it is shown that the renormalized electron-phonon energies produces $d_{x^2-y^2}$-wave gap symmetry along with a small component ($< 3\%$) of s (or d_{xy})-wave [218]. Also, the gap Eq. (3.14) and (3.15) depend on the renormalized phonon and electron energies.

Therefore, apparently it can be inferred that the new results for the SG are more appropriate for HTS which has an anisotropic gap and dominating $d_{x^2-y^2}$ pairing along with small a component of s-wave pairing.

3.3 The Effect of Antiferromagnetic Spin fluctuations on Superconducting Gap

In addition to the basic requirement of electron-phonon interaction for superconductivity, sufficient pieces of evidence reveal substantial effects of AF spin fluctuations in the pairon formation and co-existence of the magnetic order with superconductivity at low temperatures in the weak doping or near to the optimal doping(≤ 0.15) [120–122, 194, 195, 219]. Since, SG is observed as a function of energy line width of interacting particles and/or quasi-particles[220], taking the advantage of additivity of line widths, the effect of AF spin fluctuations has been included in it and the effect of antiferromagnetism is explicitly explored on SG as follows:

Let us consider the total line width as:

$$\Gamma^{total} = \Gamma^{ep} + \Gamma^{m} \tag{3.16}$$

where Γ^m stands for the magnon line width. Using Γ^{total} in EDOS, the effect of electron-phonon and AF spin fluctuations cab be analysed, simultaneously. The magnetic order being effective in the low-temperature regime, the SG equation can be derived as a function of Γ^m (in terms of energy) for AF spin fluctuations [221] and the electron-phonon line width[189] Γ^{ep}, where:

$$\Gamma^{m} = 2\hbar\omega_E S^{-2}\varepsilon_m^2(2\pi)^{-3}(a|ln\tau| + a') \tag{3.17}$$

$$\Gamma_q^{ep}(\varepsilon) = 16\pi \sum_k |g_k|^2 \Bigg[\xi(\varepsilon) \left(\frac{-8\tilde{\varepsilon}_k^2}{\varepsilon_k} + \frac{2\varepsilon_k^3}{\varepsilon_{qc}^2} \right) N(\varepsilon_{kc}) \times \delta(\varepsilon^2 - \tilde{\varepsilon}_k^2) + \left(\frac{\varepsilon_k^2 n_k}{\varepsilon_{qc}^2} + \frac{4\varepsilon \tilde{n}_k}{\varepsilon_{qc}} + \tilde{n}_k \right) \delta(\varepsilon - \tilde{\varepsilon}_{qc}) \Bigg] \tag{3.18}$$

where

$$\xi(\varepsilon) = \begin{cases} 1 & \text{for } \varepsilon > 0 \\ -1 & \text{for } \varepsilon < 0 \end{cases} \tag{3.19}$$

The modified form of the EDOS ($D_{AF}(\varepsilon)$) which is also influenced by the AF spin fluctuations can be managed in the form:

$$D_{AF}(\varepsilon) = \sum_q \frac{\varepsilon_{qc}^2 \Gamma_q^{total}(\varepsilon)}{2\pi(\varepsilon^2 - \bar{\varepsilon}_q^2)^2} \tag{3.20}$$

Therefore using simple Copper pair formalism [205] one can obtain SG equation from:

$$V^{-1} = \int_{2\varepsilon_F}^{2(\varepsilon_F + \hbar\omega_D)} (\varepsilon - 2\varepsilon_F + 2\Delta)^{-1} D_{AF}(\varepsilon) d\varepsilon \tag{3.21}$$

Using Eq. (3.20) in Eq. (3.21) and followed by some algebraic simplification one obtains:

$$\frac{\alpha(\tilde{\varepsilon}_k, \bar{\varepsilon}_q)}{(\tilde{\varepsilon}_k - 2\varepsilon_F + 2\Delta)} + \frac{\gamma(\tilde{\varepsilon}_{qc}, \bar{\varepsilon}_q)}{(\tilde{\varepsilon}_{qc} - 2\varepsilon_F + 2\Delta)} - \frac{A_m}{\Delta} + V^{-1} = 0 \tag{3.22}$$

where

$$\alpha(\tilde{\varepsilon}_k, \bar{\varepsilon}_q) \equiv \alpha = \frac{\tilde{\varepsilon}_{qc}^2 |g_k|^2 (2\varepsilon_k^4 - 8\tilde{\varepsilon}_k^2 \varepsilon_{qc}^2) N(\varepsilon_{kc})}{4\pi \varepsilon_k \tilde{\varepsilon}_k (\tilde{\varepsilon}_k^2 - \bar{\varepsilon}_q^2)^2} \tag{3.23}$$

$$\gamma(\tilde{\varepsilon}_{qc}, \bar{\varepsilon}_q) \equiv \gamma = \frac{\tilde{\varepsilon}_{qc}^2 |g_k|^2 (\varepsilon_k^2 n_k + 4\varepsilon_k \varepsilon_{qc} \tilde{n}_k + \varepsilon_{qc}^2 \tilde{n}_k)}{4\pi (\tilde{\varepsilon}_{qc}^2 - \bar{\varepsilon}_q^2)^2} \tag{3.24}$$

and

$$A_m = \frac{\hbar\omega_E 2\varepsilon_{km}^2 \tau^3 (a|ln\tau| + a')\hbar\omega_D \varepsilon_{qc}^2}{S^2(2\pi)^4(4\varepsilon_F^2 - \bar{\varepsilon}_q^2)^2} \tag{3.25}$$

where ω_E is exchange frequency, S is spin quantum number, $\tau = 2k_BT/\hbar\omega_E$, ε_{km} is reduced spin wave energy, ω_D is Debye frequency, a and a' are numerical constant.

Since the value of Δ for HTSC is large therefore the gap Eq. (3.22) can be further simplified as:

$$4\Delta^2 + 2V(\alpha + \gamma - 2A_m)\Delta - V[\alpha(\tilde{\varepsilon}_k - 2\varepsilon_F) + \gamma(\tilde{\varepsilon}_{qc} - 2\varepsilon_F)] = 0 \tag{3.26}$$

Solving the Eq. (3.26) two expression of SG obtained as:

$$\begin{aligned}\Delta_{\substack{1m\\2m}}(T) =& \frac{V}{4}(2A_m - \alpha - \gamma) \pm \frac{V}{4}\{(\alpha + \gamma - 2A_m)^2 \\ & - 4V^{-1}[\alpha(\tilde{\varepsilon}_k - 2\varepsilon_F) + \gamma(\tilde{\varepsilon}_{qc} - 2\varepsilon_F)]\}^{1/2}\end{aligned} \tag{3.27}$$

where subscript '$1m$' and '$2m$' stand for '+' and '-' sign, respectively. The first term of square root is greater than second term (numerically compared for $La_{2-x}Sr_xCuO_4$), therefore the obtained SG Eq. (3.27) cab be further simplified as:

$$\Delta_{1m}(T) = \frac{\alpha(\tilde{\varepsilon}_k - 2\varepsilon_F) + \gamma(\tilde{\varepsilon}_{qc} - 2\varepsilon_F)}{2(2A_m - \alpha - \gamma)} \tag{3.28}$$

$$\Delta_{2m}(T) = \frac{V}{2}(2A_m - \alpha - \gamma) - \frac{\alpha(\tilde{\varepsilon}_k - 2\varepsilon_F) + \gamma(\tilde{\varepsilon}_{qc} - 2\varepsilon_F)}{2(2A_m - \alpha - \gamma)} \tag{3.29}$$

Obviously, the SG equations (Eq. (3.28) and (3.29)) is affected by AF spin fluctuations and depend on the function A_m. The two SG equations may be useful in the study of multi-gap superconductors but in the present case of $La_{2-x}Sr_xCuO_4$ the SG Eq.(3.28) is found suitable. The temperature dependence of the $\Delta_{1m}(T)$ and $\Delta_1(T)$ for $La_{2-x}Sr_xCuO_4$ at the optimal doping $x = 0.15$ is depicted in Fig. (3.3).

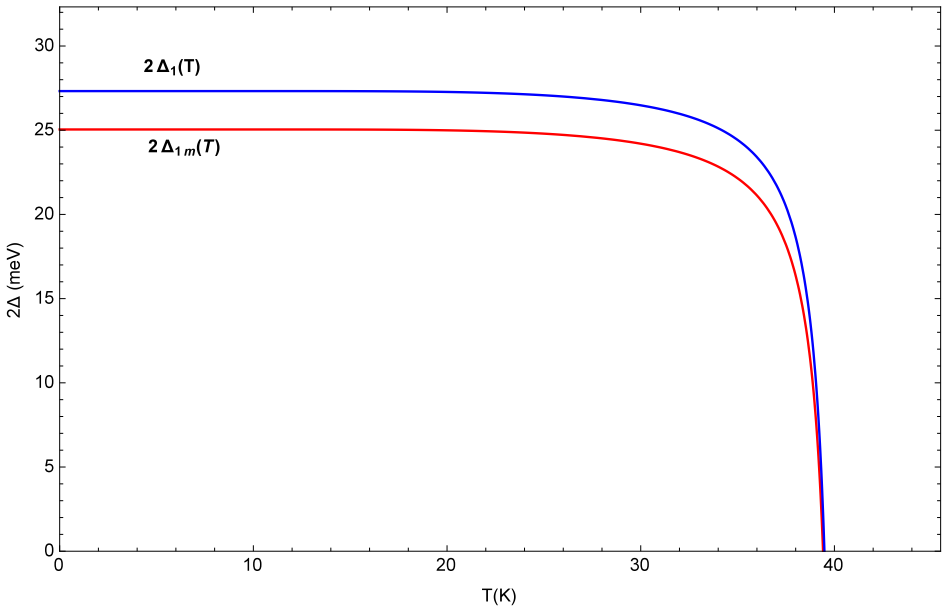

FIGURE 3.3: Variation of SG with temperature for $La_{2-x}Sr_xCuO_4$. $\Delta_1(T)$ (blue curve)-in absence of AF spin fluctuations and $\Delta_{1m}(T)$ (red curve)-in presence of AF spin fluctuations.

A reduction in the SG is observed due to the influence of AF spin fluctuations by 9% at $0K$, supporting the fact that the superconductivity is educed/destroyed due to the magnetic effect which is a consequence of pairing and depairing effect of AF spin fluctuations [222]. With the rising temperature, the difference between $\Delta_{1m}(T)$ and $\Delta_1(T)$ reduces continuously and near the transition temperature both the gap curves overlap at 39K. Presumably, the superconductivity and magnetism cannot coexist but exceptionally this convention weakens in the case of $La_{2-x}Sr_xCuO_4$ and the experiment exhibit the co-existence of AF spin fluctuations and superconductivity at low concentration (doping) in low-temperature regime. The present analysis thus supports the possible effects of the AF spin fluctuations on the SG. The change in the SG due to the AF spin fluctuations can also lead to the pairing symmetry up to some degree. However, the change in the SG observed maximum by 9% (at $0K$) at the optimum doping, therefore the change in pairing symmetry should be minimal which is discussed in chapter (4). The reduced gap ratio at 0K for $La_{2-x}Sr_xCuO_4$ is found as: $2\Delta_1/k_BT_c = 8.44$ which is a little bit higher than reduced gap ratio of HTS

and $2\Delta_{1m}/k_BT_c = 7.76$ and is close to the experimental value [219] ($2\Delta/k_BT_c = 7.7$) making the present formulation more and more reliable.

3.4 The Effect of Doping on Superconducting Gap

3.4.1 *Lattice Dynamics of $YBa_2Cu_3O_{7-\delta}$ and $La_{2-x}Sr_xCuO_4$*

The lattice dynamical calculations of the $YBa_2Cu_3O_{7-\delta}$ and $La_{2-x}Sr_xCuO_4$ is given using the MBMHP since it provides a significant insight into underlying physics of the phenomenon of superconductivity [173, 223]. The development of the lattice dynamics carried out in a very generalized way instead of numerically equal force constant environment. After a very precise calculation we observe that the interatomic force constant from the different layers of $YBa_2Cu_3O_{7-\delta}$ to the central atom Y and different layers of $La_{2-x}Sr_xCuO_4$ to the central atom Cu is not equal and therefore different set of force constants are calculated (in the subsequent sections). These calculated force constants further utilized to get the phonon dispersion relation (ω_k) via the dynamical matrix. The usual equation of motion of the lattice can be written as [164]

$$M\ddot{u}_\alpha(l) = -\sum_{\alpha,\beta} V_{\alpha\beta}(l,l')u_\beta(l') \tag{3.30}$$

this equation of motion yields the secular determinant for dynamical matrix $D_{\alpha\beta}(k)$ in the form

$$|D_{\alpha\beta}(k) - \omega^2\delta_{\alpha\beta}| = 0 \tag{3.31}$$

The Eq. (3.31) provides $3r$ branches (for r atom per unit cell), 3 of which are acoustical and $3r-3$ optical. The secular determinant for $YBa_2Cu_3O_{7-\delta}$ and $La_{2-x}Sr_xCuO_4$ crystal becomes

$$\begin{vmatrix} D_{xx} & D_{xy} & D_{xz} \\ D_{yx} & D_{yy} & D_{yz} \\ D_{zx} & D_{zy} & D_{zz} \end{vmatrix} = 0$$

The each element of above matrix is given as [224]:

$$D_{xx} = \frac{1}{\sqrt{M}} \sum_{l=1}^{N-1} \frac{\alpha_l x_l x_l}{\sqrt{M_l} r_l^2} (1 - exp(2\pi i \vec{k}.\vec{r_l})) \tag{3.32}$$

$$D_{xy} = \frac{1}{\sqrt{M}} \sum_{l=1}^{N-1} \frac{\alpha_l x_l y_l}{\sqrt{M_l} r_l^2} (1 - exp(2\pi i \vec{k}.\vec{r_l})) \tag{3.33}$$

$$D_{xz} = \frac{1}{\sqrt{M}} \sum_{l=1}^{N-1} \frac{\alpha_l x_l z_l}{\sqrt{M_l} r_l^2} (1 - exp(2\pi i \vec{k}.\vec{r_l})) \tag{3.34}$$

$$D_{yx} = \frac{1}{\sqrt{M}} \sum_{l=1}^{N-1} \frac{\alpha_l y_l x_l}{\sqrt{M_l} r_l^2} (1 - exp(2\pi i \vec{k}.\vec{r_l})) \tag{3.35}$$

$$D_{yy} = \frac{1}{\sqrt{M}} \sum_{l=1}^{N-1} \frac{\alpha_l y_l y_l}{\sqrt{M_l} r_l^2} (1 - exp(2\pi i \vec{k}.\vec{r_l})) \tag{3.36}$$

$$D_{yz} = \frac{1}{\sqrt{M}} \sum_{l=1}^{N-1} \frac{\alpha_l y_l z_l}{\sqrt{M_l} r_l^2} (1 - exp(2\pi i \vec{k}.\vec{r_l})) \tag{3.37}$$

$$D_{zx} = \frac{1}{\sqrt{M}} \sum_{l=1}^{N-1} \frac{\alpha_l z_l x_l}{\sqrt{M_l} r_l^2} (1 - exp(2\pi i \vec{k}.\vec{r_l})) \tag{3.38}$$

$$D_{zy} = \frac{1}{\sqrt{M}} \sum_{l=1}^{N-1} \frac{\alpha_l z_l y_l}{\sqrt{M_l} r_l^2} (1 - exp(2\pi i \vec{k}.\vec{r_l})) \tag{3.39}$$

$$D_{zz} = \frac{1}{\sqrt{M}} \sum_{l=1}^{N-1} \frac{\alpha_l z_l z_l}{\sqrt{M_l} r_l^2} (1 - exp(2\pi i \vec{k}.\vec{r_l})) \tag{3.40}$$

where $\vec{k} = k_x\hat{x} + k_y\hat{y} + k_z\hat{z}$, α_l is force constant between l^{th} atom to central atom, M

is the mass of central atom of unit cell, M_l is the mass of l^{th} atom, $\vec{r}_l$ is position vector of l^{th} atom from central atom, x_l, y_l and z_l are x, y and z component of position vector of l^{th} atom, respectively. The upper limit of summation $N-1$ is due to the fact that the central atom should not interact with itself. The computation of matrix element and consequently the eigenvalue (dispersion relation) of the determinant of a real system with a large number of the atom is a very tedious job and we have used modern technical computing system (Wolfram Mathematica). In chapter (2), using many-body quantum dynamics and Dyson's equation formalism the phonon Green's functions is developed by utilizing a generalized Hamiltonian that include the contribution of harmonic electron and phonon field and their interactions, phonon field anharmonicities and defects. Using the phonon dispersion relation (ω_k) in phonon's Green's functions [192] the renormalized electron-phonon dispersions ($\tilde{\omega}_{kq}$) are obtained in the representative HTS $La_{2-x}Sr_xCuO_4$ and $YBa_2Cu_3O_{7-\delta}$ that are further used to analyze the SG properties in the following sections.

3.4.2 Superconducting Gap Analysis in $La_{2-x}Sr_xCuO_4$

The model cuprate HTS $La_{2-x}Sr_xCuO_4$ has perovskite structure with different layers of LaO and CuO_2. To investigate the different interactions in unit cell of $La_{2-x}Sr_xCuO_4$, we have considered the Cu at the center of the unit cell which consist a mesh of 41 atoms. Using the MBMHP the second order force constant has been calculated from central Cu to different layers of unit cell namley; LaO and CuO_2. The third and fourth order average force constants have been calculated from Cu as central atom to entire mesh. Various physical constants of $La_{2-x}Sr_xCuO_4$ crystal used in the computation for the renormalized electron-phonon energy spectrum, are: lattice constants $a = 3.778\,\mathring{A}$, $b = 3.778\,\mathring{A}$ and $c = 13.266\,\mathring{A}$ [225], electron-phonon coupling constant $g_k = 0.7$, transition temperature $T_c = 37.5\,K$, phonon velocity $v_p = 5 \times 10^5\,\mathrm{cm\,s^{-1}}$, $\omega_Q = 3.0343 \times 10^{13}\,\mathrm{s^{-1}}$, $\omega_Q^c = 1.1783 \times 10^{14}\,\mathrm{s^{-1}}$. The second order force constant from central atom Cu to the different layers can be summarized as:

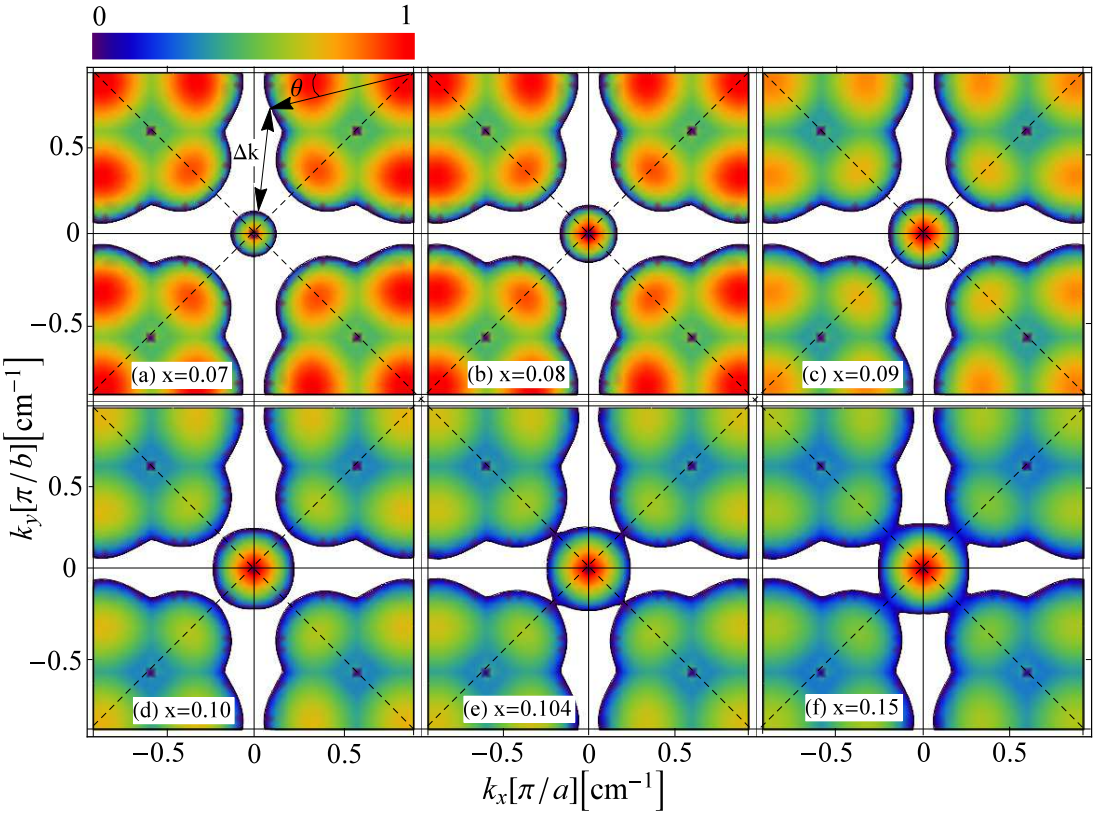

FIGURE 3.4: Renormalized electron-phonon dispersion plot for $La_{2-x}Sr_xCuO_4$ at different doping.

$Cu-CuO_2(0)$: $2.027\times10^3\,\mathrm{dyn\,cm^{-2}}$ (force constant between central atom and other oxygen atom in central layer), $Cu-LaO(I)$: $2.017\times10^3\,\mathrm{dyn\,cm^{-2}}$ (between central atom and first layer), $Cu-LaO(II)$: $1.943\times10^3\,\mathrm{dyn\,cm^{-2}}$ (between central atom and second layer), $Cu-CuO_2(III)$: $1.779\times10^3\,\mathrm{dyn\,cm^{-2}}$ (between central atom and third layer). Third and fourth order interaction force constant are $-5.360\times10^{11}\,\mathrm{dyn\,cm^{-3}}$ and $5.223\times10^{19}\,\mathrm{dyn\,cm^{-4}}$.

The renormalized electron-phonon dispersion ($\tilde{\omega}_{kq}$) plot of $La_{2-x}Sr_xCuO_4$ is shown in Fig. (3.4) at different doping level for $x = 0.07$ to 0.15 (optimal doping) at $T = 12K$ are not simple but show their dependence on several quantities such as electron-phonon interaction, doping, anharmonicities, and defects. The renormalized (quasi-particle) dispersion plots furnish the information of SG in momentum space through

quasi-particle Fermi surface. The Fermi surface (FS) angle (θ) has been specified via a traditional scheme in Fig. (3.4*a*) and the corresponding SG is measured as Δk in the momentum space. Employing the relation $\Delta = \hbar v_p \Delta k$, the equivalent the SG has been calculated, where v_p is quasiparticle velocity. It is quite obvious from these plots that the SG is highly anisotropic.

Doping Dependence of Nodal and Antinodal Superconducting Gap in $La_{2-x}Sr_xCuO_4$

Although the BCS theory has well explained the reduced gap of conventional superconductors ($R = 3.5$), the higher reduced gap value ($R = 5 - 8$) and doping dependence of gap in HTS [93–98, 103] may question the mechanism of superconductivity based on the BCS theory. There are theoretical attempts [226] to justify higher reduced gap ratio value using Bolgiubov de Greens (BdG) equation by eight band model [227, 228]. In the present work, we have measured the average SG with the help of the renormalized electron-phonon dispersion plot. The mass change parameter depends on doping (Sr in $La_{2-x}Sr_xCuO_4$) which leads to the drastic changes in renormalized dispersion. The estimated SG plot in Fig. (3.5) shows that SG increases with a decrease in doping and the SG decreases rapidly up to optimal doping and afterwards it decreases slowly with the increase in doping.

Apart from the SG, the appearance of the nodal and antinodal gap in HTS has been observed as a very complex and have distinct property [107]. Much theoretical work is available [229–231] but there is no comprehensive mechanism found which can interpret this energy scale scenario. The gap for nodal direction (FS angle $\theta = 45°$) and antinodal direction (FS angle $\theta = 0°$ or $90°$) is calculated in momentum space at different doping and plotted in Fig. (3.5). It is observed that the nodal gap remains zero up to doping for $x = 0.104$ and opens in underdoped regime ($x < 0.104$) which monotonically increases with the decrement of the doping in agreement with similar variation of Y. Peng *et al.* [232]. The antinodal gap also found increasing with

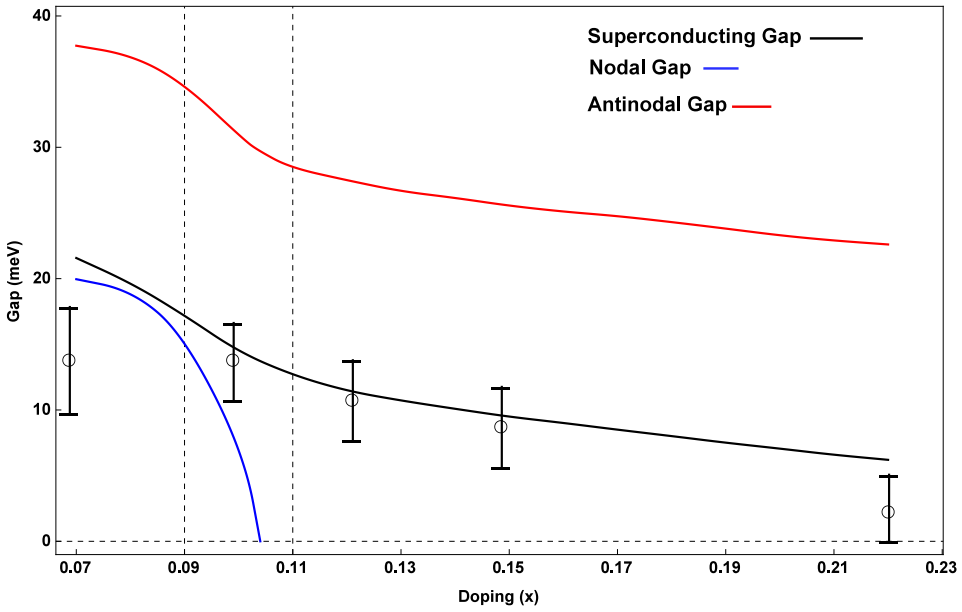

FIGURE 3.5: Variation of the nodal, antinodal and superconducting gap with the doping for $La_{2-x}Sr_xCuO_4$.

decreasing doping is in agreement with the theoretical study of M. Aichhorn *et al.* [233]. Although there are different methods to study this strange behaviour, the renormalized frequency produces similar results. Therefore it can be concluded that the anharmonicity and defect both play important role in this phenomenon.

3.4.3 Superconducting Gap Analysis in $YBa_2Cu_3O_{7-\delta}$

Similar to the analysis of SG in the previous section, the renormalized electron-phonon dispersion ($\tilde{\omega}_{kq}$) of $YBa_2Cu_3O_{7-\delta}$ are furnished in Fig. (3.6) at the optimum doping ($\delta_0 = 0.16$) in the momentum space. The quasiparticle dispersion curves give SG in momentum space (i.e. Δk) and using relation $\Delta = \hbar v_p \Delta k$ the corresponding SG has been calculated, where v_p is quasiparticle velocity. Various physical constants used for $YBa_2Cu_3O_{7-\delta}$ crystal are given as follows: lattice constants $a = 3.8227\mathring{A}$, $b = 3.8872\mathring{A}$ and $c = 11.6802\mathring{A}$, electron-phonon coupling constant $g_k = 0.7$, transition temperature $T_c = 92K$, phonon velocity $v_p = 5.5 \times 10^5\, cm\, sec^{-1}$,

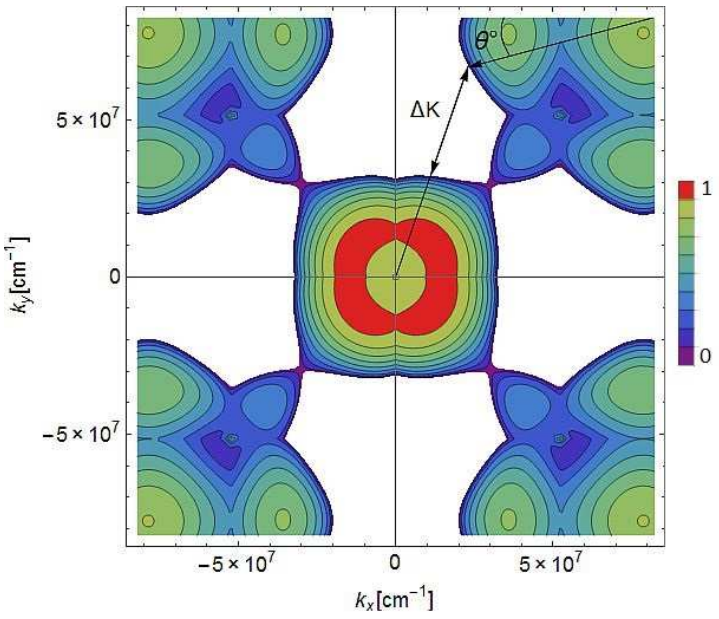

FIGURE 3.6: Renormalized electron-phonon dispersion plot for $YBa_2Cu_3O_{7-\delta}$ at optimum doping ($\delta = 0.16$).

$\omega_Q = 3.0343 \times 10^{13}\, sec^{-1}$, $\omega_Q^c = 1.1783 \times 10^{14}\, sec^{-1}$. The second order force constants of cental atom Y with different layers are: $Y - CuO_2$ $(1.633 \times 10^3\, dyn\, cm^{-2})$, $Y - BaO$ $(4.614 \times 10^3\, dyn\, cm^{-2})$ and $Y - CuO$ $(1.268 \times 10^3\, dyn\, cm^{-2})$, third and fourth order force constants are $-3.688 \times 10^{10}\, dyn\, cm^{-3}$ and $2.528 \times 10^{17}\, dyn\, cm^{-4}$, respectively.

Doping Dependence of Superconducting Gap in $YBa_2Cu_3O_{7-\delta}$

Using the renormalized electron-phonon dispersion plot of $YBa_2Cu_3O_{7-\delta}$, the HTS-reduced gap ratio Δ_R $(= 2\Delta/k_BT_c)$ with reduced doping δ_R $(= \delta/\delta_0)$ has been plotted in the Fig. (3.7) along with experimental data of Deutscher[93]. The obtained results are very close to the experimental results. However, Deustscher reports that Δ_c is associated with the coherence energy range of superconducting state whereas Szotek *et al.* [226] confirm that Δ_c is SG. Since we have taken the various interaction terms to investigate the superconducting gap which is in agreement to the experimental results. Therefore, we conclude that the pairing mechanism is a very

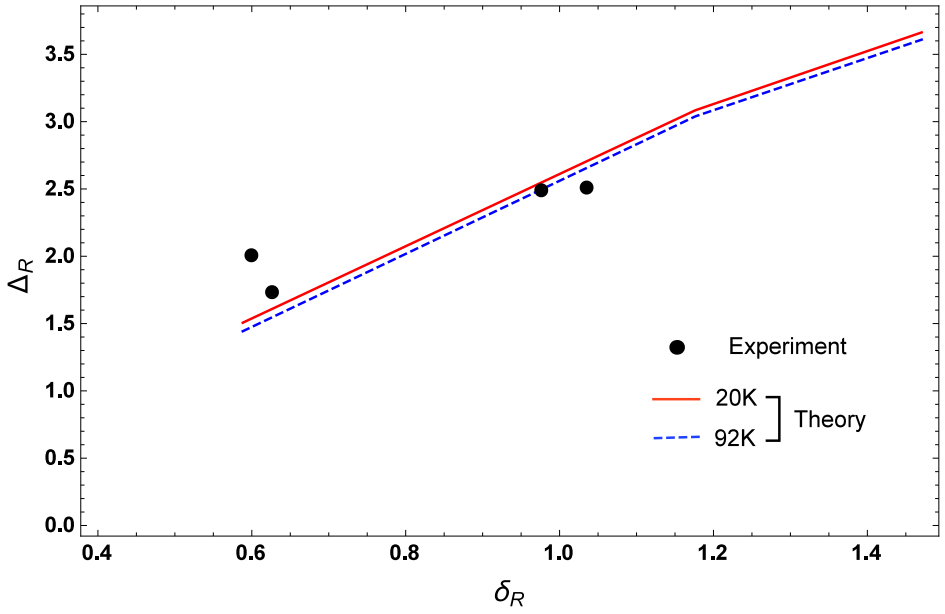

FIGURE 3.7: Variation of reduced superconducting gap with doping for $YBa_2Cu_3O_{7-\delta}$.

complex phenomenon in HTSC and the effect of the electron-phonon, anharmonicity and defects are essential in the pairon formation.

It should be noted that the SG in $YBa_2Cu_3O_{7-\delta}$ and $La_{2-x}Sr_xCuO_4$ have opposite nature of variation with doping. In the case of $YBa_2Cu_3O_{7-\delta}$, the SG shows increment the increasing doping, but in $La_{2-x}Sr_xCuO_4$ the SG decreases with increasing doping. The different behaviour of these two superconductor due to doping can be understand from the crystal structure. In the case of $La_{2-x}Sr_xCuO_4$, Sr act as a impurity atom which have Sr^{2+} state in compound form, but in $YBa_2Cu_3O_{7-\delta}$, O act as impurity atom which O^{2-} state in compound form. The oxidation state of impurity atoms in $La_{2-x}Sr_xCuO_4$ and $YBa_2Cu_3O_{7-\delta}$ are opposite, therefore their interaction with central atom of respective unit cell will be different duo to Coulombic term in the Born-Mayer-Huggins potential. In the case of $La_{2-x}Sr_xCuO_4$, the Coulombic interaction of impurity atom with central atom is $Cu^{2+} - Sr^{2+}$ while in $YBa_2Cu_3O_{7-\delta}$ the interaction of impurity atom with central atom is $Y^{3+} - O^{2-}$. These two different interaction change the phonon spectrum in different way with variation in

doping concentration, which consequently change the renormalized electron-phonon dispersion. This is the possible reason why the SG show opposite behaviour in $YBa_2Cu_3O_{7-\delta}$ and $La_{2-x}Sr_xCuO_4$ with change in doping.

3.5 The Pairing Potential

With the pairing potential being the prime requirement for pairon formation, the matrix elements for electron-phonon interaction are replaced by an averaged pairing (attractive) potential to simply the problem the in BCS theory. Qualitative analysis of the pairing potential for the HTS [234, 235] shows that the pairing potential leads to SG formation, but these results could not provide appropriate justification for the pairing potential. We take the advantage of the fact that the SG disappears just above T_c and the pairing potential can be obtained using the equations $\Delta_1(T) = \varepsilon_F - \frac{1}{2}[\tilde{\varepsilon}_k - \varepsilon_1]$ (Eq. (3.14)) and $\Delta_2(T) = \varepsilon_F - \frac{1}{2}\{\tilde{\varepsilon}_{qc} + V[\alpha(\tilde{\varepsilon}_k, \bar{\varepsilon}_q) + \gamma(\tilde{\varepsilon}_{qc}, \bar{\varepsilon}_q)] + \varepsilon_1\}$ (Eq. (3.15)). This leads to the condition just above critical temperature (at T_{c^+}) when both the SG gaps are vanished;

$$\Delta_1(T_{c^+}) = \Delta_2(T_{c^+}) = 0 \tag{3.41}$$

Using the Eqs. (3.14), (3.15) and (3.41) the following equation of V is obtained

$$V[\alpha(\tilde{\varepsilon}_k, \bar{\varepsilon}_q) + \gamma(\tilde{\varepsilon}_{qc}, \bar{\varepsilon}_q)] + \frac{2\alpha(\tilde{\varepsilon}_k, \bar{\varepsilon}_q)V(\tilde{\varepsilon}_k - \tilde{\varepsilon}_{qc})}{V[\alpha(\tilde{\varepsilon}_k, \bar{\varepsilon}_q) + \gamma(\tilde{\varepsilon}_{qc}, \bar{\varepsilon}_q)] - (\tilde{\varepsilon}_k - \tilde{\varepsilon}_{qc})} - (\tilde{\varepsilon}_k - \tilde{\varepsilon}_{qc}) = 0 \tag{3.42}$$

The solution of Eq. (3.42) gives the pairing potential in the form:

$$V_{\pm} = \frac{(\tilde{\varepsilon}_k - \tilde{\varepsilon}_{qc})\gamma(\tilde{\varepsilon}_{qc}, \bar{\varepsilon}_q) \pm (\tilde{\varepsilon}_k - \tilde{\varepsilon}_{qc})\sqrt{-\alpha(\tilde{\varepsilon}_k, \bar{\varepsilon}_q)[\alpha(\tilde{\varepsilon}_k, \bar{\varepsilon}_q) + 2\gamma(\tilde{\varepsilon}_{qc}, \bar{\varepsilon}_q)]}}{[\alpha(\tilde{\varepsilon}_k, \bar{\varepsilon}_q) + \gamma(\tilde{\varepsilon}_{qc}, \bar{\varepsilon}_q)]^2} \tag{3.43}$$

using

$$\frac{\alpha(\tilde{\varepsilon}_k, \bar{\varepsilon}_q)}{\gamma(\tilde{\varepsilon}_{qc}, \bar{\varepsilon}_q)} = R \tag{3.44}$$

where

$$R = \frac{(\tilde{\varepsilon}_{qc}^2 - \bar{\varepsilon}_q^2)^2(\varepsilon_k^4 - 4\tilde{\varepsilon}_k^2\varepsilon_{qc}^2)N(\varepsilon_{kc})}{\varepsilon_k\tilde{\varepsilon}_k(\tilde{\varepsilon}_k^2 - \bar{\varepsilon}_q^2)^2(\varepsilon_k^2 + 4\tilde{\varepsilon}_k\varepsilon_{qc} + \varepsilon_{qc}^2\tilde{\varepsilon}_k/\varepsilon_k)n_k} \tag{3.45}$$

Eq. (3.43) can be further simplified as:

$$V_{\pm} = \frac{(\tilde{\varepsilon}_k - \tilde{\varepsilon}_{qc})(1 \pm \sqrt{-R(2+R)})}{\gamma(\tilde{\varepsilon}_{qc}, \bar{\varepsilon}_q)(1+R)^2} \tag{3.46}$$

Eq. (3.46) is the general form of the pairing potential, which has complicated dependence on renormalized phonon and electron energy. For $YBa_2Cu_3O_{7-\delta}$ we obtained $R = -6.46 \times 10^{-9}$ at $T_c = 92K$ and hence $\sqrt{-R(2+R)} = 1.13 \times 10^{-4}$ which is much less than unity. Therefore, the approximated form of the pairing potential (for $YBa_2Cu_3O_{7-\delta}$) can be written as $V = (\tilde{\varepsilon}_k - \tilde{\varepsilon}_{qc})/\gamma(\tilde{\varepsilon}_{qc}, \bar{\varepsilon}_q)$. Using this expression, the pairing potential (V_{cal}) has been calculated for weak ($g_k \ll 1$), intermediate ($g_k \sim 1$) and strong ($g_k > 1$) coupling [236] for $YBa_2Cu_3O_{7-\delta}$ and summarized in Tab. (3.1). Using the EDOS of $YBa_2Cu_3O_{7-\delta}$ at the Fermi level [237], the pairing (attractive) potential (V_{BCS}) per unit cell has been calculated following the BCS approximation ($D(\varepsilon_F)V_{BCS} \simeq g_k$) at different g_k and the results are further summarized in Tab. (3.1). The obtained pairing potential (V_{cal}) is close to the BCS values for intermediate coupling, but slightly differs for weak and strong coupling. The temperature-dependent behavior of $\Delta_1(T)$ is shown in Fig. (3.8) at $g_k = 0.3$ using V_{cal} and V_{BMH} which predicts a slightly different value of T_c.

It is obvious from Fig. (3.8) that for $V_{cal} = 0.3655 \times 10^{-13}$ erg a lower T_c ($91.6K$) is obtained, which is close to the experimental results as compared to $V_{BMH} =$

g_k	0.3	0.5	0.7	1.0	1.5
$V_{cal}(\times 10^{-13}\,\mathrm{erg})$	0.3655	1.0154	1.9902	4.0615	9.1385
$V_{BCS}(\times 10^{-13}\,\mathrm{erg})$	1.3348	2.3081	3.2312	4.6162	6.9244

TABLE 3.1: Comparison of the pairing potential for $YBa_2Cu_3O_{7-\delta}$ at different coupling constant g_k.

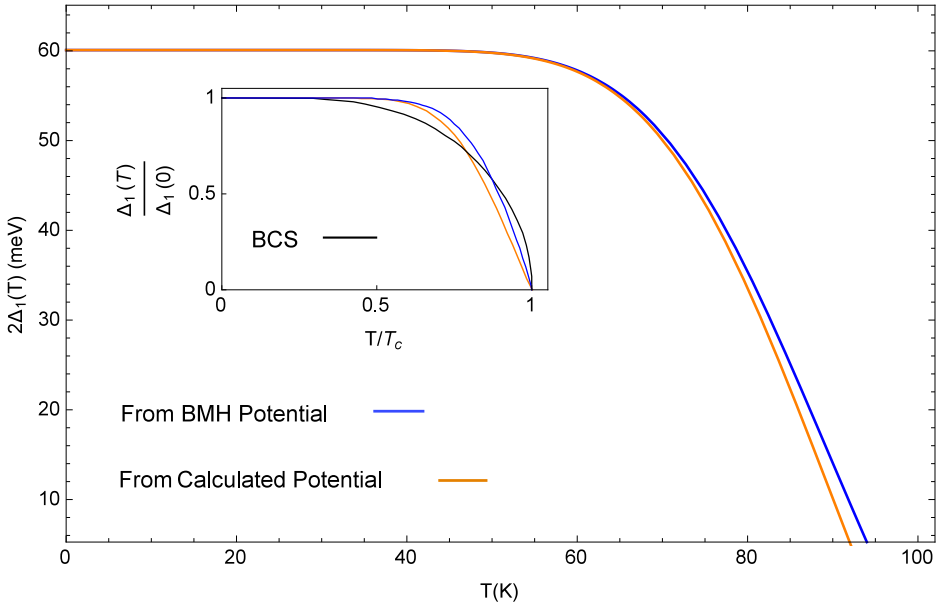

FIGURE 3.8: At $g_k = 0.3$, the SG $\Delta_1(T)$ plotted using BMH and calculated potential. Inset shows the normalized SG curve. Both SGs are in agreement with the BCS gap curve in the low temperature regime.

1.0410×10^{-12} erg, which gives the higher T_c $(93.8K)$. This suggests that the higher pairing potential is responsible for higher T_c from which it can be inferred that higher pairing potential strongly bound the pairons (Cooper-pair for the electronic system) and hence higher T_c. The dependence of T_c on the pairing potential ensures that by choosing a proper potential, there emerges the possibility of increasing the critical temperature T_c.

3.6 Conclusions

From the SG equation formulation and renormalized electron-phonon dispersion, the following conclusions are obtained. Based on many-body quantum dynamics of electrons and phonons the two SG equations have been successfully obtained via EDOS. Both $\Delta_1(T)$ and $\Delta_2(T)$ depend on temperature, Fermi energy and renormalized electron and phonon energies heralding the signatures of anharmonic effect on SG structure. Both SG equations predict the same $T_c = 93.8K$ (for $YBa_2Cu_3O_{7-\delta}$) from MBMHP, but $T_c = 91.6K$ from the calculated potential. At $g_k = 0.3$, the normalized gaps $\Delta_1(T)/\Delta_1(0)$ and $\Delta_2(T)/\Delta_2(0)$ are compared with the normalized BCS gap curve, which demonstrate the same variation in low-temperature region, but deviate near T_c. The reduced gap ratio (for $YBa_2Cu_3O_{7-\delta}$ $2\Delta_1(0)/k_BT_c = 7.2-7.5$) is found in the upper limit of gap ratio of HTS and the SG equations infer the anisotropic gap structure. General expressions for pairing potential are also obtained and numerically calculated for $YBa_2Cu_3O_{7-\delta}$, which is found close to the calculated pairing potential via BCS approach in intermediate coupling range, while it slightly deviates in the weak and strong coupling range. The results that the higher pairing potential responsible for higher T_c, opens a new window to explore the possibility to fabricate the new HTS with an elevated transition temperature. The SG gap equation derived including the effects of AF spin fluctuations along with electron-phonon interaction and analysed for $La_{2-x}Sr_xCuO_4$. It is found that that the SG is reduced by 9% at 0K and at the optimum doping. The addition of AF spin fluctuations in the SG formulation provides the reduced gap ratio ($2\Delta_{1m}/k_BT_c = 7.76$), which is much closer to experimental value ($2\Delta/k_BT_c = 7.7$).

Using Green's functions technique the renormalized electron-phonon dispersion is analysed for the $La_{2-x}Sr_xCuO_4$ and $YBa_2Cu_3O_{7-\delta}$. The SG analysis show that for the $La_{2-x}Sr_xCuO_4$, the SG found increasing with decreasing doping. The nodal and antinodal gap in $La_{2-x}Sr_xCuO_4$ also found increasing with decreasing doping but the nodal gap vanishes at the doping $x = 0.104$. In the case of $YBa_2Cu_3O_{7-\delta}$, the

SG found increasing with increasing doping. The different behaviour of SG with the doping in the $La_{2-x}Sr_xCuO_4$ and $YBa_2Cu_3O_{7-\delta}$ is due to their dopant atom.

Chapter 4

Anisotropic Superconducting Gap and Pairing Symmetry

"It doesn't matter how beautiful your theory is, it doesn't matter how smart you are. If it doesn't agree with experiment, it's wrong."

- - - Richard Feynman

Work presented in this chapter is partially published as follows:

1. Superconducting gap anisotropy and d-wave pairing in $YBa_2Cu_3O_{7-\delta}$.
   S. K. Verma, A. Gupta, A. Kumari, B. D. Indu.
   Int. J. Mod. Phys. B, **32**, 1850035 (2018).
   DOI: https://doi.org/10.1142/S0217979218500352.

2. The high-temperature superconductor gap equation.
   S. K. Verma, A. Kumari, A. Gupta, B. D. Indu.
   Phys. Scr., **94**, 035701 (2019).
   DOI: https://doi.org/10.1088/1402-4896/aafbc5.

3. Pairing symmetry, nodal and antinodal superconducting gap in $La_{2-x}Sr_xCuO_4$: A doping scenario.
   S. K. Verma, A. Gupta, A. Kumari, B. D. Indu.
   J. Low Temp. Phys., **196**, 442-457, (2019).
   DOI: https://doi.org/10.1007/s10909-019-02199-2.

4. Superconducting gap in cuprates high temperature superconductors.
   S. K. Verma, A. Kumari, A. Gupta, B. D. Indu.
   AIP Conf. Proc., **1953**, 120020, (2018).
   DOI: https://doi.org/10.1063/1.5033085.

5. Anisotropy in superconducting gap in $YBa_2Cu_3O_{7-\delta}$.
   S. K. Verma, A. Kumari, A. Gupta, B. D. Indu.
   AIP Conf. Proc., **1942**, 130036, (2018).
   DOI: https://doi.org/10.1063/1.5029106.

6. **S. K. Verma**, A. Gupta, A. Kumari, B. D. Indu, "Angular superconducting gap in $YBa_2Cu_3O_{7-\delta}$", 12th International Conference on Materials and Mechanisms of Superconductivity and High Temperature Superconductors, Beijing, China, August 19-24, (2018).

4.1 Introduction

The superconducting gap (SG) which defined as the energy separation between ground state and lowest excited state of the superconductor [174] formed in the close vicinity of the FS [119, 176–178] exhibit many interesting and mysterious properties. In a conventional superconductor the SG is symmetric around the FS, i.e., the SG is isotropic. The doping dependent SG was observed in HTS by several authors [93–98, 103] with highly anisotropic characteristics [103–106]. The anisotropy of SG is related to the pairing symmetry [196, 218, 238, 239]. In a conventional superconductor, the isotropic SG leads to the s- wave pairing symmetry while in cuprate HTS the anisotropic SG leads to dominant $d_{x^2-y^2}$ pairing states [196, 218, 238, 239]. The

above facts emphasize that the pairing symmetry of a superconductor is a kind of anisotropic assessment of the SG and consequently, from the study of SG the pairing symmetry of superconductor can be understood. The BCS theory successfully explains the formation of the s-wave pairing symmetry in the conventional superconductor. After the discovery of HTS, the elevated reduced SG ratio ($2\Delta/k_BT_c$) emerges in the range of 5-8 [47, 100–102]. Along with the high value of reduced SG ratio, the experimental observation strongly supports the dominant $d_{x^2-y^2}$ pairing symmetry in HTS [102–106, 240, 241] in contrast to the isotropic gap and s-wave pairing symmetry in the conventional superconductors. It is also observed that the pairing symmetry of HTS primarily exhibits a mixture of $d_{x^2-y^2}$ and s or d_{xy} ($< 5\%$) component [105, 242] along with the effect of doping which is worked out in underdoped and overdoped regimes [105]. The phase of the SG for bound pairs is measured using two superconducting-normal-superconducting (S-N-S) sandwich by Wallman *et al.* [78] and nearly π phase shift is observed in $YBa_2Cu_3O_{7-\delta}$ while in conventional superconductors no such phase shift is observed. The phase sensitive technique settled the controversy of pairing symmetry in the favour of predominant $d_{x^2-y^2}$-wave pairing symmetry for a number of optimal hole and electron-doped cuprate [238, 239]. The existence of $d_{x^2-y^2}$ pairing symmetry in HTS cuprate have many implications on its physical properties. The SG along $\theta = 0°$ (or $90°$), i.e., along [100] (or [010]) direction is maximum, while along $\theta = 45°$, i.e., along [110] direction is minimum (not necessarily zero), where θ being the FS angle.

The nodal and antinodal SG have been evidenced by a large number of experimental out come that describe the fundamental characteristics of the SG structure in cuprate HTS [232, 243–245]. The electronic Raman spectroscopy (ERS) is a powerful tool to probe quasiparticle study in the superconducting state in the nodal and antinodal region where the amplitude of SG reaches its maximum (antinodal gap)value and vanishes (nodal gap) otherwise, respectively [239, 246]. Various experiments on antinodal gap studies using ARPES [247] and ERS [246, 248–251] show that it monotonically increases as one goes deeply into the underdoped regime. The

behaviour of the nodal SG with doping shows very ambiguous nature. There are experimental results showing monotonic increment in the nodal gap with decreased doping and become zero for optimum doping case [232] while other evidence shows a non-monotonic variation in the nodal gap with doping [251]. It is also believed that nodal and antinodal gaps are correlated [252]. The appearance of the nodal and antinodal SG in HTS makes it more difficult to understand the mechanism of HTSC and these anomalies could not be resolved by BCS theory. Several efforts [213, 218, 253–257] have been made to interpret this mechanism of HTSC but the success is still awaited. Further, the experimental evidence shows that the nodal SG becomes non-zero with small in magnitude if superconductor is in the sate other than optimal doping, e.g., in $YBa_2Cu_3O_{7-\delta}$ the nodal SG becomes non-zero in the underdoped and overdoped regime [106] while in $La_{2-x}Sr_xCuO_4$ the nodal SG becomes zero in the overdoped region [241]. It is observed that the nodal SG emerges as a key point to decide the presence of other components of pairing symmetry (s or d_{xy}) [238, 239]. For pure $d_{x^2-y^2}$ pairing symmetry the SG along the nodal direction is zero for optimal doping, which makes the thermodynamics properties thoroughly distinct [107, 258] from those of conventional superconductors. The presence of non-zero SG along nodal direction prove that there are other components (s or d_{xy}) along with the pure $d_{x^2-y^2}$ pairing symmetry and the general state of the superconductor are in the mixed state [239]. It is generally defines as $\Delta_{mix} = \Delta_{d_{x^2-y^2}} + is$ or $\Delta_{mix} = \Delta_{d_{x^2-y^2}} + id_{xy}$, in the form of order parameter [239]. There are theoretical approaches to explain this unique character of high T_c cuprate superconductor, the famous one is Hubbard model [258] which describes electron hoping on a lattice parameterized in terms of the bandwidth $W = 8t$ (where t is the measure of hoping energy) and on-site electron-electron repulsion U. In the copper oxide, U and W are compared and the approximate solution of the doped Hubbard model invariably point to a $d_{x^2-y^2}$-pairing state.

The pairing mechanism is also influenced by antiferromagnetic (AF) spin fluctuations in some cuprate superconductors at low temperature and low doping concentrations,

e.g., in $La_{2-x}Sr_xCuO_4$ [120–122, 194, 195]. The presence of antiferromagnetic phase with the superconducting phase in low temperature and low doping regime is a mysterious phenomenon. The experimental observations [120–122] of the AF phase along with superconductivity certainly motivate to study this strange behaviour. In chapter (3), the effect of AF spin fluctuations have been described on the SG. As discussed above that the study of SG leads to the understanding of pairing symmetry, therefore, the effect of AF spin fluctuations on pairing symmetry is analyzed via the effect of AF spin fluctuations on the SG. The detailed study of the impact of AF spin fluctuations on the SG which is already available in the chapter (3), the effect of AF spin fluctuations on pairing symmetry is further studied in the present chapter.

The study of pairing symmetry and anisotropy of the SG in the present chapter is based on the renormalized electron-phonon dispersion for the model cuprates, namely, $YBa_2Cu_3O_{7-\delta}$, and $La_{2-x}Sr_xCuO_4$ HTS. The anisotropy in the SG has been directly observed from the renormalized electron-phonon dispersion itself. Further, the pairing symmetry studied via angular parametric plot the SG obtained from the renormalized electron-phonon dispersion. The doping dependent renormalized electron-phonon dispersion leads to the doping dependent anisotropy in the SG and consequently doping dependent pairing symmetry in $YBa_2Cu_3O_{7-\delta}$ and $La_{2-x}Sr_xCuO_4$. The effect of AF spin fluctuations on pairing symmetry in $La_{2-x}Sr_xCuO_4$ has been analyzed via the effect of AF spin fluctuations on the SG in $La_{2-x}Sr_xCuO_4$. In $YBa_2Cu_3O_{7-\delta}$ such effect are either minimal or absent [193], therefore the effect of AF spin fluctuation on pairing symmetry is not considered for $YBa_2Cu_3O_{7-\delta}$.

4.2 Angular Superconducting Gap

Various experiments [103–106] reveal the strong anisotropic nature of SG in HTS. In the momentum space for the FS angle θ, it is spotted that gap magnitude is

maximal along $\theta = 0°$ (and $\theta = 90°$) referred to as antinodal gap and minimal (not consistently zero) along $\theta = 45°$ known as the nodal gap. Here the angular nature of SG has been investigated with the help of renormalized electron-phonon dispersion of $La_{2-x}Sr_xCuO_4$ and $YBa_2Cu_3O_{7-\delta}$ and are given in the subsequent sections.

4.2.1 Angular Superconducting Gap in $La_{2-x}Sr_xCuO_4$

By measuring the gap (Δk) in momentum space (in k_xk_y plane) with respect to FS angle from the renormalized electron-phonon dispersion plot of $La_{2-x}Sr_xCuO_4$ and using relation $\Delta = \hbar v_p \Delta k$, the SG been converted into energy scale. The Δk drops to zero along $k_x = \pm k_y$ direction at doping $x = 0.104$ and in overdoped regime (Fig. (3.4)), which is fundamental characteristic of $d_{x^2-y^2}$ symmetry gap function. However in underdoped regime Δk becomes non zero along $k_x = \pm k_y$ and forms a nodeless gap which indicates the presence of s or d_{xy} type of pairing state. The angular gap plotted in Fig. (4.1) as a function of FS angle (θ) for the doping $x = 0.08, 0.09, 0.10, 0.105$ and has been observed a v- shaped gap which is in agreement with experimental results of Shi *et al.* [240] (for $x = 0.105$) and Razzoli *et al.* [241] (for $x = 0.08$). The experimental measurement of SG with FS angle shows that it also depends on doping [240] introducing even further complexity. The change in doping leads to change in renormalized electron-phonon dispersion plot via mass change parameter and change in the SG observed accordingly. Further, the angular gap plotted in Fig. (4.2) as a function of d-wave order parameter $|cos(k_xa) - cos(k_ya)|/2$ which are in well agreement with experimental results of Yoshida *et al.* [102] for $x = 0.10, 0.15$.

4.2.2 Angular Superconducting Gap in $YBa_2Cu_3O_{7-\delta}$

Utilizing the same method as in case of $La_{2-x}Sr_xCuO_4$, the anisotropy in the SG studied from the renormalized electron-phonon dispersion plot of $YBa_2Cu_3O_{7-\delta}$ (Fig.

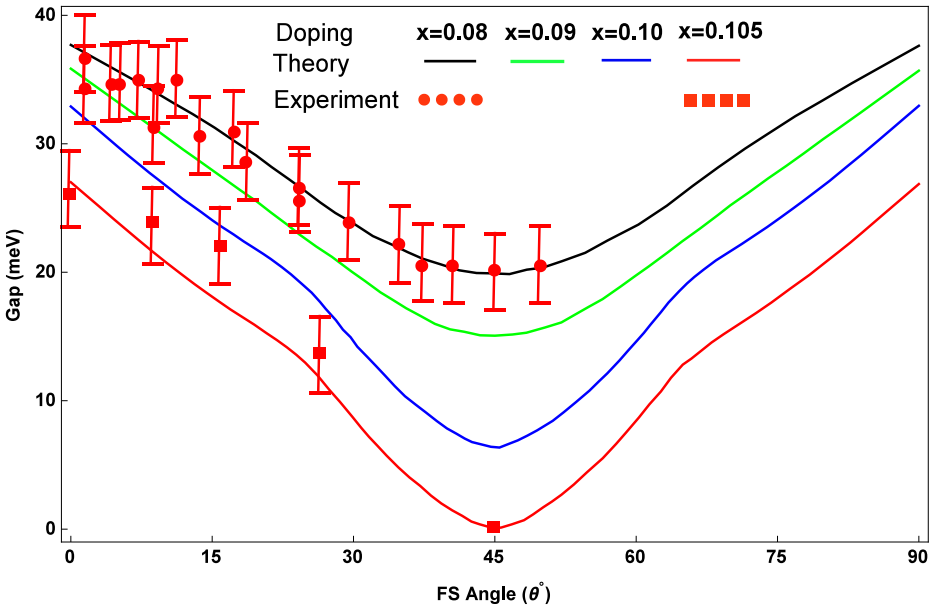

FIGURE 4.1: Angular gap for $La_{2-x}Sr_xCuO_4$ as function of FS angle ($\theta°$).

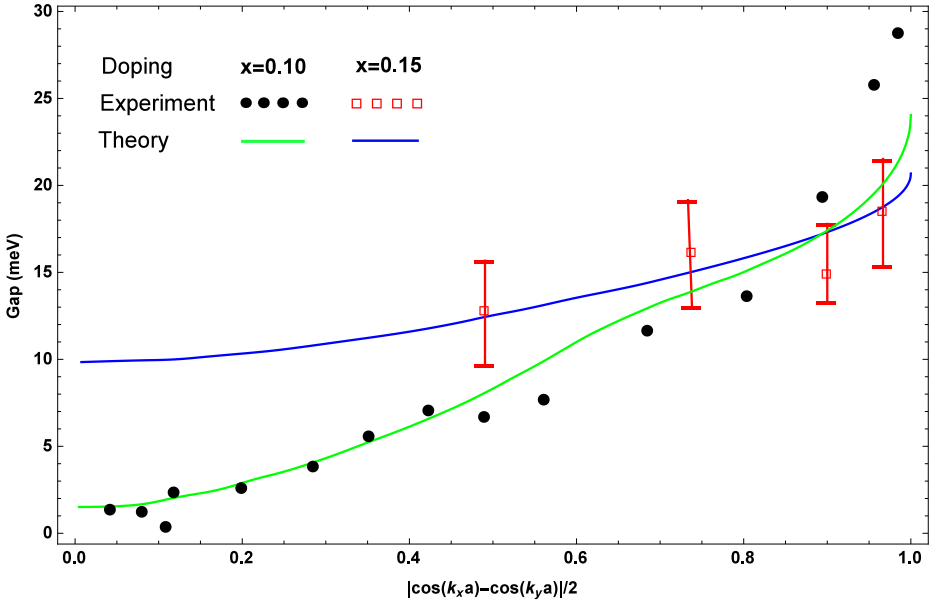

FIGURE 4.2: Angular gap for $La_{2-x}Sr_xCuO_4$ as function of d-wave order parameter $|cos(k_x a) - cos(k_y a)|/2$.

(3.6)). The Δk drops to zero along $k_x = \pm k_y$ direction at optimum doping ($\delta_0 = 0.16$), but in underdoped and overdoped regime Δk becomes non zero along $k_x = \pm k_y$ and forms a nodeless gap which indicates the presence of s or d_{xy} type of pairing state. Energy gap or superconducting order parameter being fundamental characteristics of HTS duly figure out its highly anisotropic behaviour [79, 259, 260]. The present investigations based on quasiparticle renormalized frequency contours (Fig. (3.6)) exhibit substantial variation in energy gap in different directions confers the signature of anisotropic behaviour of superconducting energy gap. The variation of gap with FS angle (θ°) as evidenced from the contour plot of $YBa_2Cu_3O_{7-\delta}$ that enables to plot the calculated the SG values with two different experimental methods [106], namely, superconducting peak (SCP) and leading - edge midpoint (LEM). A v-shape of gap has been observed (Fig. (4.3)) with a node (zero gap) in [110] (at $\theta = 45^\circ$) direction for optimum doping ($\delta = 0.16$) and maximum gap at antinode in [100] and [010] directions which is consistent with the experimental observations [106]. A careful study of angular gap with different doping concentrations shows that there emerges a small opening of gap at nodal point where the gap assumes to be zero making a nodeless SG and this possibility has also been emphasized by Ming-Qiang Ren *et al.* [261]. As discussed earlier, the small gap at nodal point can be attributed to the presence of s or d_{xy} type of gap mixed with pure $d_{x^2-y^2}$ gap and varies with doping concentration. It is clear from Fig. (4.3) that the nodal gap increases in underdoped and overdoped regime which infers that the presence of s or d_{xy} type of gap tend to increase away from optimum doping. The angular gap plotted in Fig. (4.4) as a function of d-wave order parameter $|cos(k_x a) - cos(k_y a)|/2$ along with the experimental results of Schabel *et al.* [103]which are in good agreement.

In both cuprates, $YBa_2Cu_3O_{7-\delta}$ and $La_{2-x}Sr_xCuO_4$, the plot of SG with the FS angle gives a v- shape of SG with the resemblance of experimental data. It should be noted that the anisotropy depend on doping differently in $YBa_2Cu_3O_{7-\delta}$ and $La_{2-x}Sr_xCuO_4$. In the case of $La_{2-x}Sr_xCuO_4$ it is found that the along nodal direction ($\theta = 45$) the SG increases with decreasing doping while in $YBa_2Cu_3O_{7-\delta}$ the

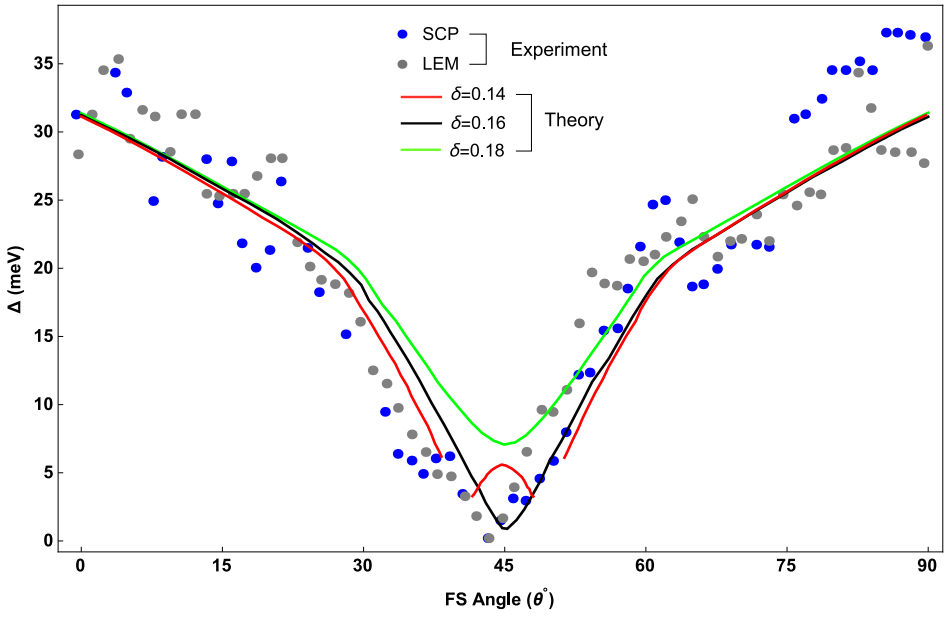

FIGURE 4.3: Variation of superconducting gap with the FS angle ($\theta°$) for $YBa_2Cu_3O_{7-\delta}$ at 20K (at $\delta = 0.14, 0.16, 0.18$) along with experimental gap observed for two different method SCP and LEM.

SG increases with increasing doping. This is because of the different ionizing state of dopant as discussed in the chapter (3).

4.3 Pairing Symmetry in High Temperature Superconductor

Pairing symmetry of superconductor is a measure of anisotropy in the SG. The $d_{x^2-y^2}$-wave pairing symmetry is the reflection of a highly anisotropic nature of SG. We use graphical method [196, 218] to examine the pairing symmetry in $La_{2-x}Sr_xCuO_4$ and $YBa_2Cu_3O_{7-\delta}$. A parameter $d = f(\Delta_\theta, \theta)$ is plotted at different doping level in angular coordinate system where Δ_θ is the magnitude of SG at FS angle θ (in degree) which give a dominated $d_{x^2-y^2}$ type of pairing symmetry along with the s (or d_{xy}) pairing state.

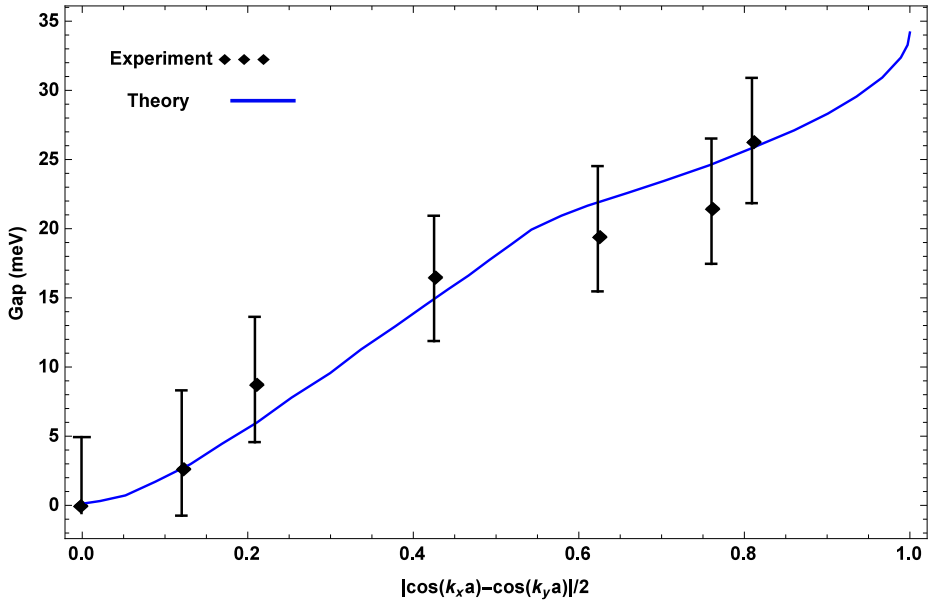

FIGURE 4.4: Angular gap for $YBa_2Cu_3O_{7-\delta}$ as function of d-wave order parameter $|cos(k_x a) - cos(k_y a)|/2$.

4.3.1 Pairing Symmetry in $La_{2-x}Sr_xCuO_4$

The experimental analysis of $La_{2-x}Sr_xCuO_4$ show that at $x = 0.105$ nodal gap is zero [240] but it become non zero at $x = 0.08$ [241] implying the presence of s or d_{xy} pairing state along with pure $d_{x^2-y^2}$ pairing symmetry and superconductor are in mixed state. The parameter $d = f(\Delta_\theta, \theta)$ is plotted at different doping for $La_{2-x}Sr_xCuO_4$: the inset (a) to (e) of Fig. (4.5). The inset (a) to (e) of Fig. (4.5) represents the evolution of d-wave pairing as function of doping. At doping level $x = 0.104$ the nodal gap become zero and a pure $d_{x^2-y^2}$ type of symmetry observed. In underdoped region the nodal gap increasing with decrease in doping consequently the presence of s or d_{xy} component increases. The numerical estimation (with the help of graphical method) of component of s or d_{xy} (Υ in %) is done at different doping levels without considering AF spin fluctuations, which are listed in Tab. (4.1) and plotted in Fig. (4.5). It is observed that variation of Υ component with doping is non-linear which shows that doping has non-linear effect on $d_{x^2-y^2}$ pairing symmetry. Since above $x = 0.104$ the nodal gap is always zero and therefore we

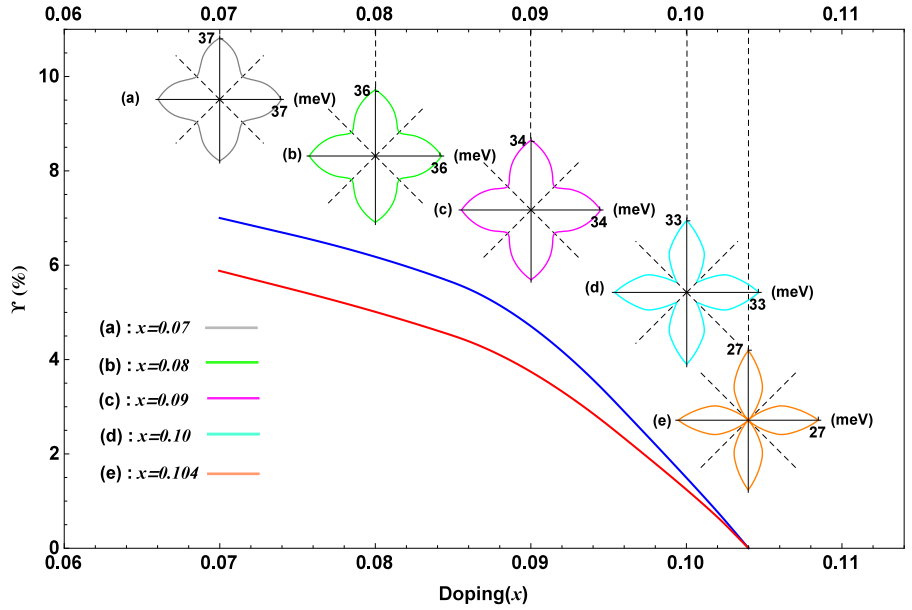

FIGURE 4.5: Variation of s or d_{xy}-wave component for $La_{2-x}Sr_xCuO_4$ with doping in the absence of AF spin fluctuations (blue curve) and in the presence of AF spin fluctuations (red curve). The insets, (a) to (e) represent pairing symmetries at different doping without AF spin fluctuations.

conclude that above $x = 0.104$ a pure $d_{x^2-y^2}$ pairing state exists. The effect of AF spin fluctuations on component s or d_{xy} is discussed in section (4.4).

x	0.07	0.08	0.09	0.10	0.104
Υ(without AF)	6.9958	6.1784	4.90815	1.4956	0
Υ(with AF)	5.8688	5.0021	3.7362	1.2417	0

TABLE 4.1: Percentage of Υ (s or d_{xy}) at different doping (x) for $La_{2-x}Sr_xCuO_4$.

4.3.2 Pairing Symmetry in $YBa_2Cu_3O_{7-\delta}$

However, the poorly understood pairing symmetry in HTS opened the debate [78, 104, 238, 239, 262, 263] that it is mainly dominated by $d_{x^2-y^2}$ in HTS cuprate, e.g., $YBa_2Cu_3O_{7-\delta}$. Various experimental results [104, 105, 239, 242, 264, 265] which implicated the presence of very small component ($< 5\%$) of s or d_{xy} pairing symmetry along with $d_{x^2-y^2}$ and its doping dependence [262]. A deeper insight

on the pairing symmetry (including deviations) in the underdoped and overdoped regions for different levels of doping is achieved by plotting the anisotropic SG in the angular coordinate system; the inset (a) and (c) of Fig. (4.6). An ideal $d_{x^2-y^2}$ type gap obtained for optimum doping $\delta_0 = 0.16$; the inset b of Fig. (4.6). These results address the presence of extended s-wave in the underdoped region while $d_{x^2-y^2}+i\Upsilon$ (Υ may be s or d_{xy}) in overdoped regime. Percentage of extended s-wave components in the underdoped ($0.11 < \delta < \delta_0$) and imaginary component Υ in overdoped ($\delta_0 < \delta < 0.21$) regime for different doping level has been calculated and summarized in the Tab. (4.2). The Fig. (4.6) depicts present results of variation of percentage of extended s and Υ-wave component with doping which figure out that these variations are not monotonic. The superconducting state drived from one phase (underdoped regime) enters the other phase (overdoped regime) for doping variation of $\delta = 0.12$ to 0.20. Such phase transition of HTS near optimum doping confirms the existence of quantum critical point (QCP) in $YBa_2Cu_3O_{7-\delta}$ [266, 267]. For $0.11 < \delta < 0.21$ theory provides maximum 2.5% s-wave component in underdoped and 2.7% s or d_{xy} in overdoped scenario which is within the limit ($< 3\%$) of experimental observations [105, 242].

The study of pairing symmetry in $La_{2-x}Sr_xCuO_4$ and $YBa_2Cu_3O_{7-\delta}$ show that the pairing symmetry in both cuprate HTS have dominating $d_{x^2-y^2}$ pairing state with the presence of component of s (or d_{xy}). In both cuprates HTS, the pairing symmetry depends on doping. In the case of $YBa_2Cu_3O_{7-\delta}$, an ideal $d_{x^2-y^2}$ pairing state found at the optimum doping but as one move from the optimum doping the presence of s (or d_{xy}) component increases. In case of $La_{2-x}Sr_xCuO_4$, as one move towards the underdoped regime the presence of s (or d_{xy}) component increases while in the overdoped regime an ideal $d_{x^2-y^2}$ pairing state remains.

$\delta(<\delta_0$, underdoped)	% of extended s	$\delta(>\delta_0$, overdoped)	% of Υ
0.12	2.56	0.17	0.08
0.13	1.36	0.18	0.44
0.14	0.52	0.19	1.73
0.15	0.09	0.20	2.79

TABLE 4.2: Percentage of extended s and Υ at different doping for $YBa_2Cu_3O_{7-\delta}$.

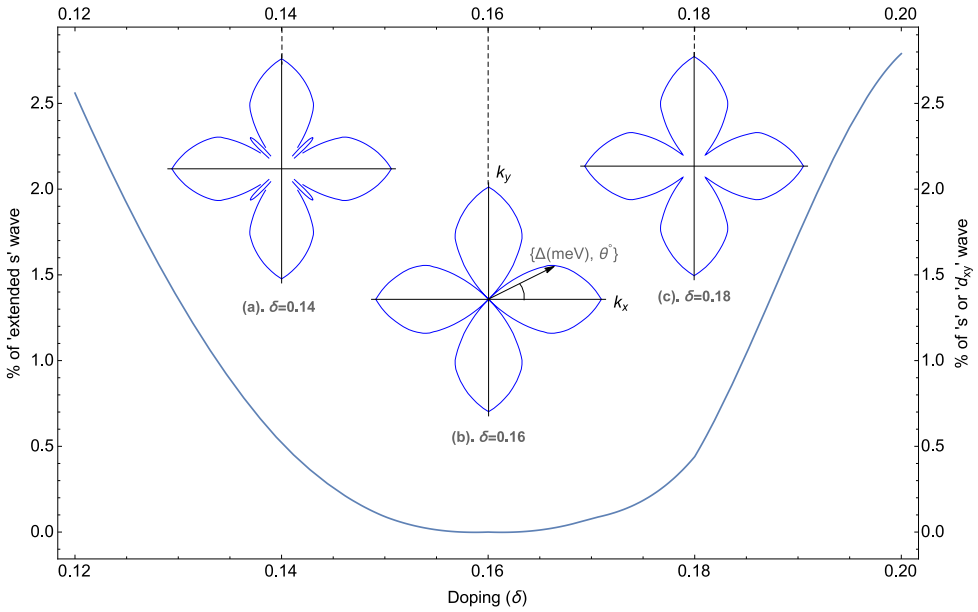

FIGURE 4.6: Variation of extended s-wave and s (or d_{xy})-wave component for $YBa_2Cu_3O_{7-\delta}$ with doping. The inset (b) represent ideal $d_{x^2-y^2}$ type of gap at $\delta = 0.16$ while (a) and (c) represents $d_{x^2-y^2}$ type of gap with some deviation at $\delta = 0.14$, 0.18 respectively.

4.4 Effect of Antiferromagnetic Spin Fluctuations on Pairing Symmetry

The co-existence of magnetic order with superconductivity is a surprising phenomenon since magnetism has a natural tendency to destroy the superconductivity. However, there are plenty of experimental facts available that confess the co-existence of AF spin fluctuations and superconductivity. Such phenomenon found in the low temperature and weak doping or near to optimum doping [120–122, 194, 195, 219]. The pairing symmetry studied in the previous section only considered the

electron-phonon interaction, anharmonicity, and defect via renormalized electron-phonon dispersion. In chapter (3), the effect of AF spin fluctuations on the SG has been studied with the newly derived SG equations. The presence of A_m in the SG equation is the direct link to the fact that the SG and consequently, pairing symmetry is directly affected by the AF spin fluctuations. Since our pairing symmetry study based on the information of SG, therefore, the effect of AF spin fluctuation on pairing symmetry worked out using the fact that the AF spin fluctuations have effects on the SG. The detailed treatment of AF spin fluctuation is given in the chapter (3). There are some cuprate HTS that have characteristics of AF spin fluctuation with superconductivity like $La_{2-x}Sr_xCuO_4$ and in some cuprate such effect are either minimum or absent like in $YBa_2Cu_3O_{7-\delta}$. In the present case the effect of AF spin fluctuations worked out for $La_{2-x}Sr_xCuO_4$. The temperature dependence of $\Delta_{1m}(T)$ and $\Delta_1(T)$ for $La_{2-x}Sr_xCuO_4$ at optimal doping $x = 0.15$ is depicted in the chapter (3) (Fig. (3.3)). A reduction in SG is observed due to the influence of AF spin fluctuations by 9% at $0K$, supporting the fact that the superconductivity is educed/destroyed due to the magnetic effect which is a consequence of pairing and depairing effect of AF spin fluctuations [222]. With rising temperature difference between $\Delta_{1m}(T)$ and $\Delta_1(T)$ reduces continuously and near transition temperature both the gap curves overlap at 39K. Presumably, the superconductivity and magnetism cannot coexist but exceptionally this convention weakens in case of $La_{2-x}Sr_xCuO_4$ and experimental exhibit the co-existence of AF spin fluctuations and superconductivity at low concentration (doping) in low-temperature regime. The present analysis thus supports the possible effects of AF spin fluctuations on SG. The change in SG due to AF spin fluctuations leads to the change in pairing symmetry up to some degree. However, the change in SG observed maximum by 9% (at $0K$) at optimum doping, therefore the change in pairing symmetry should be minimal. The reduction in SG due to AF spin fluctuations leads to change in the component of s or d_{xy}, i.e., it affects the pairing symmetry. The percentage of s or d_{xy} component calculated considering the reduction in SG due to AF spin fluctuations at the different doping level which is given in Tab. (4.2) and plotted in Fig. (4.5). It should be noted

that the presence of AF suppresses the s or d_{xy} component. Therefore it can be concluded that the AF spin fluctuations endorse the $d_{x^2-y^2}$ pairing symmetry.

4.5 Conclusions

From the study of anisotropic SG and pairing symmetry in HTS cuprates $La_{2-x}Sr_xCuO_4$ and $YBa_2Cu_3O_{7-\delta}$ via renormalized electron-phonon dispersion the following conclusion has been pointed out. The plot of SG as a function of FS angle (θ) gives a v-shape confessing the anisotropicity of the SG in $La_{2-x}Sr_xCuO_4$ and $YBa_2Cu_3O_{7-\delta}$. The plot of SG as a function order parameter $|cos(k_xa)-cos(k_yb)|$ confirms the highly anisotropic nature of SG in both the cuprate HTS. It is found that the anisotropy also affected by the doping.

In the case of $La_{2-x}Sr_xCuO_4$ a dominating $d_{x^2-y^2}$ pairing symmetry observed along with the existence of Υ (s or d_{xy} component) in the underdoped regime which also affected by doping in the non-linear fashion. The maximum magnitude of component Υ (s or d_{xy} component) found as 6% and 7% in the presence and absence of AF spin fluctuation, respectively. It is observed that from doping $x = 0.104$ towards the optimum and overdoped regime, the pairing symmetry follows pure $d_{x^2-y^2}$. In chapter (3), it is seen that the nodal and antinodal SG change rapidly from the doping level $x = 0.09$ to 0.11 and the pairing symmetry also change rapidly in the same doping range. Therefore, it is apparent that there exists a rapid phase transition in the $La_{2-x}Sr_xCuO_4$ in the doping range of $x = 0.09$ to 0.11.

Further, in the case of $YBa_2Cu_3O_{7-\delta}$ a dominant $d_{x^2-y^2}$ type of pairing symmetry is observed at optimum doping with node in $k_x = \pm k_y$ direction. The node disappears in the underdoped and overdoped regime confirming the possibility of nodeless SG. An ideal $d_{x^2-y^2}$ pairing symmetry observed at optimum doping with the presence of a very small component of extended s-type pairing symmetry in the underdoped regime which signified increases up to 2.5% with the decrease in doping. On the

other hand in the overdoped regime presence of s (or d_{xy}) pairing symmetry is established and its weight also increases up to 2.7% as doping is increased. It emerges from the present formulation that the study of superconducting gap, anisotropy and pairing symmetry can be successfully made for a wide spectrum of underdoped and overdoped regions with a sound inference about the existence of QCP at optimum doping $\delta = 0.16$ for $YBa_2Cu_3O_{7-\delta}$.

The renormalized electron-phonon dispersion which is heavily influenced by anharmonicities, impurities (defects) and their interference leads to the successful explanation of pairing symmetry therefore, it can be pointed out that electron-phonon interaction, anharmonicity, and defects are essential for pair formation in HTS in $YBa_2Cu_3O_{7-\delta}$ while in the case of $La_{2-x}Sr_xCuO_4$ an additional quantity, the AF spin fluctuations also participate in the pair formation.

Chapter 5

Theory of Renormalized Phonon Group Velocity in High Temperature Superconductors

"Natural science, does not simply describe and explain nature; it is part of the interplay between nature and ourselves."

- - - Werner Heisenberg

Work presented in this chapter is partially published as follows:

1. Theory of renormalized phonon group velocity in high temperature superconductors.
   S. K. Verma, A. Gupta, A. Kumari, B. D. Indu.
   Mod. Phys. Lett. B, 1950337, (2019).
   DOI: https://doi.org/10.1142/S0217984919503378.

5.1 Introduction

The interaction of electrons and phonons is the key to understand the mechanism of both the conventional and high temperature superconductivity. Unlike conventional

superconductors the HTS exhibit strange behavior like antiferromagnetic state [120–122, 195, 268] and doping dependent superconducting state [93, 94, 96, 262, 269, 270]. It is experimentally observed that the coupling of an electron with phonon change the electron velocity as well as scattering rate when the electron energy is close to the phonon energy [109]. Gadermaier *et al.* [110] figure out the importance of electron-phonon interaction in superconductivity pairing mechanism based on the determination of electron-relaxation time via pump-prob optical spectroscopy. Therefore, it is fair to say that even the BCS theory can't explain these features of HTS, the role of electron-phonon interactions [109–112] still remain important factor in the understanding of HTSC. The effect of anharmonic phonons on superconducting phenomenon evaluated by Vincent *et al.* [114] while examining the anharmonic effects on reduced gap ratio $2\Delta/k_BT_c$ with the conclusion that the reduced gap ratio was increased by 5 -10 % due to anharmonicity. In the case of multi-gap superconductivity in MgB_2 the electron-phonon coupling was determined with the conclusion that the phonon are strongly anharmonic in pairing phenomenon [115]. The anharmonic effects on superconductivity has also been confirmed by several experiments in cuprate HTS[116]. The various studies of anharmonic effects [113–118] in superconductivity show that the anharmonicity plays an important role in determining the dynamical as well as superconducting properties of cuprate HTS and therefore the contribution of anharmonicity must be taken into account in any theoretical formalism. The importance of phonon is further seen in terms of change in T_c in various cuprate HTS as one substitute ^{18}O with ^{16}O implying the contribution of phonon in pairing mechanism [271–277].

It is observed that the in-plane electronic transport of bipolarons is largely affected by the acoustic phonon due to scattering [135]. Alexandrov [143] show that the anisotropic sound velocity in crystal are responsible for phonon mediated attraction of electron that provides unconventional Cooper pair as well as for the *d*- wave pairing symmetry in cuprate superconductor. Experiments also reveal that the lattice thermal conductivity of HTS depends on doping concentration [94, 278]. Among

the many properties of cuprate HTS like large value to superconducting gap (SG) [47, 100–102], anisotropy in SG [103–106], doping dependent SG [93, 94] the transport property is an important problem to be understand. The transport property of superconductors like lattice thermal conductivity depends on phonon velocity (sound velocity) along with various other parameters [136–138, 140, 141]. The lattice thermal conductivity which is one of the most important dynamical property of solids depends on the phonon group velocity (v_g) in the form [279]

$$\kappa = \frac{k_B(\beta\hbar)^2}{2\pi^2 v_g}\int_0^{\omega_D}\tau(\omega)\omega^4 e^{\beta\hbar\omega}(e^{\beta\hbar\omega}-1)^{-2}d\omega \tag{5.1}$$

where $\tau(\omega)$ is the total relaxation time for all scattering processes [136, 280, 281]. Due to additive nature of line width (inverse of relaxation time), the total (inverse) relaxation time is given as [170, 172] $\tau^{-1}(\omega) = \tau_{CB}^{-1}+\tau_R^{-1}+\Gamma_k^D(\omega)+\Gamma_k^{3A}(\omega)+\Gamma_k^{3D}(\omega)+\Gamma_q^{eph}(\omega)$ where the notations τ_{CB}^{-1}, τ_R^{-1}, $\Gamma_k^D(\omega)$, $\Gamma_k^{3A}(\omega)$, $\Gamma_k^{3D}(\omega)$ and $\Gamma_q^{eph}(\omega)$ stands for combined boundary relaxation time, resonance scattering relaxation time, line width due to impurity scattering, phonon-phonon scattering, impurity-anharmonicity interference scattering and electron-phonon scattering, respectively. The study of thermal conductivity requires the detailed knowledge of these parameters which is out of the scope of the present work. In the transport problems, obviously, the phonon group velocity emerges as a very important entity and needs the in depth consideration which has yet not been studied rigorously. Present work leads to the detailed study of renormalized phonon group velocity (RPGV) evaluated from the phonon Green's functions [192] which have been obtained via many-body quantum dynamics using a general HTSC Hamiltonian. The expression for RPGV thus obtained show dependence on phonon frequency, doping (impurity concentration), anharmonicity and temperature.

5.2 Formulation of the Problem

The importance of phonon in cuprate HTS motivate to study the properties of the phonon in detail. The phonon group velocity is defined as $v_g = \partial\omega/\partial k$ where ω is phonon dispersion relation. In order to study the phonon group velocity, a dispersion relation is needed that should take care of defect as well as anharmonicity. Using the renormalized phonon dispersion relation such effect can be taken into account in the RPGV. Using the many-body quantum dynamical formulation followed by Dyson's equation formalism the systemic development of renormalized phonon dispersion is given in chapter (2). The term mass change parameter $C(k_1, k_2)$ and force constant change parameter $D(k_1, k_2)$ take care of doping/impurity. The renormalized phonon dispersion which is given as; $\tilde{\omega}_k^2 = \omega_k^2 - \omega_k[\omega_k^D + \omega_k^A + \omega_k^{AD}]$, contains the terms ω_k^D, ω_k^A, ω_k^{AD} in which the term ω_k^{AD} can be dropped since its effect is appear only at very large temperature. Therefore the used renormalized dispersion in the present case is given as: $\tilde{\omega}_k^2 = \omega_k^2 - \omega_k[\omega_k^D + \omega_k^A]$ where ω_k^D and ω_k^A is given as [192]:

$$\begin{aligned}\omega_k^D =& 8D(k_1,-k) + 8C(k_1,-k) + 32\omega_k^{-1}C(k_1,-k)D(k_1,-k_1) \\ &+ 32\omega_k^{-1}\sum_{k_1} C(k_1,-k_1)D(k_1,-k) + 32\omega_k^{-1}\sum_{k_1} C(k_1,-k_1)C(k_1,-k) \\ &+ 128\omega_k^{-2}\sum_{k_1} C(k_1,-k_1)C(k_1,-k)D(k_1,-k_1)\end{aligned} \tag{5.2}$$

$$\omega_k^A = 48\sum_{k_1,k_2} V_4(k_1,k_2,k_1,-k)n_{k_1} \tag{5.3}$$

5.3 Derivation of Renormalized Phonon Group Velocity

Considering the fact that the impurity anharmonicity interaction effects are substantial in the classical hydrodynamic regime, the renormalized phonon dispersion, $\tilde{\omega}$ ($\equiv \tilde{\omega_k}$) can be reasonably simplified to the form

$$\tilde{\omega} = [\omega^2 - \omega(\omega^D + \omega^A)]^{1/2} \tag{5.4}$$

which leads to the evaluation of renormalized group velocity ($\tilde{v}_g$) as:

$$\tilde{v}_g = \frac{\partial\tilde{\omega}}{\partial k} = \frac{\partial}{\partial k}[\omega^2 - \omega(\omega^D + \omega^A)]^{1/2} = \frac{\partial}{\partial \omega}[\omega^2 - \omega(\omega^D + \omega^A)]^{1/2} v_g \tag{5.5}$$

This can be simplified to the form

$$\tilde{v}_g = \frac{2\omega - \zeta(\omega)}{2\tilde{\omega}} v_g \tag{5.6}$$

where

$$\zeta(\omega) = \omega^D + \omega^A + \omega\frac{\partial\omega^D}{\partial\omega} + \omega\frac{\partial\omega^A}{\partial\omega} \tag{5.7}$$

The terms $\zeta(\omega)$ and $\tilde{\omega}$ take care of the effects of doping and anharmonicity on phonon group velocity and in the absence of these two effects the renormalized group velocity becomes usual group velocity, i.e., $\tilde{v}_g = v_g$. Since the effects of doping and anharmonicity on superconductivity is well established fact and hence the need of considering $\tilde{v}_g$ appears well justified.

The mass change parameter [282] ($C(k_1, k_2)$), force constant change parameter [282] ($D(k_1, k_2)$) and anharmonic fourth order potential [32] ($V_4(k_1, k_2, k_1, -k)$) are given by

$$C(k_1, k_2) = \left(\frac{M_0}{4N\mu}\right)(\omega_{k_1}\omega_{k_2})^{1/2}[e(k_1).e(k_2)]\left[\sum_{l}^{N} ce^{i(k_1+k_2).R_l} - \sum_{\mathrm{i}}^{n} e^{i(k_1+k_2).R_{\mathrm{i}}}\right] \quad (5.8)$$

$$D(k_1, k_2) = (4N)^{-1}(\omega_{k_1}\omega_{k_2})^{-1/2}\sum_{l,l'}\left(\frac{\phi_{l,l'}}{M_0}\right)[e(k_1).e(k_2)]e^{i(k_1\cdot R_l + k_2\cdot R_{l'})} \quad (5.9)$$

$$V_4(k_1, k_2, k_3, k_4) = \frac{1}{4!}\left(\frac{\hbar}{4N}\right)\frac{\Delta(k_1, k_2, k_3, k_4)\phi_4(k_1, k_2, k_3, k_4)}{(\omega_{k_1}\omega_{k_2}\omega_{k_3}\omega_{k_4})^{1/2}} \quad (5.10)$$

To examine the effects of mass change and force constant parameters on RPGV due to substitutional point impurities; let us consider a crystal consisting of N atom hypothesized such that impurities of equal mass M' are randomly scattered at n lattice sites and rest sites $(N - n)$ are occupied by atoms of mass M. In the present case n is taken as a variable while considering the impurity concentration $c = n/N$ which appears as a very important parameter [192]. Under a reasonable approximation, taking $\omega_{k_1} = \omega_{k_2} = \omega_{k_3} = \omega_{k_4} = \omega$ and the Debye relation $\omega = vk$; Eqs. (5.8), (5.9) and (5.10), after some algebriac simplifications one can obtain

$$C(\omega) = \left(\frac{M_0}{4N\mu}\right)\omega\left[\sum_{l}^{N} ce^{i\frac{2\omega}{v}.R_l} - \sum_{\mathrm{i}}^{n} e^{i\frac{2\omega}{v}.R_{\mathrm{i}}}\right] \quad (5.11)$$

$$D(\omega) = \frac{(4N)^{-1}}{\omega}\sum_{l,l'}\left(\frac{\phi_{l,l'}}{M_0}\right)e^{i\frac{\omega}{v}(R_l+R_{l'})} \quad (5.12)$$

$$V_4(\omega) = \frac{\hbar\phi_4}{96N\omega^2} \quad (5.13)$$

Using Eqs. (5.11), (5.12) and (5.13), Eqs. (5.2) and (5.3) can be simplified to the following form:

$$\begin{aligned}\omega^D &= 8D(\omega) + 8C(\omega) + 32\omega^{-1}C(\omega)D(\omega) + 32\omega^{-1}C(\omega)D(\omega) \\ &\quad + 32\omega^{-1}C(\omega)C^*(\omega) + 128\omega^{-2}C(\omega)C^*(\omega)D(\omega) \end{aligned} \tag{5.14}$$

$$\omega^A = \frac{\hbar\phi_4}{2N}\frac{\coth(\beta\hbar\omega/2)}{\omega^2} \tag{5.15}$$

where $C^*(\omega)$ is complex conjugate of $C(\omega)$.

The derivatives of $C(\omega)$ and $D(\omega)$ can be obtained as

$$\frac{\partial C(\omega)}{\partial\omega} = \frac{C(\omega)}{\omega} + i\left(\frac{M_0}{4N\mu}\right)\left(\frac{2\omega}{v}\right)S_1 \tag{5.16}$$

$$\frac{\partial D(\omega)}{\partial\omega} = -\frac{D(\omega)}{\omega} + i\frac{(4N)^{-1}}{\omega v}S_2 \tag{5.17}$$

where

$$S_1 = \left[\sum_l^N cR_l e^{i\frac{2\omega}{v}.R_l} - \sum_{\mathrm{i}}^n R_{\mathrm{i}} e^{i\frac{2\omega}{v}.R_{\mathrm{i}}}\right] \tag{5.18}$$

$$S_2 = \sum_{l,l'}\left(\frac{\phi_{l,l'}}{M_0}\right)(R_l + R_{l'})e^{i\frac{\omega}{v}(R_l+R_{l'})} \tag{5.19}$$

Using Eqs. (5.11), (5.12), (5.16) and (5.17) in Eq. (5.14) the term $\omega\frac{\partial\omega^D}{\partial\omega}$ can be evaluated in the form

$$\begin{aligned}\omega\frac{\partial\omega^D}{\partial\omega} &= -8D(\omega)+8C(\omega)+i\frac{(4N)^{-1}}{\omega v}+i(\frac{M_0}{4N\mu})(\frac{2\omega}{v})S_1-i32D(\omega)(\frac{M_0}{4N\mu})(\frac{2\omega}{v})S_1\\ &-\frac{32}{\omega}C(\omega)D(\omega)+i32C(\omega)\frac{(4N)^{-1}}{\omega v}S_2+i32C^*(\omega)(\frac{M_0}{4N\mu})(\frac{2\omega}{v})S_1\\ &+\frac{32}{\omega}C(\omega)C^*(\omega)-i32(\frac{M_0}{4N\mu})(\frac{2\omega}{v})C(\omega)S_1^*+i\frac{128}{\omega}C^*(\omega)D(\omega)(\frac{M_0}{4N\mu})(\frac{2\omega}{v})S_1\\ &-i\frac{128}{\omega}C(\omega)D(\omega)(\frac{M_0}{4N\mu})(\frac{2\omega}{v})S_1^*-\frac{128}{\omega^2}C(\omega)C^*(\omega)D(\omega)\\ &+i\frac{128}{\omega}C(\omega)C^*(\omega)\frac{(4N)^{-1}}{\omega v}S_2 \qquad (5.20)\end{aligned}$$

Where, S_1^* being the complex conjugate of S_1. Similarly use of Eq. (5.15) yields the term $\omega\frac{\partial\omega^A}{\partial\omega}$ as

$$\omega\frac{\partial\omega^A}{\partial\omega} = -96\coth(\beta\hbar\omega/2)V_4(\omega)-48(\beta\hbar\omega/2)\,\mathrm{csch}^2(\beta\hbar\omega/2)V_4(\omega) \qquad (5.21)$$

Using Eqs. (5.14), (5.15), (5.20), and (5.21), the $\zeta(\omega)$ takes the form

$$\begin{aligned}\zeta(\omega) &= 16C(\omega)+\frac{32}{\omega}C(\omega)D(\omega)+\frac{64}{\omega}|C(\omega)|^2-96\coth(\beta\hbar\omega/2)V_4(\omega)\\ &-48(\beta\hbar\omega/2)\,\mathrm{csch}^2(\beta\hbar\omega/2)V_4(\omega)+i\left[\frac{(4N)^{-1}}{\omega v}+\omega\left(\frac{M_0}{4N\mu}\right)\left(\frac{2\omega}{v}\right)S_1\right.\\ &-32D(\omega)\left(\frac{M_0}{4N\mu}\right)\left(\frac{2\omega}{v}\right)S_1+32C(\omega)\frac{(4N)^{-1}}{\omega v}S_2\\ &\left.+\frac{128}{\omega}|C(\omega)|^2\frac{(4N)^{-1}}{\omega v}S_2\right] \qquad (5.22)\end{aligned}$$

The fourth order anharmonic term ($V_4(\omega)$) contributes at high temperatures and therefore in the interest of low temperature region these terms can be dropped. $\zeta(\omega)$ being complex function and in order to derive the expression for RPGV the following equations are used to resolve the real part of $\zeta(\omega)$, i. e., $\mathbb{R}\mathrm{e}[\zeta(\omega)] \equiv \xi(\omega)$:

$$\mathbb{R}\mathrm{e}[C(\omega)] = \left(\frac{M_0}{4N\mu}\right)\omega\left[\sum_{l}^{N} cC^{l} - \sum_{\mathrm{i}}^{n} C^{\mathrm{i}}\right]; \mathbb{I}\mathrm{m}[C(\omega)] = \left(\frac{M_0}{4N\mu}\right)\omega\left[\sum_{l}^{N} cS^{l} - \sum_{\mathrm{i}}^{n} S^{\mathrm{i}}\right] \tag{5.23}$$

$$\mathbb{R}\mathrm{e}[D(\omega)] = \frac{(4N)^{-1}}{\omega}\sum_{l,l'}\left(\frac{\phi_{l,l'}}{M_0}\right)C^{ll'}; \quad \mathbb{I}\mathrm{m}[D(\omega)] = \frac{(4N)^{-1}}{\omega}\sum_{l,l'}\left(\frac{\phi_{l,l'}}{M_0}\right)S^{ll'} \tag{5.24}$$

$$\mathbb{R}\mathrm{e}[S_1] = \sum_{l}^{N} cR_l C^{l} - \sum_{\mathrm{i}}^{n} R_{\mathrm{i}} C^{\mathrm{i}}; \quad \mathbb{I}\mathrm{m}[S_1] = \sum_{l}^{N} cR_l S^{l} - \sum_{\mathrm{i}}^{n} R_{\mathrm{i}} S^{\mathrm{i}} \tag{5.25}$$

$$\mathbb{R}\mathrm{e}[S_2] = \sum_{l,l'}\left(\frac{\phi_{l,l'}}{M_0}\right)(R_l + R_{l'})C^{ll'}; \mathbb{I}\mathrm{m}[S_2] = \sum_{l,l'}\left(\frac{\phi_{l,l'}}{M_0}\right)(R_l + R_{l'})S^{ll'} \tag{5.26}$$

Using Eqs. (5.23) to (5.26) in Eq. (5.22) and after a tedious algebraic and trigonometric simplifications, the $\xi(\omega)$ can be obtained as

$$\begin{aligned}\xi(\omega) &= \left(\frac{4M_0}{N\mu}\right)\omega\left[\sum_{l}^{N} cC^{l} - \sum_{\mathrm{i}}^{n} C^{\mathrm{i}}\right] + \left(\frac{2M_0}{N^2\mu}\right)\frac{1}{\omega}\sum_{l_1,l'}\left(\frac{\phi_{l_1,l'}}{M_0}\right)\left[\sum_{l}^{N} cC^{ll_1l'} - \sum_{\mathrm{i}}^{n} C^{\mathrm{i}l_1l'}\right] \\ &+\left(\frac{2M_0}{N\mu}\right)^2\omega\left[\sum_{l,l_1} c^2(C^{ll_1}+S^{ll_1}) + \sum_{\mathrm{i},\mathrm{i}_1}(C^{\mathrm{i}\mathrm{i}_1}+S^{\mathrm{i}\mathrm{i}_1}) - 2\sum_{l,\mathrm{i}} cC^{l\mathrm{i}}\right] \\ &-\left(\frac{M_0}{2N\mu v}\right)\omega^2\left[\sum_{l}^{N} cR_lS^{l} - \sum_{\mathrm{i}}^{n} R_{\mathrm{i}}S^{\mathrm{i}}\right] - \left(\frac{2M_0}{N^2\mu v}\right)\sum_{l_1,l'}\left(\frac{\phi_{l_1,l'}}{M_0}\right)\left[\sum_{l}^{N} cS^{ll_1l'} - \sum_{\mathrm{i}}^{n} S^{\mathrm{i}l_1l'}\right] \\ &+\left(\frac{4M_0}{N^2\mu v}\right)\sum_{l_1,l'}\left(\frac{\phi_{l_1,l'}}{M_0}\right)\left[\sum_{l}^{N} cR_lS^{ll_1l'} - \sum_{\mathrm{i}}^{n} R_{\mathrm{i}}S^{\mathrm{i}l_1l'}\right] \qquad (5.27)\end{aligned}$$

where

$$C^{l} = \cos\Omega_l; \quad C^{\mathrm{i}} = \cos\Omega_{\mathrm{i}}; \quad S^{l} = \sin\Omega_l; \quad S^{\mathrm{i}} = \sin\Omega_{\mathrm{i}}; \quad C^{l\mathrm{i}} = \cos\Omega_{l\mathrm{i}} \qquad (5.28)$$

$$C^{ll_1} = \cos\Omega^{+}_{ll_1}; \quad C^{\mathrm{i}\mathrm{i}_1} = \cos\Omega^{+}_{\mathrm{i}\mathrm{i}_1}; \quad S^{ll_1} = \sin\Omega^{-}_{ll_1}; \quad S^{\mathrm{i}\mathrm{i}_1} = \sin\Omega^{-}_{\mathrm{i}\mathrm{i}_1} \qquad (5.29)$$

$$C^{ll_1l'} = \cos\Omega_{ll_1l'}; \quad C^{\mathrm{i}l_1l'} = \cos\Omega_{\mathrm{i}l_1l'}; \quad S^{ll_1l'} = \sin\Omega_{ll_1l'}; \quad S^{\mathrm{i}l_1l'} = \sin\Omega_{\mathrm{i}l_1l'} \qquad (5.30)$$

$$C^{ll'} = \cos\Omega_{ll'}; \quad S^{ll'} = \sin\Omega_{ll'} \qquad (5.31)$$

and

$$\Omega_l = \frac{2\omega}{v}R_l; \quad \Omega_{\mathrm{i}} = \frac{2\omega}{v}R_{\mathrm{i}}; \quad \Omega_{l\mathrm{i}} = \frac{2\omega}{v}(R_l + R_{\mathrm{i}}) \qquad (5.32)$$

$$\Omega^{\pm}_{ll_1} = \frac{2\omega}{v}(R_l \pm R_{l_1});\ \Omega^{\pm}_{\mathrm{ii}_1} = \frac{2\omega}{v}(R_{\mathrm{i}} \pm R_{\mathrm{i}_1});\ \Omega_{ll'} = \frac{\omega}{v}(R_l + R_{l'}) \tag{5.33}$$

$$\Omega_{ll_1l'} = \frac{\omega}{v}(2R_l + R_{l_1} + R_{l'});\quad \Omega_{\mathrm{i}l_1l'} = \frac{\omega}{v}(2R_{\mathrm{i}} + R_{l_1} + R_{l'}); \tag{5.34}$$

Therefore, the final form of RPGV can be written as

$$\tilde{v}_g = \frac{2\omega - \xi(\omega)}{2\tilde{\omega}} v_g \tag{5.35}$$

In the above equations the summation index l, l_1, l' stands for total atoms in the system and index i, i_1 stands for impurity atoms.

5.4 Renormalized Phonon Group Velocity in $La_{2-x}Sr_xCuO_4$

The expression obtained for RPGV ($\tilde{v}_g$) includes the effects of phonon frequency, doping concentration, temperature, and anharmonicity. However, the anharmonicity appears in the form of fourth order anharmonic terms which is not much significant in the low temperature regime for superconducting materials. For the purpose of analysis of $\tilde{v}_g$ the model high temperature superconducting cuprate crystal $La_{2-x}Sr_xCuO_4$ has been taken. The Cu atom has been taken at the center of a system consisting of 41 atoms surrounded by other atoms of $La_{2-x}Sr_xCuO_4$ with impurity atom Sr taken at random lattice site replacing the La atom. To this configuration of the system, Eq. (5.35) is analyzed and the behavior of $\tilde{v}_g$ with phonon frequency is depicted in Fig. (5.1) at different doping concentrations. A similar variation in phonon group

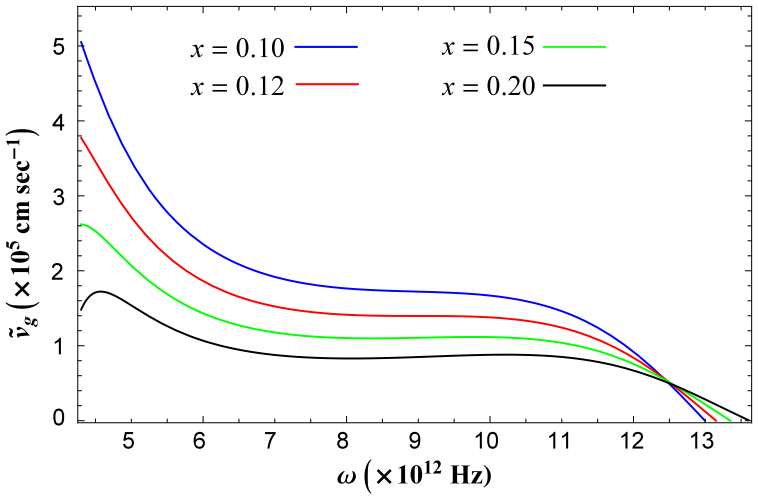

FIGURE 5.1: Variation of RPGV ($\tilde{v}_g$) with the frequency (ω) for $La_{2-x}Sr_xCuO_4$ at different doping.

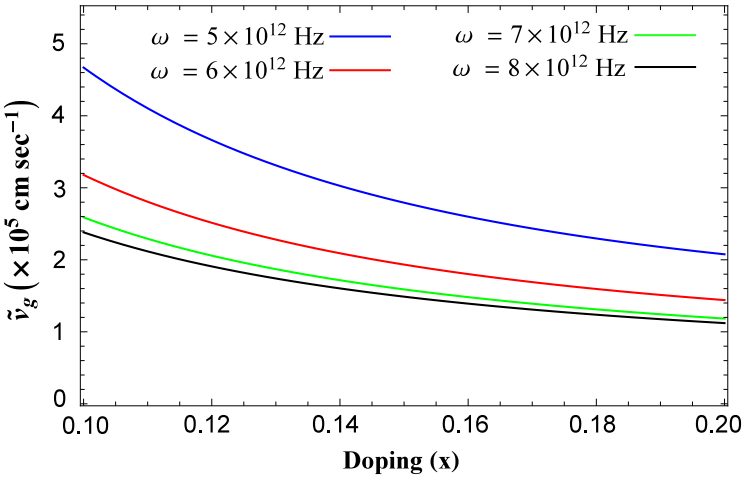

FIGURE 5.2: Variation of RPGV ($\tilde{v}_g$) with the doping (x) for $La_{2-x}Sr_xCuO_4$ at different frequency.

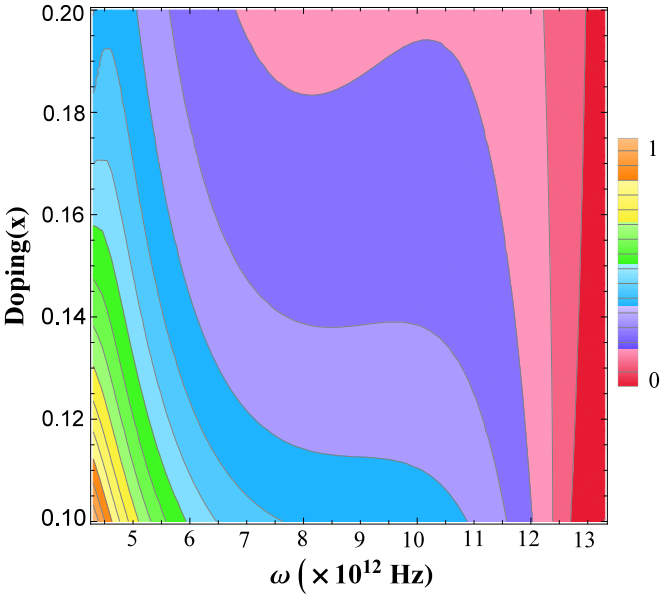

FIGURE 5.3: Contour plot of RPGV ($\tilde{v}_g$) for $La_{2-x}Sr_xCuO_4$.

velocity with frequency has also been found in the available literature for some other materials [283]. In superconductors RPGV shows readily decreasing trend with doping concentration which has been furnished in Fig. (5.2). This change occurs as a result of changes in the interacting force constants among atoms due to the difference in mass of dopant/impurity atoms. Such behavior of decrease in phonon group velocity with increasing doping in $La_{2-x}Sr_xCuO_4$ superconductor also confirmed by other authors [284]. The RPGV contours depicted in Fig. (5.3) also confirm its non-linear behavior with simultaneous variation in frequency and doping concentration. Obviously, this sensitive nature of RPGV adds a feather to the very complex phenomenon of energy transport. The advantage of present formulation of RPGV is that it includes the crystal/system details to depict the phonon energy transport therefore for the different system it can provide RPGV according to the system, i.e., the obtained result is system oriented, hence it is closer to the real situation.

5.5 Conclusions

Using the renormalized phonon dispersion obtained via phonon Green's functions, the results for RPGV are developed. It appears from the current investigation that the RPGV depends on doping concentration, phonon frequency, anharmonicity, and temperature. The anharmonicity and temperature dependence has not been taken into account in the interest of the low-temperature regime.

The RPGV plots for $La_{2-x}Sr_xCuO_4$ superconductor reveal a complicated variation with doping concentration and frequency. Since, the present formulation being system oriented appears more close to the real situations.

Chapter 6

Summary and Futuristic Scenario

"Our virtues and our failings are inseparable, like force and matter. When they separate, man is no more."

- - - Nikola Tesla

6.1 Summary of Present Work

Using the electron and phonon Green's functions followed by the MBMHP, the following properties of cuprate superconductor $La_{2-x}Sr_xCuO_4$ and $YBa_2Cu_3O_{7-\delta}$ are summarized as below.

6.1.1 The Superconducting Gap

Using the generalized EDOS of HTS followed by BCS formalism the two SG equations have been successfully obtained which shows dependence on temperature, Fermi energy and renormalized electron and phonon energies. Both SG equations $\Delta_1(T)$ and $\Delta_2(T)$, predict the $T_c = 93.8K$ for $YBa_2Cu_3O_{7-\delta}$. The normalized gaps $\Delta_1(T)/\Delta_1(0)$ and $\Delta_2(T)/\Delta_2(0)$ show the similar variation to the BCS gap curve in low-temperature region, but deviate near T_c. The reduced gap ratio of

$YBa_2Cu_3O_{7-\delta}$ is observed as $2\Delta_1(0)/k_BT_c$=7.2 to 7.5. The effect of AF spin fluctuations on the SG also seen in $La_{2-x}Sr_xCuO_4$ and it is found that the SG is reduced by 9% at 0K and at the optimum doping. General expressions for pairing potential are obtained and numerically calculated for $YBa_2Cu_3O_{7-\delta}$, which is found close to the calculated pairing potential via BCS approach in intermediate coupling range, while it slightly deviates in the weak and strong coupling range. Using Green's functions technique the renormalized electron-phonon dispersion is analysed for the $La_{2-x}Sr_xCuO_4$ and $YBa_2Cu_3O_{7-\delta}$. The SG, nodal and antinodal gap in $La_{2-x}Sr_xCuO_4$ are found increasing with decrement in doping but the nodal gap vanished at the doping $x = 0.104$. In the case of $YBa_2Cu_3O_{7-\delta}$, the SG increases with increment in doping.

6.1.2 Anisotropic Superconducting Gap and Pairing Symmetry

The plot of SG as a function of FS angle (θ) gives a v- shape gap confessing the anisotropicity of the SG in $La_{2-x}Sr_xCuO_4$ and $YBa_2Cu_3O_{7-\delta}$. The plot of SG as a function order parameter $|cos(k_xa) - cos(k_yb)|$ confirms the highly anisotropic nature of SG in both the cuprate HTS with doping dependence. A dominating $d_{x^2-y^2}$ pairing symmetry are observed in $La_{2-x}Sr_xCuO_4$ and $YBa_2Cu_3O_{7-\delta}$. In the both superconductors the pairing symmetry are affected by the doping in non-linear way and the existence of s or d_{xy} component is seen in the underdoped regime. In the overdoped regime a pure $d_{x^2-y^2}$ pairing symmetry is observed in $La_{2-x}Sr_xCuO_4$ while in $YBa_2Cu_3O_{7-\delta}$ s or d_{xy} component is observed. The effect of AF spin fluctuations on pairing symmetry is observed in $La_{2-x}Sr_xCuO_4$.

6.1.3 Theory of Renormalized Phonon Group Velocity in High Temperature Superconductors

A theory of RPGV is developed using the renormalized phonon dispersion obtained via phonon Green's functions. It emerges from the present study that the RPGV depends on doping concentration, phonon frequency, anharmonicity, and temperature. The RPGV plots for $La_{2-x}Sr_xCuO_4$ superconductor reveal a complicated variation with doping concentration and frequency.

6.2 Future aspects

6.2.1 Study of Penetration Depth

The experimental fact that the energy gap has effects on the penetration depth of superconductor which can be studied with the help of the newly formulated SG equations.

6.2.2 Thermal Conductivity

The developed model of RPGV ($\tilde{v}_g$) can be further utilized in the study of phonon thermal conductivity of HTS with the following equation.

$$\kappa = \frac{k_B(\beta\hbar)^2}{2\pi^2 v_g} \int_0^{\omega_D} \tau(\omega)\omega^4 e^{\beta\hbar\omega}(e^{\beta\hbar\omega} - 1)^{-2} d\omega \tag{6.1}$$

6.2.3 Doping Dependent Debye Temperature

The dependence of Debye temperature on sound (group) velocity ($\theta_D = \frac{\hbar v_g}{k_B}.(\frac{6\pi^2 N}{V})^{1/3}$) can utilized to study the doping dependent Debye temperature in HTS via developed model of RPGV ($\tilde{v}_g$).

Bibliography

[1] S. R. Acherman. "Studies on the temperature dependence of electric conductivity for metals in the nineteenth century: a neglected chapter in the history of superconductivity". *Rev. Bras. Ensino. Fis.*, **33**(4):4602–4302, 2011.

[2] H. K. Onnes. "The liquefaction of helium". *Commun. Phys. Lab. Univ. Leiden*, **108**, 1908.

[3] H. K. Onnes. "The resistance of pure mercury at helium temperatures". *Commun. Phys. Lab. Univ. Leiden, b*, **120**, 1911.

[4] J. D. Nobel and P. Lindenfeld. "The discovery of superconductivity". *Phys. Today*, **49**(9):40–42, 1996.

[5] W. Meissner and R. Ochsenfeld. "Ein neuer effekt bei eintritt der supraleitfähigkeit". *Naturwissenschaften*, **21**(44):787–788, 1933.

[6] B. T. Matthias, T. H. Geballe, and V. B. Compton. "Superconductivity". *Rev. Mod. Phys.*, **35**(1):1–22, 1963.

[7] J. Schmalian. "Failed theories of superconductivity". *Mod. Phys. Lett. B*, **24**(27):2679–2691, 2010.

[8] C. K. Poole, H. A. Farach, and R. J. Creswick. *"Handbook of superconductivity"*. Elsevier, 1999.

[9] C. J. Gorter and H. Casimir. "On supraconductivity I". *Physica*, **1**(1-6):306–320, 1934.

[10] F. London and H. London. "The electromagnetic equations of the supraconductor". *Proc. R. Soc. Lond. A*, **149**(866):71–88, 1935.

[11] L. V. Shubnikov, V. I. Khotkevich, Y. D. Shepelev, and Y. N. Ryabinin. "Magnetic properties of superconducting metals and alloys". *Zh. Eksp. Teor. Fiz*, **7**:221–237, 1937. [Ukrainian J. Phys. **53**: 42–52, Reprint in English, 2008].

[12] A. A. Abrikosov. "On the magnetic properties of superconductors of the second group". *Sov. Phys. JETP*, **5**:1174–1182, 1957. [*Zh. Eksp. Teor. Fiz.* **32**, 1442-1452 (1957)].

[13] V. L. Ginzburg and L. D. Landau. "On the theory of superconductivity". *Zh. Eksper. Teor. Fiz.*, **20**:1064–1082, 1950. [V. L. Gingburg, "On Superconductivity and Superfluidity", Chapter 4, Page: 113–137, Moscow, 2008].

[14] H. F. Hess, R. B. Robinson, R. C. Dynes, J. M. Valles Jr, and J. V. Waszczak. "Scanning-tunneling-microscope observation of the Abrikosov flux lattice and the density of states near and inside a fluxoid". *Phys. Rev. Lett.*, **62**(2):214–216, 1989.

[15] H. F. Hess, R. B. Robinson, and J. V. Waszczak. "Vortex-core structure observed with a scanning tunneling microscope". *Phys. Rev. Lett.*, **64**(22):2711–2714, 1990.

[16] H. Frölich. "The Isotope Effect in Superconductivity, Procc". In *Phys. Soc. A*, volume **63**, page 778, 1950.

[17] H. Fröhlich. "Theory of the superconducting state. I. The ground state at the absolute zero of temperature". *Phys. Rev.*, **79**(5):845–856, 1950.

[18] E. Maxwell. "Isotope effect in the superconductivity of mercury". *Phys. Rev.*, **78**(4):477, 1950.

[19] C. A. Reynolds, B. Serin, W. H. Wright, and L. B. Nesbitt. "Superconductivity of isotopes of mercury". *Phys. Rev.*, **78**(4):487, 1950.

[20] J. Bardeen, L. N. Cooper, and J. R. Schrieffer. "Theory of superconductivity". *Phys. Rev.*, **108**(5):1175–1204, 1957.

[21] L. D. Landau. "Diamagnetismus der metalle". *Zeitschrift für Physik*, **64**(9-10):629–637, 1930.

[22] L. D. Landau. "EM Lifshitz Statistical Physics". *Course of Theoretical Physics*, **5**:396–400, 1980.

[23] L. N. Cooper. "Bound electron pairs in a degenerate Fermi gas". *Phys. Rev.*, **104**(4):1189–1190, 1956.

[24] W. S. Corak, B. B. Goodman, C. B. Satterthwaite, and A. Wexler. "Exponential temperature dependence of the electronic specific heat of superconducting vanadium". *Phys. Rev.*, **96**(5):1442–1444, 1954.

[25] L. P. Gor'kov. "Microscopic derivation of the Ginzburg-Landau equations in the theory of superconductivity". *Sov. Phys. JETP*, **9**(6):1364–1367, 1959.

[26] P. W. Anderson. "Random-phase approximation in the theory of superconductivity". *Phys. Rev.*, **112**(6):1900–1916, 1958.

[27] N. N. Bogoliubov. "A New Method in the Theory of Superconductivity". *Sov. Phys. JETP*, **7**(1):41–46, 1958.

[28] N. N. Bogoljubov, V. V. Tolmachov, and D. V. Širkov. "A new method in the theory of superconductivity". *Fortschr. Phys.*, **6**(11-12):605–682, 1958.

[29] L. P. Gor'kov. "On the energy spectrum of superconductors". *Sov. Phys. JETP*, **7**(3):505–508, 1958.

[30] X. L. Lei and C. S. Ting. "Green's-function approach to nonlinear electronic transport for an electron-impurity-phonon system in a strong electric field". *Phys. Rev. B*, **32**(2):1112–1132, 1985.

[31] K. N. Pathak. "Mean-square velocity of an atom in anharmonic crystals". *Proc. Phys. Soc.*, **92**(4):998–1001, 1967.

[32] K. N. Pathak. "Theory of anharmonic crystals". *Phys. Rev.*, **139**(5A):A1569–A1580, 1965.

[33] K. N. Pathak and Y. P. Varshni. "Thermodynamics of anharmonic crystals". *Phys. Lett. A*, **28**(8):539–540, 1969.

[34] A. Mookerjee. "Fermion-field theory and configuration averaging. II. Two-particle Green functions". *J. Phys. C: Solid State Phys.*, **8**(17):2688–2694, 1975.

[35] A. Mookerjee. "Fermion-field theory and configuration averaging". *J. Phys. C: Solid State Phys.*, **8**(10):1524–1534, 1975.

[36] A. B. Migdal. "Interaction between electrons and lattice vibrations in a normal metal". *Sov. Phys. JETP*, **7**(6):996–1001, 1958.

[37] G. M. Eliashberg. "Interactions between electrons and lattice vibrations in a superconductor". *Sov. Phys. JETP*, **11**(3):696–702, 1960.

[38] Y. Nambu. "Quasi-particles and gauge invariance in the theory of superconductivity". *Phys. Rev.*, **117**(3):648–663, 1960.

[39] W. L. McMillan. "Transition temperature of strong-coupled superconductors". *Phys. Rev.*, **167**(2):331–344, 1968.

[40] P. B. Allen and R. C. Dynes. "Transition temperature of strong-coupled superconductors reanalyzed". *Phys. Rev. B*, **12**(3):905–922, 1975.

[41] B. D. Josephson. "Possible new effects in superconductive tunnelling". *Phys. Lett.*, **1**(7):251–253, 1962.

[42] P. W. Anderson and J. M. Rowell. "Probable observation of the Josephson superconducting tunneling effect". *Phys. Rev. Lett.*, **10**(6):230–232, 1963.

[43] B. T. Matthias, T. H. Geballe, S. Geller, and E. Corenzwit. "Superconductivity of Nb_3Sn". *Phys. Rev.*, **95**(6):1435, 1954.

[44] D. C. Johnston, H. Prakash, W. H. Zachariasen, and R. Viswanathan. "High temperature superconductivity in the $Li_{1+x}Ti_{2-x}O_4$ ternary system". *Mater. Res. Bull.*, **8**(7):777–784, 1973.

[45] A. W. l. Sleight, J. L. Gillson, and P. E. Bierstedt. "High-temperature superconductivity in the $BaPb_{1-x}Bi_xO_3$ system". *Solid State Commun.*, **88**(11-12):841–842, 1993.

[46] G. I. Oya and E. J. Saur. "Preparation of Nb_3Ge films by chemical transport reaction and their critical properties". *J. Low Temp. Phys.*, **34**(5-6):569–583, 1979.

[47] J. G. Bednorz and K. A. Müller. "Possible high T_c superconductivity in the Ba- La- Cu- O system". *Z. Phys.*, **64**(2):189–193, 1986.

[48] M. K. Wu, J. R. Ashburn, C. l. J. Torng, P. H. Hor, R. l. L. Meng, L. Gao, Z. J. Huang, Y. Q. Wang, and C. W. Chu. "Superconductivity at 93 K in a new mixed-phase Y-Ba-Cu-O compound system at ambient pressure". *Phys. Rev. Lett.*, **58**(9):908–910, 1987.

[49] H. Maeda, Y. Tanaka, M. Fukutomi, and T. Asano. "A new high-T_c oxide superconductor without a rare earth element". *Jpn. J. Appl. Phys.*, **27**(2A):L209–L210, 1988.

[50] A. Schilling, M. Cantoni, J. .D. Guo, and H. R. Ott. "Superconductivity above 130 K in the Hg–Ba–Ca–Cu–O system". *Nature*, **363**(6424):56–58, 1993.

[51] C. W. Chu, Li Gao, F. Chen, Z. J. Huang, R. L. Meng, and Y. Y. Xue. "Superconductivity above 150 K in $HgBa_2Ca_2Cu_3O_{8+\delta}$ at high pressures". *Nature*, **365**(6444):323–325, 1993.

[52] J. Nagamatsu, N. Nakagawa, T. Muranaka, Y. Zenitani, and J. Akimitsu. "Superconductivity at 39 K in magnesium diboride". *Nature*, **410**(6824):63–64, 2001.

[53] Y. Kamihara, T. Watanabe, M. Hirano, and H. Hosono. "Iron-based layered superconductor La[$O_{1-x}F_x$]FeAs (x= 0.05- 0.12) with T_c= 26 K". *J. Am. Chem. Soc.*, **130**(11):3296–3297, 2008.

[54] X. H. Chen, T. Wu, G. Wu, R. H. Liu, H. Chen, and D. F. Fang. "Superconductivity at 43 K in $SmFeAsO_{1-x}F_x$". *Nature*, **453**(7196):761–762, 2008.

[55] G. F. Chen, Z. Li, D. Wu, G Li, W. Z. Hu, J. Dong, P. Zheng, J. L. Luo, and N. L. Wang. "Superconductivity at 41 K and its competition with spin-density-wave instability in layered $CeO_{1-x}F_xFeAs$". *Phys. Rev. Lett.*, **100**(24):247002, 2008.

[56] Z. A. Ren, J. Yang, W. Lu, W. Yi, X. L. Shen, Z. C. Li, G. C. Che, X. L. Dong, L. L. Sun, F. Zhou, et al. "Superconductivity in the iron-based F-doped layered quaternary compound Nd[$O_{1-x}F_x$]FeAs". *EPL (Europhysics Letters)*, **82**(5):57002, 2008.

[57] Z. A. Ren, W. Lu, J. Yang, W. Yi, X. L. Shen, Z. C. Li, G. C. Che, X. L. Dong, L. L. Sun, F. Zhou, et al. "Superconductivity at 55 K in iron-based F-doped layered quaternary compound Sm [O1-xFx] FeAs". *arXiv preprint arXiv:0804.2053*, 2008.

[58] L. P. Gor'kov Sokol and A. V. "Phase stratification of an electron liquid in the new superconductors". *JETP Lett.*, **46**(8):420–423, 1987 [Zh. Teor. Fiz. **46**(8): 333–336].

[59] V. Z. Kresin. "On the relation between the energy gap and the critical temperature". *Solid State Commun*, **63**(8):725–727, 1987.

[60] I. Affleck and J. B. Marston. "Large-n limit of the Heisenberg-Hubbard model: Implications for high-T_c superconductors". *Phys. Rev. B*, **37**(7):3774(R), 1988.

[61] J. B. Marston and I. Affleck. "Large-n limit of the Hubbard-Heisenberg model". *Phys. Rev. B*, **39**(16):11538, 1989.

[62] X. G. Wen and P. A. Lee. "Theory of underdoped cuprates". *Phys. Rev. Lett.*, **76**(3):503–506, 1996.

[63] J. I. Kishine, P. A. Lee, and X. G. Wen. "Staggered local density of states around the vortex in underdoped cuprates". *Phys. Rev. Lett.*, **86**(23):5365–5368, 2001.

[64] O. Zachar, S. A. Kivelson, and V. J. Emery. "Landau theory of stripe phases in cuprates and nickelates". *Phys. Rev. B*, **57**(3):1422–1426, 1998.

[65] S. R. White and D. J. Scalapino. "Density matrix renormalization group study of the striped phase in the 2D t- J model". *Phys. Rev. Lett.*, **80**(6):1272–1275, 1998.

[66] C. M. Varma. "Proposal for an experiment to test a theory of high-temperature superconductors". *Phys. Rev. B*, **61**(6):R3804–R3807, 2000.

[67] P. W. Anderson. "The resonating valence bond state in La_2CuO_4 and superconductivity". *Science*, **235**(4793):1196–1198, 1987.

[68] P. W. Anderson, G. Baskaran, Z. Zou, and T. Hsu. "Resonating–valence-bond theory of phase transitions and superconductivity in La_2CuO_4-based compounds". *Phys. Rev. Lett.*, **58**:2790–2793, 1987.

[69] G. Baskaran and P. W. Anderson. "Gauge theory of high-temperature superconductors and strongly correlated Fermi systems". *Phys. Rev. B*, **37**(1):580–583, 1988.

[70] V. J. Emery. "Theory of high-T_c superconductivity in oxides". *Phys. Rev. Lett.*, **58**(26):2794–2797, 1987.

[71] B. K. Agrawal, S. Kumar, S. Agrawal, and P. S. Yadav. "Theoretical evidence for the correlation between hole density and T_c in high-T_c Tl-based superconductors". *Phys. Rev. B*, **48**(10):7364–7375, 1993.

[72] B. K. Agrawal, S. Kumar, S. Agrawal, and P. S. Yadav. "Theoretical evidence for correlation between hole density and T_c in high-T_c $Tl_2Ba_2Ca_{n-1}$, Cu_n $O2_{n+4}$ superconductors". *Appl. Supercond.*, **1**(3-6):351–358, 1993.

[73] F. C. Zhang and T. M. Rice. "Effective Hamiltonian for the superconducting Cu oxides". *Phys. Rev. B*, **37**(7):3759–3761, 1988.

[74] K. Miyake, S. S. Rink, and C. M. Varma. "Spin-fluctuation-mediated even-parity pairing in heavy-fermion superconductors". *Phys. Rev. B*, **34**(9):6554–6556, 1986.

[75] T. Moriya and K. Ueda. "Spin fluctuation spectra and high temperature superconductivity". *J. Phys. Soc. Jpn.*, **63**(5):1871–1880, 1994.

[76] T. Moriya and K. Ueda. "Spin fluctuations and high temperature superconductivity". *Adv. Phys.*, **49**(5):555–606, 2000.

[77] T. Moriya. "Developments of the theory of spin fluctuations and spin fluctuation-induced superconductivity". *Proc. Jpn. Acad. Ser. B*, **82**(1):1–16, 2006.

[78] D. A. Wollman, D. J. Van Harlingen, W. C. Lee, D. M. Ginsberg, and A. J. Leggett. "Experimental determination of the superconducting pairing state in YBCO from the phase coherence of YBCO-Pb dc SQUIDs". *Phys. Rev. Lett.*, **71**(13):2134–2137, 1993.

[79] C. C. Tsuei, J. R. Kirtley, C. C. Chi, L. S. Y. Jahnes, A. Gupta, T. Shaw, J. Z. Sun, and M. B. Ketchen. "Pairing symmetry and flux quantization in a tricrystal superconducting ring of $YBa_2Cu_3O_{7-\delta}$". *Phys. Rev. Lett.*, **73**(4):593–598, 1994.

[80] D. J. Scalapino, E. Loh Jr, and J. E. Hirsch. "D-wave pairing near a spin-density-wave instability". *Phys. Rev. B*, **34**(11):8190–8192, 1986.

[81] P. Monthoux, A. V. Balatsky, and D. Pines. "Toward a theory of high-temperature superconductivity in the antiferromagnetically correlated cuprate oxides". *Phys. Rev. Lett.*, **67**(24):3448–3451, 1991.

[82] M. Inui, S. Doniach, P. J. Hirschfeld, and A. E. Ruckenstein. "Coexistence of antiferromagnetism and superconductivity in a mean-field theory of high-T_c superconductors". *Phys. Rev. B*, **37**(4):2320–2323, 1988.

[83] G. Kotliar and J. Liu. "Superexchange mechanism and d-wave superconductivity". *Phys. Rev. B*, **38**(7):5142–5145, 1988.

[84] C. Gros, D. Poilblanc, T. M. Rice, and F. C. Zhang. "Superconductivity in correlated wavefunctions". *Physica C*, **153**:543–548, 1988.

[85] J. H. Xu, Y. Ren, and C. S. Ting. "Structures of single vortex and vortex lattice in a d-wave superconductor". *Phys. Rev. B*, **53**(6):R2991–R2994, 1996.

[86] K. Ramakrishna, B. Das, A. K. Singh, R. S. Tiwari, and O. N. Srivastava. "Electron microscopic studies of local structures of high temperature $YBa_2Cu_3O_{7-x}$ superconductor". *Solid. State. Commun.*, **65**(8):831–834, 1988.

[87] S. Feng. "Kinetic energy driven superconductivity in doped cuprates". *Phys. Rev. B*, **68**(18):184501, 2003.

[88] S. Feng, T. Ma, and H. Guo. "Magnetic nature of superconductivity in doped cuprates". *Physica C*, **436**(1):14–24, 2006.

[89] S. Feng, H. Zhao, and Z. Huang. "Two gaps with one energy scale in cuprate superconductors". *Phys. Rev. B*, **85**(5):054509, 2012.

[90] S. Feng, Y. Lan, Huaisong Z., L. Kuang, L. Qin, and X. Ma. "Kinetic-energy-driven superconductivity in cuprate superconductors". *Int. J. Mod. Phys. B*, **29**(16):1530009, 2015.

[91] Q. Wang, C. R. Hu, and C. S. Ting. "Impurity effects on the quasiparticle spectrum of the Fulde-Ferrell-Larkin-Ovchinnikov state of a d-wave superconductor". *Phys. Rev. B*, **74**(21):212501, 2006.

[92] T. M. Shaw, S. L. Shinde, D. Dimos, R. F. Cook, P. R. Duncombe, and C. Kroll. "The effect of grain size on microstructure and stress relaxation in polycrystalline $Y_1Ba_2Cu_3O_{7-\delta}$". *J. Mater. Res.*, **4**(2):248–256, 1989.

[93] G. Deutscher. "Coherence and single-particle excitations in the high-temperature superconductors". *Nature*, **397**(6718):410–412, 1999.

[94] M. Sutherland, D. G. Hawthorn, R. W. Hill, F. Ronning, S. Wakimoto, H. Zhang, C. Proust, E. Boaknin, C. Lupien, L. Taillefer, et al. "Thermal conductivity across the phase diagram of cuprates: Low-energy quasiparticles and doping dependence of the superconducting gap". *Phys. Rev. B*, **67**(17):174520, 2003.

[95] T. Nakano, N. Momono, M. Oda, and M. Ido. "Correlation between the Doping Dependences of Superconducting Gap Magnitude $2\Delta_0$ and Pseudogap Temperature T* in High-T_c Cuprates". *J. Phys. Soc. Jpn.*, **67**(8):2622–2625, 1998.

[96] A. Ino, C. Kim, M. Nakamura, T. Yoshida, T. Mizokawa, A. Fujimori, Z. X. Shen, T. Kakeshita, H. Eisaki, and S. Uchida. "Doping-dependent evolution of the electronic structure of $La_{2-x}Sr_xCuO_4$ in the superconducting and metallic phases". *Phys. Rev. B*, **65**(9):094504, 2002.

[97] M. Hashimoto, T. Yoshida, K. Tanaka, A. Fujimori, M. Okusawa, S. Wakimoto, K. Yamada, T. Kakeshita, H. Eisaki, and S. Uchida. "Distinct doping dependences of the pseudogap and superconducting gap of $La_{2-x}Sr_xCuO_4$ cuprate superconductors". *Phys. Rev. B*, **75**(14):140503, 2007.

[98] T. Yoshida, M. Hashimoto, S. Ideta, A. Fujimori, K. Tanaka, N. Mannella, Z. Hussain, Z. X. Shen, M. Kubota, K. Ono, et al. "Universal versus

material-dependent two-gap behaviors of the high-T_c cuprate superconductors: Angle-resolved photoemission study of $La_{2-x}Sr_xCuO_4$". *Phys. Rev. Lett.*, **103**(3):037004, 2009.

[99] A. F. Bangura, J. D. Fletcher, A. Carrington, J. Levallois, M. Nardone, B. Vignolle, P. J. Heard, N. D. Leyraud, D. LeBoeuf, L. Taillefer, et al. "Small Fermi surface pockets in underdoped high temperature superconductors: Observation of Shubnikov–de Haas oscillations in $YBa_2Cu_4O_8$". *Phys. Rev. Lett.*, **100**(4):047004, 2008.

[100] H. L. Edwards, J. T. Markert, and A. L. D. Lozanne. "Energy gap and surface structure of $YBa_2Cu_3O_{7-x}$ probed by scanning tunneling microscopy". *Phys. Rev. Lett.*, **69**(20):2967–2970, 1992.

[101] B. Friedl, C. Thomsen, and M. Cardona. "Determination of the superconducting gap in $RBa_2Cu_3O_{7-\delta}$". *Phys. Rev. Lett.*, **65**(7):915–918, 1990.

[102] T. Yoshida, W. Malaeb, S. Ideta, D. H. Lu, R. G. Moor, Z. X. Shen, M. Okawa, T. Kiss, K. Ishizaka, S. Shin, et al. "Coexistence of a pseudogap and a superconducting gap for the high-T_c superconductor $La_{2-x}Sr_xCuO_4$ studied by angle-resolved photoemission spectroscopy". *Phys. Rev. B*, **93**(1):014513, 2016.

[103] M. C Schabel, C. H. Park, A. Matsuura, Z. X. Shen, D. A. Bonn, R. Liang, and W. N. Hardy. "Superconducting-gap anisotropy in $YBa_2Cu_3O_{7-\delta}$: Photoemission results on untwinned crystals". *Phys. Rev. B*, **55**(5):2796–2799, 1997.

[104] J. Y. T. Wei, N. C. Yeh, D. F. Garrigus, and M. Strasik. "Directional tunneling and Andreev reflection on $YBa_2Cu_3O_{7-\delta}$ single crystals: Predominance of d-wave pairing symmetry verified with the generalized Blonder, Tinkham, and Klapwijk theory". *Phys. Rev. Lett.*, **81**(12):2542–2545, 1998.

[105] J. R. Kirtley, C. C. Tsuei, A. Ariando, C. J. M. Verwijs, S. Harkema, and H. Hilgenkamp. "Angle-resolved phase-sensitive determination of the in-plane gap symmetry in $YBa_2Cu_3O_{7-\delta}$". *Nat. Phys.*, **2**(3):190–194, 2006.

[106] D. Fournier, G. Levy, Y. Pennec, J. L. McChesney, A. Bostwick, E. Rotenberg, R. Liang, W. N. Hardy, D. A. Bonn, I. S. Elfimov, et al. "Loss of nodal quasiparticle integrity in underdoped $YBa_2Cu_3O_{6+x}$". *Nat. Phys.*, **6**(11):905–911, 2010.

[107] X. J. Zhou, T. Yoshida, D. H. Lee, W. L. Yang, V. Brouet, F. Zhou, W. X. Ti, J. W. Xiong, Z. X. Zhao, T. Sasagawa, et al. "Dichotomy between nodal and antinodal quasiparticles in underdoped $(La_{2-x}Sr_x)CuO_4$ superconductors". *Phys. Rev. Lett.*, **92**(18):187001, 2004.

[108] C. Ulrich, G. Khaliullin, M. Guennou, H. Roth, T. Lorenz, and B. Keimer. "Spin-Orbital Excitation Continuum and Anomalous Electron-Phonon Interaction in the Mott Insulator $LaTiO_3$". *Phys. Rev. Lett.*, **115**(15):156403, 2015.

[109] A. Lanzara, P. V. Bogdanov, X. J. Zhou, S. A. Kellar, D. L. Feng, E. D. Lu, T. Yoshida, H. Eisaki, A. Fujimori, K. Kishio, et al. "Evidence for ubiquitous strong electron–phonon coupling in high-temperature superconductors". *Nature*, **412**(6846):510–514, 2001.

[110] C. Gadermaier, A. S. Alexandrov, V. V. Kabanov, P. Kusar, T. Mertelj, X. Yao, C. Manzoni, D. Brida, G. Cerullo, and D. Mihailovic. "Electron-phonon coupling in high-temperature cuprate superconductors determined from electron relaxation rates". *Phys. Rev. Lett.*, **105**(25):257001, 2010.

[111] A. S. Mishchenko. "Electron–phonon coupling in underdoped high-temperature superconductors". *Phys. Usp.*, **52**(12):1193–1212, 2009.

[112] Z. X. Shen, A. Lanzara, S. Ishihara, and N. Nagaosa. "Role of the electron-phonon interaction in the strongly correlated cuprate superconductors". *Philos. Mag. B*, **82**(13):1349–1368, 2002.

[113] A. B. Holder and A. R. Bishop. "Anharmonicity-induced multiphonon processes in high-temperature superconductors". *Phys. Rev. B*, **44**(6):2853–2856, 1991.

[114] V. H. Crespi and M. L. Cohen. "Anharmonic phonons and high-temperature superconductivity". *Phys. Rev. B*, **48**(1):398–406, 1993.

[115] A. Y. Liu, I. I. Mazin, and J. Kortus. "Beyond Eliashberg superconductivity in MgB_2: Anharmonicity, two-phonon scattering, and multiple gaps". *Phys. Rev. Lett.*, **87**(8):087005, 2001.

[116] K. A. Müller. "On the oxygen isotope effect and apex anharmonicity in high-T_c cuprates". *Z. Phys. B*, **80**(2):193–201, 1990.

[117] G. M. Vujičić, V. L. Aksenov, N. M. Plakida, and S. Stamenković. "On the role of quasilocal excitations in the lattice of high-T_c superconductors". *Phys. Lett. A*, **73**(5-6):439–441, 1979.

[118] N. M. Plakida, V. L. Aksenov, and S. L. Drechsler. "Anharmonic model for high-T_c superconductors". *Int. J. of Mod. Phys. B*, **1**(03n04):1071–1088, 1987.

[119] C. Renner, B. Revaz, J. Y. Genoud, K. Kadowaki, and Ø Fischer. "Pseudogap precursor of the superconducting gap in under-and overdoped $Bi_2Sr_2CaCu_2O_{8+\delta}$". *Phys. Rev. Lett.*, **80**(1):149–152, 1998.

[120] H. Kitazawa, K. Katsumata, E. Torikai, and K. Nagamine. "Coexistence of magnetic ordering and superconductivity in $La_{2-x}Sr_xCuO_4$ system revealed by positive muon spin relaxation". *Solid State Commun.*, **67**(12):1191–1195, 1988.

[121] A. Weidinger, C. Niedermayer, A. Golnik, R. Simon, E. Recknagel, J. I. Budnick, B. Chamberland, and C. Baines. "Observation of Magnetic Ordering in Superconducting $La_{2-x}Sr_xCuO_4$ by Muon Spin Rotation". *Phys. Rev. Lett.*, **62**(1):102–105, 1989.

[122] C. Panagopoulos, B. D. Rainford, J. R. Cooper, and C. A. Scott. "Antiferromagnetic correlations versus superfluid density in $La_{2-x}Sr_xCuO_4$". *Physica C*, **341**:843–856, 2000.

[123] A. A. Abrikosov and L. P. Gor'kov. "Contribution to the theory of superconducting alloys with paramagnetic impurities". *Sov. Phys. JETP*, **12**:1243, 1960 [*Zhur. Eksptl'. i Teoret. Fiz.* **39**, 1960].

[124] N. Hollmann, M. W. Haverkort, M. Benomar, M. Cwik, M. Braden, and T. Lorenz. "Evidence for a temperature-induced spin-state transition of Co^{3+} in $La_{2-x}Sr_xCuO_4$". *Phys. Rev. B*, **83**(17):174435, 2011.

[125] S. Fujita and D. L. Morabito. "Formation of d-Wave Pairons in Cuprates via Longitudinal-Optical-Phonon Exchange". *Mod. Phys. Lett. B*, **12**(25):1061–1068, 1998.

[126] S. Fujita and S. Godoy. "Quantum statistical foundation to the fermi liquid model and Ginzburg-Landau wave function". *J. Supercond.*, **6**(6):373–379, 1993.

[127] S. Fujita and S. Godoy. "Quantum Statistical Derivation of the Ginzburg–Landau Equation. Energy Gap, Condensed Pairon Density and Penetration Depth". *Int. J. Mod. Phys. B*, **12**(01):99–111, 1998.

[128] W. Sacks, A. Mauger, and Y. Noat. "Cooper pairs without "glue" in high-Tc superconductors: A universal phase diagram". *EPL (Europhysics Letters)*, **119**(1):17001, 2017.

[129] W. Sacks, A. Mauger, and Y. Noat. "Origin of the Fermi arcs in cuprates: a dual role of quasiparticle and pair excitations". *J. Phys. Condens. Matter*, **30**(47):475703, 2018.

[130] S. Fujita. "On the Bose-Einstein condensation of nonzero-momentum cooper pairs. A second-order phase transition". *J. Supercond.*, **4**(4):297–310, 1991.

[131] S. Fujita and S. Watanabe. "Theory of superconductivity. 3. 2D conduction bands for high T_c. Bose-Einstein condensation transition of the third order". *J. Supercond.*, **5**(3):219–237, 1992.

[132] A. J. Coleman, E. P. Yukalova, and V. I. Yukalov. "Pairon distributions and the spectra of reduced Hamiltonians". *Int. J. Quantum Chem.*, **54**(4):211–222, 1995.

[133] S. Fujita and S. Godoy. *"Theory of high temperature superconductivity"*, volume **121**. Springer Science & Business Media, 2001.

[134] J. Chang, I. Eremin, and P. Thalmeier. "Cooper-pair formation by anharmonic rattling modes in the β-pyrochlore superconductor KOs_2O_6". *New J. Phys.*, **11**(5):055068, 2009.

[135] D. Emin. "Large-bipolaron transport and cuprate superconductors". *Phys. Rev. B*, **45**(10):5525–5529, 1992.

[136] J. Callaway. "Low-temperature lattice thermal conductivity". *Phys. Rev.*, **122**(3):787–790, 1961.

[137] J. Callaway. "Model for lattice thermal conductivity at low temperatures". *Phys. Rev.*, **113**(4):1046–1051, 1959.

[138] C. Uher. "Thermal conductivity of high-T_c superconductors". *J. Supercond.*, **3**(4):337–389, 1990.

[139] C. Uher and A. B. Kaiser. "Thermal transport properties of $YBa_2Cu_3O_7$ superconductors". *Phys. Rev. B*, **36**(10):5680–5683, 1987.

[140] J. Bardeen, G. Rickayzen, and L. Tewordt. "Theory of the thermal conductivity of superconductors". *Phys. Rev.*, **113**(4):982–994, 1959.

[141] M. D. Tiwari and B. K. Agrawal. "Analysis of the Lattice Thermal Conductivity of Germanium". *Phys. Rev. B*, **4**(10):3527–3532, 1971.

[142] S. L. Shinde and J. Goela. *"High thermal conductivity materials"*, volume **91**. Springer, 2006.

[143] A. S. Alexandrov. "Unconventional pairing symmetry of layered superconductors caused by acoustic phonons". *Phys. Rev. B*, **77**(9):094502, 2008.

[144] K. Ramakrishna, B. Das, A. K. Singh, R. S. Tiwari, and O. N. Srivastava. "Studies on structural characteristics of high Tc superconducting Bi-Ca-Sr-Cu-O phases". *Solid State Commun*, **68**(7):629–634, 1988.

[145] A. K. Saxena. *"High-temperature superconductors"*, volume **125**. Springer Science & Business Media, 2012.

[146] W. Thomson and G. Green. "An Essay on the Application of mathematical Analysis to the theories of Electricity and magnetism". *Journal für die reine und angewandte Mathematik*, **39**:73–89, 1850.

[147] J. Schwinger. "On the Green's functions of quantized fields. I". *Proc. of Natl. Acad. of Sci.*, **37**(7):452–455, 1951.

[148] J. Schwinger. "On the Green's functions of quantized fields. II". *Proc. of Natl. Acad. of Sci.*, **37**(7):455–459, 1951.

[149] H. Lehmann. "Über eigenschaften von ausbreitungsfunktionen und renormierungskonstanten quantisierter felder". *Il Nuovo Cimento (1943-1954)*, **11**(4):342–357, 1954.

[150] N. N. Bogolyubov and S. V. Tyablikov. "Retarded and advanced Green functions in statistical physics". In *Soviet Physics Doklady*, volume **4**, page 589, 1959.

[151] N. N. Bogolyubov, D. N. Zubarev, and Y. A. Tserkovnikov. "An Asymptotically Exact Solution for the Model Hamiltonian of the Theory of Superconductivity". *Sov. Phys. JETP*, **12**(1):88–93, 1961.

[152] N. Plakida. *"High-Temperature Cuprate Superconductors: Experiment, Theory, and Applications"*, volume 166. Springer Science & Business Media, 2010.

[153] D. N. Zubarev. "Double-time Green functions in statistical physics". *Sov. Phys. Usp*, **3**(3):320–345, 1960.

[154] F. J. Dyson. "The S matrix in quantum electrodynamics". *Phys. Rev.*, **75**(11):1736–1755, 1949.

[155] J. R. Schrieffer. "Theory of Superconductivity Addison-Wesley". *New York*, 1964.

[156] R. D. Parks. "Superconductivity Marcel Dekker Inc". *New York USA*, 1969.

[157] G. D. Mahan. "Introductory Material". In *Many-Particle Physics*, pages 1–64. Springer, 2000.

[158] G. Rickayzen. *"Green's functions and condensed matter"*. Courier Corporation, 2013.

[159] W. Nolting. *"Fundamentals of Many-body Physics"*. Springer, 2008.

[160] L. P. Kadanoff and G. Baym. "Quantum Statistical Mechanics WA benjamin Inc". *New York*, 1962.

[161] P. C. K. Kwok. "Green's function method in lattice dynamics". In *Solid State Physics*, volume **20**, pages 213–303. Elsevier, 1968.

[162] T. H. K. Barron, M. L. Klein, G. K. Horton, and A. A. Maradudin. "Dynamical Properties of Solids". 1974.

[163] A. A. Maradudin. "Solid State Physics, Vols. 18 and 19, Eds., F. Seitz and D. Turnbull". *Academic Press, New York*, **18**:273–420, 1966.

[164] M. Born and K. Huang. "Dynamical theory of crystal lattices Oxford University Press". *London, New York*, 1954.

[165] R. A. Cowley. "Anharmonic crystals". *Rep. Prog. Phys.*, **31**(1):123, 1968.

[166] A. A. Maradudin. "Some effects of point defects on the vibrations of crystal lattices". *Rep. Prog. Phys.*, **28**(1):331–380, 1965.

[167] R. A. Cowley. "The lattice dynamics of an anharmonic crystal". *Adv. Phys.*, **12**(48):421–480, 1963.

[168] S. Ganguly, A. Venkatasubramanian, K. Tarafder, I. Dasgupta, and A. Mookerjee. "Augmented space recursion study of the effect of disorder on superconductivity". *Phys. Rev. B*, **79**(22):224204, 2009.

[169] A. Alam and A. Mookerjee. "Lattice thermal conductivity of disordered binary alloys". *Phys. Rev. B*, **72**:214207, 2005.

[170] B. D. Indu. "Enhanced phonon density of states in impure anharmonic crystals". *Mod. Phys. Lett. B*, **6**(26):1665–1672, 1992.

[171] A. A. Maradudin, P. A. Flinn, and R. A. C. Horsfall. "Anharmonic contributions to vibrational thermodynamic properties of solids: Part I. General formulation and application to the linear chain". *Ann. Phys.*, **15**(3):337–359, 1961.

[172] B. D. Indu. "Theory of lattice specific heat of an isotopically disordered anharmonic crystal". *Int. J. Mod. Phys. B*, **4**(07n08):1379–1393, 1990.

[173] H. Singh, A. Singh, and B. D. Indu. "The Born–Mayer–Huggins potential in high temperature superconductors". *Mod. Phys. Lett. B*, **30**(21):1650283, 2016.

[174] M. Tinkham. *"Introduction to superconductivity"*. Courier Corporation, 2004.

[175] M. A. Biondi, M. P. Garfunkel, and A. O. McCoubrey. "Millimeter wave absorption in superconducting aluminum". *Phys. Rev.*, **101**(4):1427–1429, 1956.

[176] H. Ding, M. R. Norman, J. C. Campuzano, M. Randeria, A. F. Bellman, T. Yokoya, T. Takahashi, T. Mochiku, and K. Kadowaki. "Angle-resolved photoemission spectroscopy study of the superconducting gap anisotropy in $Bi_2Sr_2CaCu_2O_{8+x}$". *Phys. Rev. B*, **54**(14):R9678–R9681, 1996.

[177] H. Ding, P. Richard, K. Nakayama, K. Sugawara, T. Arakane, Y. Sekiba, A. Takayama, S. Souma, T. Sato, T. Takahashi, et al. "Observation of Fermi-surface–dependent nodeless superconducting gaps in $Ba_{0.6}K_{0.4}Fe_2As_2$". *Europhys. Lett.*, **83**(4):47001, 2008.

[178] D. Mou, S. Liu, X. Jia, J. He, Y. Peng, L. Zhao, L. Yu, G. Liu, S. He, X. Dong, et al. "Distinct Fermi surface topology and nodeless superconducting gap in a $(TI_{0.58}Rb_{0.42})Fe_{1.72}Se_2$ superconductor". *Phys. Rev. Lett.*, **106**(10):107001, 2011.

[179] M. A. Biondi and M. P. Garfunkel. "Millimeter wave absorption in superconducting aluminum. I. Temperature dependence of the energy gap". *Phys. Rev.*, **116**(4):853–861, 1959.

[180] A. Vansevenant. "The gap equation in superconductivity theory". *Physica D*, **17**(3):339–344, 1985.

[181] M. Gladysiewicz, R. Gonczarek, and M. Mulak. "The form of energy gap and critical temperature of superconductor implied by fluctuations of density of states". *Acta Phys. Pol. A*, **97**(6):1039–1051, 2000.

[182] Y. Sun, M. Guidry, and C. L. Wu. "Pairing gaps, pseudogaps, and phase diagrams for cuprate superconductors". *Phys. Rev. B*, **75**(13):134511, 2007.

[183] C. Hainzl and R. Seiringer. "Critical temperature and energy gap for the BCS equation". *Phys. Rev. B*, **77**(18):184517, 2008.

[184] C. Hainzl, E. Hamza, R. Seiringer, and J. P. Solovej. "The BCS functional for general pair interactions". *Commun. Math. Phys.*, **281**(2):349–367, 2008.

[185] S. Watanabe. "The solution to the BCS gap equation and the second-order phase transition in superconductivity". *J. Math. Anal. Appl.*, 383(**2**):353–364, 2011.

[186] S. Watanabe. "Addendum to "The solution to the BCS gap equation and the second-order phase transition in superconductivity [J. Math. Anal. Appl. 383 (2011) 353–364]". *J. Math. Anal. Appl.*, **405**(2):742–745, 2013.

[187] S. Watanabe. "The Solution to the BCS Gap Equation for Superconductivity and Its Temperature Dependence". *Abstr. Appl. Anal.*, **2013**:1–5, 2013.

[188] H. Caldas, F. S. Batista, M. A. Continentino, F. Deus, and D. Nozadze. "A two-band model for p-wave superconductivity". *Ann. Phys.*, **384**:211–224, 2017.

[189] A. Singh, H. Singh, and B. D. Indu. "The electronic heat capacity of $YBa_2Cu_3O_{7-\delta}$ superconductor". *AIP Adv.*, **6**(7):075102, 2016.

[190] A. B. Chen, G. Weisz, and A. Sher. "Temperature dependence of the electron density of states and dc electrical resistivity of disordered binary alloys". *Phys. Rev. B*, **5**(8):2897–924, 1972.

[191] J. J. M. Valles, R. C. Dynes, and J. P. Garno. "Temperature dependence of the two-dimensional electronic density of states in disordered metal films". *Phys. Rev. B*, **40**(11):7590–7593, 1989.

[192] V. Ashokan, B. D. Indu, and A. K. Dimri. "Signature of electron-phonon interaction in high temperature superconductors". *AIP Adv.*, **1**(3):032101, 2011.

[193] B. M. Andersen, P. J. Hirschfeld, A. P. Kampf, and M. Schmid. "Disorder-induced static antiferromagnetism in cuprate superconductors". *Phys. Rev. Lett.*, **99**(14):147002, 2007.

[194] G. Shirane, R. J. Birgeneau, Y. Endoh, and M. A. Kastner. "Spin fluctuations in insulating, weakly metallic and superconducting $La_{2-x}Sr_xCuO_4$". *Physica B*, **197**(1-4):158–174, 1994.

[195] M. H. Julien. "Magnetic order and superconductivity in $La_{2-x}Sr_xCuO_4$: a review". *Physica B*, **329**:693–696, 2003.

[196] S. K. Verma, A. Gupta, A. Kumari, and B. D. Indu. "Pairing Symmetry, Nodal and Antinodal Superconducting Gap in $La_{2-x}Sr_xCuO_4$: A Doping Scenario". *Unpublished results*, 2019.

[197] M. L. Kulić and O. V. Dolgov. "The electron-phonon interaction renormalized by strong correlations: The way to HTS". *Physica C*, **341**:111–112, 2000.

[198] H. M. Tutuncu, E. Karaca, and G. P. Srivastava. "Electron–phonon interaction and superconductivity in the borocarbide superconductor". *Philos. Mag.*, **97**(29):2669–2688, 2017.

[199] E. G. Maksimov, A. E. Karakozov, B. P. Gorshunov, E. S. Zhukova, Y. G. Ponomarev, and M. Dressel. "Electronic specific heat of two-band layered superconductors: analysis within the generalized two-band α model". *Phys. Rev. B*, **84**(17):174504, 2011.

[200] J. K Freericks and V. Zlatić. "Gap ratio in anharmonic charge-density-wave systems". *Phys. Rev. B*, **64**(7):073109, 2001.

[201] A. Ino, T. Mizokawa, K. Kobayashi, A. Fujimori, T. Sasagawa, T. Kimura, K. Kishio, K. Tamasaku, H. Eisaki, and S. Uchida. "Doping dependent density of states and pseudogap behavior in $La_{2-x}Sr_xCuO_4$". *Phys. Rev. Lett.*, **81**(10):2124–2127, 1998.

[202] I. I. Mazin, D. J. Singh, M. D. Johannes, and M. H. Du. "Unconventional superconductivity with a sign reversal in the order parameter of $LaFeAsO_{1-x}F_x$". *Phys. Rev. Lett.*, **101**(5):057003, 2008.

[203] X. L. Zhang and W. M. Liu. "Electron-Phonon Coupling and its implication for the superconducting topological insulators". *Sci. Rep.*, **5**:8964, 2015.

[204] C. M. Varma, P. B. Littlewood, S. S. Rink, E. Abrahams, and A. E. Ruckenstein. "Phenomenology of the normal state of Cu-O high-temperature superconductors". *Phys. Rev. Lett.*, **63**(18):1996–1999, 1989.

[205] M. S. Rogalski and S. B. Palmer. *"Solid State Physics"*. Gordon and Breach Science Publishers, 2000.

[206] G. P. Malik. "On the Equivalence of the Binding Energy of a Cooper Pair and the BCS Energy Gap: A Framework for Dealing with Composite Superconductors". *Int. J. Mod. Phys. B*, **24**(09):1159–1172, 2010.

[207] G. Blumberg, A. Mialitsin, B. S. Dennis, N. D. Zhigadlo, and J. Karpinski. "Multi-gap superconductivity in MgB_2: Magneto-Raman spectroscopy". *Physica C*, **456**(1):75–82, 2007.

[208] A. Perucchi, L. Baldassarre, S. Lupi, J. Y. Jiang, J. D. Weiss, E. E. Hellstrom, S. Lee, C. W. Bark, C. B. Eom, M. Putti, et al. "Multi-gap superconductivity in a $BaFe_{1.84}Co_{0.16}As_2$ film from optical measurements at terahertz frequencies". *Eur. Phys. J. B*, **77**(1):25–30, 2010.

[209] S. Souma, Y. Machida, T. Sato, T. Takahashi, H. Matsui, S. C. Wang, H. Ding, A. Kaminski, J. C. Campuzano, S. Sasaki, et al. "The origin of multiple superconducting gaps in MgB_2". *Nature*, **423**(6935):65–67, 2003.

[210] T. E. Shanygina, Y. G. Ponomarev, S. A. Kuzmichev, M. G. Mikheev, S. N. Tchesnokov, O. E. Omel'yanovskii, A. V. Sadakov, Y. F. Eltsev, A. S. Dormidontov, V. M. Pudalov, et al. "Observation of multi-gap superconductivity in GdO(F)FeAs by Andreev spectroscopy". *JETP Lett.*, **93**(2):94–98, 2011.

[211] H. Suhl, B. T. Matthias, and L. R. Walker. "Bardeen-Cooper-Schrieffer theory of superconductivity in the case of overlapping bands". *Phys. Rev. Lett.*, **3**(12):552–554, 1959.

[212] A. S. Alexandrov. "nonadiabatic polaronic superconductivity in MgB_2 and cuprates. *Physica C*, **363**(4):231–236, 2001.

[213] P. Monthoux, A. V. Balatsky, and D. Pines. "Weak-coupling theory of high-temperature superconductivity in the antiferromagnetically correlated copper oxides". *Phys. Rev. B*, **46**(22):14803–14817, 1992.

[214] C. H. Pao and N. E. Bickers. "Anisotropic superconductivity in the 2D Hubbard model: Gap function and interaction weight". *Phys. Rev. Lett.*, **72**(12):1870–1873, 1994.

[215] R. Liang, D. A. Bonn, and W. N. Hardy. "Evaluation of CuO_2 plane hole doping in $YBa_2Cu_3O_{6+x}$ single crystals". *Phys. Rev. B*, **73**(18):180505, 2006.

[216] L. Boeri, M. Calandra, I. I. Mazin, O. V. Dolgov, and F. Mauri. "Effects of magnetism and doping on the electron-phonon coupling in $BaFe_2As_2$". *Phys. Rev. B*, **82**(2):020506, 2010.

[217] V. Ashokan and B. D. Indu. "Renormalization effects and phonon density of states in high temperature superconductors". *AIP Adv.*, **3**(2):022108, 2013.

[218] S. K. Verma, A. Gupta, A. Kumari, and B. D. Indu. "Superconducting gap anisotropy and d-wave pairing in $YBa_2Cu_3O_{7-\delta}$". *Int. J. Mod. Phys. B*, **32**:1850035, 2018.

[219] X. K. Chen, J. C. Irwin, H. J. Trodahl, T. Kimura, and K. Kishio. "Investigation of the Superconducting Gap in $La_{2-x}Sr_xCuO_4$ by Raman Spectroscopy". *Phys. Rev. Lett.*, **73**(24):3290–3293, 1994.

[220] S. K. Verma, A. Kumari, A. Gupta, and B. D. Indu. "The high temperature superconductor gap equation". *Phys. Scr.*, **94**:035701, 2019.

[221] A. B. Harris, D. Kumar, B. I. Halperin, and P. C. Hohenberg. "Dynamics of an antiferromagnet at low temperatures: spin-wave damping and hydrodynamics". *Phys. Rev. B*, **3**(3):961–1024, 1971.

[222] Y. Ohashi and H. Shiba. "Pairing and Depairing Effects of Antiferromagnetic Spin Fluctuations in High-T_c Superconductivity". *J. Phys. Soc. Jpn.*, **62**(8):2783–2802, 1993.

[223] W. Kress, U. Schröder, J. Prade, A. D. Kulkarni, and F. W. D. Wette. "Lattice dynamics of the high-T_c superconductor $YBa_2Cu_3O_{7-x}$". *Phys. Rev. B*, **38**(4):2906–2909, 1988.

[224] A. K. Ghatak and L. S. Kothari. "Introduction to Lattice Dynamics". 1972.

[225] R. J. Cava, A. Santoro, D. W. Johnson Jr, and W. W. Rhodes. "Crystal structure of the high-temperature superconductor $La_{1.85}Sr_{0.15}CuO_4$ above and below T_c". *Phys. Rev. B*, **35**(13):6716–6720, 1987.

[226] Z. Szotek, B. L. Gyorffy, and W. M. Temmerman. "Doping dependence of the superconducting gap in $YBa_2Cu_3O_{7-\delta}$". *Physica C*, **353**(1-2):23–28, 2001.

[227] O. K. Andersen, O. Jepsen, A. I. Liechtenstein, and I. I. Mazin. "Plane dimpling and saddle-point bifurcation in the band structures of optimally doped high-temperature superconductors: a tight-binding model". *Phys. Rev. B*, **49**(6):4145–4157, 1994.

[228] O. K. Andersen, A. I. Liechtenstein, O. Jepsen, and F. Paulsen. "LDA energy bands, low-energy hamiltonians, $t', t'', t_\perp(k)$ and $J_\perp$". *J. Phys. Chem. Solids*, **56**(12):1573–1591, 1995.

[229] H. Fu and D. H. Lee. "Dichotomy between the nodal and antinodal excitations in high-temperature superconductors". *Phys. Rev. B*, **74**(17):174513, 2006.

[230] V. I. Belyavsky, V. V. Kapaev, and Y. V. Kopaev. "Checkerboard superconducting order and antinodal Bogoliubov quasiparticle interference". *Phys. Rev. B*, **80**(21):214524, 2009.

[231] D. Wulin, C. C. Chien, D. K. Morr, and K. Levin. "Contrasting nodal and antinodal behavior in the cuprates via multiple gap spectroscopies". *Phys. Rev. B*, **81**(10):100504, 2010.

[232] Y. Peng, J. Meng, D. Mou, J. He, L. Zhao, Y. Wu, G. Liu, X. Dong, S. He, Jun Z., et al. "Disappearance of nodal gap across the insulator–superconductor transition in a copper-oxide superconductor". *Nat. Commun.*, **4**:2459, 2013.

[233] M. Aichhorn, E. Arrigoni, Z. B. Huang, and W. Hanke. "Superconducting Gap in the Hubbard Model and the Two-Gap Energy Scales of High-T_c Cuprate Superconductors". *Phys. Rev. Lett.*, **99**:257002, 2007.

[234] J. R. Schrieffer, X. G. Wen, and S. C. Zhang. "Spin-bag mechanism of high-temperature superconductivity". *Phys. Rev. Lett.*, **60**(10):944–947, 1988.

[235] J. R. Schrieffer, X. G. Wen, and S. C. Zhang. "Dynamic spin fluctuations and the bag mechanism of high-T_c superconductivity". *Phys. Rev. B*, **39**(16):11663–11679, 1989.

[236] A. S. Alexandrov. *"Theory of Superconductivity: From Weak to Strong Coupling"*. CRC Press, 2003.

[237] Y. M. Gerbstein, N. E. Timoshchenko, and F. A. Chudnovskii. "Measurement of electron density of states at the Fermi level in YBCO by means of an "oxygen pump"". *Physica C*, **162**:961–962, 1989.

[238] D. J. V. Harlingen. "Phase-sensitive tests of the symmetry of the pairing state in the high-temperature superconductors—evidence for $d_{x^2-y^2}$ symmetry". *Rev. Mod. Phys.*, **67**(2):515–537, 1995.

[239] C. C. Tsuei and J. R. Kirtley. "Pairing symmetry in cuprate superconductors". *Rev. Mod. Phys.*, **72**(4):969–1016, 2000.

[240] M. Shi, J. Chang, S. Pailhés, M. R. Norman, J. C. Campuzano, M. Månsson, T. Claesson, O. Tjernberg, A. Bendounan, L. Patthey, et al. "Coherent d-wave

superconducting gap in underdoped $La_{2-x}Sr_xCuO_4$ by angle-resolved photoemission spectroscopy". *Phys. Rev. Lett.*, **101**(4):047002, 2008.

[241] E. Razzoli, G. Drachuck, A. Keren, M. Radovic, N. C. Plumb, J. Chang, Y. B. Huang, H. Ding, J. Mesot, and M. Shi. "Evolution from a Nodeless Gap to $d_{x^2-y^2}$ -Wave in Underdoped $La_{2-x}Sr_xCuO_4$". *Phys. Rev. Lett.*, **110**(4):047004, 2013.

[242] J. R. Kirtley, C. C. Tsuei, J. Z. Sun, C. C. Chi, L. S. Y. Jahnes, A. Gupta, M. Rupp, and M. B. Ketchen. "Symmetry of the order parameter in the high-Tc superconductor $YBa_2Cu_3O_{7-\delta}$". *Nature*, **373**(6511):225–228, 1995.

[243] H. Jacobsen, I. A. Zaliznyak, A. T. Savici, B. L. Winn, S. Chang, M Hücker, G. D. Gu, and J. M. Tranquada. "Neutron scattering study of spin ordering and stripe pinning in superconducting $La_{1.93}Sr_{0.07}CuO_4$". *Phys. Rev. B*, **92**(17):174525, 2015.

[244] T. Kurosawa, T. Yoneyama, Y. Takano, M. Hagiwara, R. Inoue, N. Hagiwara, K. Kurusu, K. Takeyama, N. Momono, M. Oda, et al. "Large pseudogap and nodal superconducting gap in $Bi_2Sr_{2-x}La_xCuO_{6+\delta}$ and $Bi_2Sr_2CaCu_2O_{8+\delta}$: Scanning tunneling microscopy and spectroscopy". *Phys. Rev. B*, **81**(9):094519, 2010.

[245] I. Kapon, D. S. Ellis, G. Drachuck, G. Bazalitski, E. Weschke, E. Schierle, J. Strempfer, C. Niedermayer, and A. Keren. "Opening a nodal gap by fluctuating spin-density wave in lightly doped $La_{2-x}Sr_xCuO_4$". *Phys. Rev. B*, **95**(10):104512, 2017.

[246] M. L. Tacon, A. Sacuto, A. Georges, G. Kotliar, Y. Gallais, D. Colson, and A. Forget. "Two energy scales and two distinct quasiparticle dynamics in the superconducting state of underdoped cuprates". *Nat. Phys.*, **2**(8):537–543, 2006.

[247] A. Damascelli, Z. Hussain, and Z. X. Shen. "Angle-resolved photoemission studies of the cuprate superconductors". *Rev. Mod. Phys.*, **75**(2):473–541, 2003.

[248] F. Venturini, M. Opel, R. Hackl, H. Berger, L. Forró, and B. Revaz. "Doping dependence of the electronic Raman spectra in cuprates". *J. Phys. Chem. Solids*, **63**(12):2345–2348, 2002.

[249] S. Sugai, H. Suzuki, Y. Takayanagi, T. Hosokawa, and N. Hayamizu. "Carrier-density-dependent momentum shift of the coherent peak and the LO phonon mode in p-type high-T_c superconductors". *Phys. Rev. B*, **68**(18):184504, 2003.

[250] T. P. Devereaux and R. Hackl. "Inelastic light scattering from correlated electrons". *Rev. Mod. Phys.*, **79**(1):175–233, 2007.

[251] W. Guyard, M. L. Tacon, M. Cazayous, A. Sacuto, A. Georges, D. Colson, and A. Forget. "Breakpoint in the evolution of the gap through the cuprate phase diagram". *Phys. Rev. B*, **77**(2):024524, 2008.

[252] H. Anzai, A. Ino, M. Arita, H. Namatame, M. Taniguchi, M. Ishikado, K. Fujita, S. Ishida, and S. Uchida. "Relation between the nodal and antinodal gap and critical temperature in superconducting Bi2212". *Nat. Commun.*, **4**:1815, 2013.

[253] K. Ueda, T. Moriya, and Y. Takahashi. "Antiferromagnetic spin fluctuations and high-T_c superconductivity". *J. Phys. Chem. Solids*, **53**(12):1515–1521, 1992.

[254] P. Monthoux and D. Pines. "$YBa_2Cu_3O_7$: A nearly antiferromagnetic Fermi liquid. *Phys. Rev. B*, **47**(10):6069–6081, 1993.

[255] P. Monthoux and D. Pines. "Spin-fluctuation-induced superconductivity and normal-state properties of $YBa_2Cu_3O_7$". *Phys. Rev. B*, **49**(6):4261–4278, 1994.

[256] D. J. Scalapino. "The case for $d_{x^2-y^2}$ pairing in the cuprate superconductors". *Phys. Rep.*, **250**(6):329–365, 1995.

[257] Y. Yildirim, W. Ku, et al. "Kinetics-Driven Superconducting Gap in Underdoped Cuprate Superconductors Within the Strong-Coupling Limit". *Phys. Rev. X*, **1**(1):011011, 2011.

[258] B. Keimer, S. A. Kivelson, M. R. Norman, S. Uchida, and J. Zaanen. "From quantum matter to high-temperature superconductivity in copper oxides". *Nature*, **518**(7538):179–186, 2015.

[259] P. W. Anderson. "The Theory of Superconductivity in the High-T_c Cuprates". *Press, Princeton New Jersey*, 1997.

[260] A. Mathai, Y. Gim, R. C. Black, A. Amar, and F. C. Wellstood. "Experimental proof of a time-reversal-invariant order parameter with a π shift in $YBa_2Cu_3O_{7-\delta}$". *Phys. Rev. Lett.*, **74**(22):4523–4526, 1995.

[261] R. M. Qiang, Y. Y. Jun, Z. Tong, and F. D. Lai. "Possible Nodeless Superconducting Gaps in $Bi_2Sr_2CaCu_2O_{8+\delta}$ and YBa_2Cu_3O Revealed by Cross-Sectional Scanning Tunneling Spectroscopy". *Chin. Phys. Lett.*, **33**(12):127402, 2016.

[262] N. C. Yeh, C. T. Chen, G. Hammerl, J. Mannhart, A. Schmehl, C. W. Schneider, R. R. Schulz, S. Tajima, K. Yoshida, D. Garrigus, et al. "Evidence of doping-dependent pairing symmetry in cuprate superconductors". *Phys. Rev. Lett.*, **87**(8):087003, 2001.

[263] C. C. Tsuei and J. R. Kirtley. "d-wave pairing symmetry in cuprate superconductors". *Physica C*, **341–348**:1625–1628, 2000.

[264] M. F. Limonov, A. I. Rykov, S. Tajima, and A. Yamanaka. "Raman Scattering Study on Fully Oxygenated $YBa_2Cu_3O_7$ Single Crystals: x-y Anisotropy in the Superconductivity-Induced Effects". *Phys. Rev. Lett.*, **80**(4):825–828, 1998.

[265] H. Aubin, K. Behnia, M. Ribault, R. Gagnon, and L. Taillefer. "Angular position of nodes in the superconducting gap of YBCO". *Phys. Rev. Lett.*, **78**(13):2624–2627, 1997.

[266] Y. Dagan and G. Deutscher. "Doping and magnetic field dependence of in-plane tunneling into $YBa_2Cu_3O_{7-x}$: possible evidence for the existence of a quantum critical point". *Phys. Rev. Lett.*, **87**(17):177004, 2001.

[267] B. J. Ramshaw, S. E. Sebastian, R. D. McDonald, J. Day, B. S. Tan, Z. Zhu, J. B. Betts, R. Liang, D. A. Bonn, W. N. Hardy, et al. "Quasiparticle mass enhancement approaching optimal doping in a high-T_c superconductor". *Science*, **348**(6232):317–320, 2015.

[268] A. P. Kampf. "Magnetic correlations in high temperature superconductivity". *Phys. Rep.*, **249**(4-5):219–351, 1994.

[269] G. Xu, W. Ming, Y. Yao, X. Dai, S. C. Zhang, and Z. Fang. "Doping-dependent phase diagram of LaOMAs (M= V–Cu) and electron-type superconductivity near ferromagnetic instability". *EPL*, **82**(6):67002, 2008.

[270] K. Gofryk, A. S. Sefat, M. A. McGuire, B. C. Sales, D. Mandrus, J. D. Thompson, E. D. Bauer, and F. Ronning. "Doping-dependent specific heat study of the superconducting gap in $Ba(Fe_{1-x}Co_x)_2As_2$". *Phys. Rev. B*, **81**(18):184518, 2010.

[271] K. J. Leary, H. C. Z. Loye, S. W. Keller, T. A. Faltens, W. K. Ham, J. N. Michaels, and A. M. Stacy. "Observation of an oxygen isotope effect in $YBa_2Cu_3O_7$". *Phys. Rev. Lett.*, **59**(11):1236–1239, 1987.

[272] G. H. Gweon, T. Sasagawa, S. Y. Zhou, J. Graf, H. Takagi, D. H. Lee, and A. Lanzara. "An unusual isotope effect in a high-transition-temperature superconductor". *Nature*, **430**(6996):187–190, 2004.

[273] D. J. Pringle, G. V. M. Williams, and J. L. Tallon. "Effect of doping and impurities on the oxygen isotope effect in high-temperature superconducting cuprates". *Phys. Rev. B*, **62**(18):12527, 2000.

[274] D. R. Temprano, J. Mesot, S. Janssen, K. Conder, A. Furrer, H. Mutka, and K. A. Müller. "Large isotope effect on the pseudogap in the high-temperature superconductor $HoBa_2Cu_4O_8$". *Phys. Rev. Lett.*, **84**(9):1990–1993, 2000.

[275] H. K. Yoshida, T. Hirooka, A. Oyamada, Y. Okabe, T. Takahashi, T. Sasaki, A. Ochiai, T. Suzuki, A. J. Mascarenhas, J. I. Pankove, et al. "Oxygen isotope effect in the superconducting Bi-Sr-Ca-Cu-O system". *Physica C*, **156**(3):481–484, 1988.

[276] V. Z. Kresin, A. Bill, S. A. Wolf, and Y. N. Ovchinnikov. "Unconventional isotope effects in superconductors". *Phys. Rev. B*, **56**(1):107–110, 1997.

[277] G. M. Zhao, H. Keller, and K. Conder. "Unconventional isotope effects in the high-temperature cuprate superconductors". *J. Phys.: Condens. Matter*, **13**(29):R569–R587, 2001.

[278] M. A. Tanatar, J. P. Reid, H. Shakeripour, X. G. Luo, N. D. Leyraud, N. N., S. L. Bud'Ko, P. C. Canfield, R. Prozorov, and L. Taillefer. "Doping Dependence of Heat Transport in the Iron-Arsenide Superconductor $Ba(Fe_{1-x}Co_x)_2As_2$: From Isotropic to a Strongly k-Dependent Gap Structure". *Phys. Rev. Lett.*, **104**(6):067002, 2010.

[279] M. A. Ansari, V. Ashokan, B. D. Indu, and R. Kumar. "Lattice Thermal Conductivity of GaAs". *Acta Phys. Pol. A.*, **121**(3):639–646, 2012.

[280] J. Callaway and H. C. V. Baeyer. "Effect of point imperfections on lattice thermal conductivity". *Phys. Rev.*, **120**(4):1149–1154, 1960.

[281] M. G. Holland. "Analysis of lattice thermal conductivity". *Phys. Rev.*, **132**(6):2461–2471, 1963.

[282] P. K. Sharma and R. Bahadur. "Thermal conductivity for phonon scattering by substitutional defects in crystals". *Phys. Rev. B*, **12**(4):1522–1530, 1975.

[283] Y. Li, Z. Tian, Y. Luo, J. Wang, L. Sun, L. Zheng, and J. Wang. "Pressure-induced low-lying phonon modes softening and enhanced thermal resistance in β-$Mg_2Al_4Si_5O_{18}$". *Phys. Rev. B*, **95**(5):054301, 2017.

[284] S. Gupta, D. S. Tomar, and S. C. Goyal. "Elastic Properties of $La_{2-x}Sr_xCuO_4$ (x= 0.10-0.20)". *J. Sci. Res.*, **2**(2):294–301, 2010.